Det Kongelige Danske Videnskabernes Selskab
Matematisk-fysiske Meddelelser, bind **27**, nr. 16

Dan. Mat. Fys. Medd. **27**, no. 16 (1953)

COLLECTIVE AND INDIVIDUAL-PARTICLE ASPECTS OF NUCLEAR STRUCTURE

BY

AAGE BOHR AND BEN R. MOTTELSON

København
i kommission hos Ejnar Munksgaard
1953

CONTENTS

Pages

I. Introduction 7
II. The Coupled System of Particles and Collective Oscillations 10
a) Formulation of the Model 10
i. Collective coordinates 10
ii. Oscillations of a shell structure 12
iii. Coupling to particle motion 14
b) Coupling of Single Particle to Nuclear Surface 16
i. Perturbation approximation 16
ii. Strong coupling approximation 18
iii. Intermediate coupling 24
c) Many-Particle Configurations 26
i. Weak surface coupling 27
ii. Strong surface coupling 27
iii. Influence of particle forces 31
III. Ground State Spins 33
i. Single-particle configurations 33
ii. Configurations of two equivalent particles. Even structures 34
iii. Configurations of three equivalent particles 34
iv. Odd-odd nuclei 37
v. Summary 39
IV. Magnetic Moments 41
a) Shell Model Moments 41
b) Moments of the Coupled System 44
c) Comparison with Empirical Data 47
V. Quadrupole Moments 53
a) Shell Model Moments 53
b) Moments of the Coupled System 54
c) Discussion of Empirical Data 58
d) Correlations with Other Nuclear Properties 61
Addendum to Chapters IV and V. Details of the Analysis of Nuclear Moments 63
i. $(1/2+)$ nuclei 63
ii. $(1/2-)$ – 67
iii. $(3/2-)$ – 69
iv. $(3/2+)$ – 72
v. $(5/2+)$ – 75
vi. $(5/2-)$ – 78
vii. $(7/2-)$ – 79
viii. $(7/2+)$ – 79
ix. $(9/2+)$ – 80
x. $(9/2-)$ – 81
xi. odd-odd nuclei 82
VI. Nuclear Level Structure 85
a) General Features of Levels in the Coupled System 85
b) Particle Excitations 86

c) Collective Excitations ... 88
i. Excitations of closed-shell nuclei ... 88
ii. Rotational states in even-even nuclei ... 89
iii. Rotational states in odd-A nuclei ... 96
iv. Vibrational excitations ... 97
d) Higher Excitation. The Compound Nucleus ... 97
VII. Electromagnetic Transitions ... 101
a) Transition Operators ... 101
b) Transitions in the Weakly Coupled System ... 103
i. Particle transitions ... 103
ii. Phonon transitions ... 105
iii. Surface moments induced by particle transitions ... 105
c) Transitions in the Strongly Coupled System ... 106
i. Particle transitions ... 106
ii. Collective transitions ... 109
d) Discussion of Empirical Data ... 110
i. $M4$ transitions; unfavoured factors ... 110
ii. $E3$ transitions; j-forbiddenness ... 113
iii. $E2$ transitions; collective excitations ... 115
VIII. Beta Transitions ... 118
a) Transition Operators ... 118
b) Evaluation of Transition Probabilities ... 120
i. Transitions in an undeformed nucleus ... 120
ii. Transitions in the strongly coupled system ... 121
c) Discussion of Empirical Data ... 123
i. Mirror transitions ... 123
ii. Allowed unfavoured transitions ... 127
iii. l-forbidden transitions ... 129
iv. Pure GT forbidden transitions ... 130
IX. Summary ... 133

Appendix I. Shell Structure and Deformability ... 136
Appendix II. Matrix Elements in the Perturbation Representation ... 138
Appendix III. Features of the Strong Coupling Solution ... 140
i. Matrix elements ... 140
ii. Strong coupling for a single $j = 3/2$ particle ... 141
Appendix IV. Solution of the Coupled Equations for Large j ... 144
Appendix V. Individual-particle and Collective Features of Nuclear Reactions ... 147
a) General Formalism ... 147
b) Scattering Cross-sections ... 150
i. Weak coupling; one-level resonance ... 151
ii. Strong coupling; many-level resonances ... 153
iii. Sum rule for scattering widths ... 156
c) Discussion ... 157
Appendix VI. Nuclear Excitation by the Electric Field of Impinging Particles 162

References ... 168

INDEX OF TABLES

		Pages
I.	Lowest spins of $(j)^{\pm 3}$ configurations	36
II.	Spins of simple odd-odd nuclei	38
III.	Properties of charge symmetrized states of type $(j = 3/2)^3_{J=3/2}$ with $T = 1/2$	44
IV.	Comparison of magnetic moments with shell model values	45
V.	Coefficients in magnetic moment shifts produced by weak surface coupling	46
VI.	Magnetic moments in strong coupling	48
VII.	Summary of magnetic moments for $A < 50$	50
VIII.	Quadrupole moments for $(j)^3$ proton configurations	54
IX.	Comparison of quadrupole moments with hydrodynamic estimates	60
X.	Moments of $(1/2+)$ nuclei	64
XI.	Moments of $(1/2-)$ nuclei	68
XII.	Moments of $(3/2-)$ nuclei	69
XIII.	Correlations between magnetic moments and quadrupole moments for $(3/2-)$ nuclei	71
XIV.	Moments of $(3/2+)$ nuclei	72
XV.	Moments of $(5/2+)$ nuclei	76
XVI.	Moments of $(5/2-)$ nuclei	78
XVII.	Moments of $(7/2-)$ nuclei	79
XVIII.	Moments of $(7/2+)$ nuclei	80
XIX.	Moments of $(9/2+)$ nuclei	81
XX.	Moments of $(9/2-)$ nuclei	81
XXI.	Moments of odd-odd nuclei	82
XXII.	Energies of $(2+)$ and $(4+)$ states in even-even nuclei with $A > 140$	92
XXIII.	Deformations deduced from properties of rotational states	94
XXIV.	Coefficients $c(j_>, j_<)$ in transition probabilities	104
XXV.	$M4$ transitions in odd-A nuclei	111
XXVI.	$E3$ transitions of $(7/2+) \leftrightarrow (1/2-)$ type	114
XXVII.	$E2$ transitions in even-even nuclei	116
XXVIII.	$E2$ transitions in odd-A nuclei	117
XXIX.	ft-values of mirror transitions	124
XXX.	Allowed unfavoured β-transitions in odd-A nuclei	128
XXXI.	l-forbidden β-transitions in odd-A nuclei	129
XXXII.	Forbidden β-transitions of pure GT type	131

INDEX OF FIGURES

Pages

1. Nuclear deformability in the hydrodynamic approximation 14
2. Frequencies of surface oscillations in the hydrodynamic approximation 14
3. Coupling scheme for strong particle-surface interaction..... 19
4. Wave function in intermediate coupling for $I = j = 3/2$ 25
5. Sharing of angular momentum between particle and surface motion... 26
6. Coupling schemes for many-particle configurations 29
7. Magnetic moments of odd-proton nuclei 42
8. Magnetic moments of odd-neutron nuclei 43
9. Quadrupole moments of odd-A nuclei 55
10. Projection factor for quadrupole moments in the coupled system..... 57
11. Magnetic moments arising from d-state admixture in $I = \Omega = 1/2$ states 66
12. Magnetic moments arising from decoupling of spin and orbit in d states with $I = \Omega = 3/2$ 73
13. First excited states in even-even nuclei with $A > 140$ 91
14. Unfavoured factors in intermediate coupling 108
15. Beta decay transition probabilities arising from d-state admixture in $I = \Omega = 1/2$ states 126
16. Scattering f-function in coupled model 155
17. Function $g_2(\xi)$ appearing in cross-sections for Coulomb excitation 166

I. Introduction.

Great progress has been achieved in recent years in the exploration of nuclear properties, and an extensive body of data is now available, giving information on many aspects of nuclear structure.

Strong evidence has been accumulated that the nucleons may be considered as occupying states of binding characteristic of independent particle motion in the averaged nuclear field. This recognition has led to the development of a nuclear shell model, which exhibits many similarities with the description of atomic constitution (MAYER, 1950; HAXEL, JENSEN and SUESS, 1950, 1952). The shell model has been an important guide in the interpretation of nuclear phenomena; besides the numerous features of the nuclear systematics associated with the discontinuities of binding energies at closed shells, the model especially explains many regularities of nuclear spins and parities.

There are, however, also essential differences between atomic and nuclear structures, arising from the fact that the nuclear field is generated by the nucleons themselves, while the atomic field, responsible for the electronic binding, is largely governed by the attraction from the central nucleus. The large mass of the atomic nucleus, as compared with the electrons, makes it possible to a first approximation to treat the atomic field as a static quantity, but, in the nuclear case, the dynamic aspects of the field, associated with collective oscillations of the structure as a whole, must be expected to play an essential role. The significance of collective features in a system where the cohesion is a result of the mutual attraction of the particles has earlier found expression in the liquid drop nuclear model (N. BOHR, 1936; N. BOHR and F. KALCKAR, 1937).

The importance of taking into account the collective aspects of the nuclear structure is clearly evidenced in the empirical

data, and ordered types of motion of the nucleons are strikingly exhibited by a number of phenomena:

1) The occurrence of the fission reaction, many features of which can be understood on the basis of the liquid drop model (MEITNER and FRISCH, 1939; BOHR and WHEELER, 1940).

2) The large quadrupole moments observed for many nuclei, which in some cases are more than 20 times larger than single-particle estimates (CASIMIR, 1936; TOWNES, FOLEY and LOW, 1949; cf. also Fig. 9 on page 55 below). It has been pointed out by RAINWATER (1950) that the magnitude of the quadrupole moments can be accounted for by the tendency of the particle structure to deform the nuclear surface.

3) The occurrence of nuclear gamma transitions of electric quadrupole type with lifetimes about a hundred times shorter than single-particle estimates (GOLDHABER and SUNYAR, 1951). The existence of collective transitions with such short lifetimes is a characteristic feature of the excitation spectra of strongly deformed nuclei (BOHR and MOTTELSON, 1953).

One is thus led to describe the nucleus as a shell structure capable of performing oscillations in shape and size. These collective oscillations involve variations of the nuclear field and are therefore strongly coupled to the particle motion. The general dynamics of such a coupled system of individual particle motion and collective oscillations has previously been considered*, **. The system exhibits many analogies to molecular structures with the interplay between electronic and nuclear motion.

In the present paper, we consider the further development of such a unified nuclear model incorporating collective and individual-particle features, and pursue its consequences, especially for the nuclear properties pertaining to the ground state and the low energy region of excitation. The available empirical evidence is analyzed in an attempt to ascertain to what extent a comprehensive interpretation is possible on the basis of such a description of the nucleus.

* A. BOHR (1951, 1952). In the following, we refer to sections and equations of the latter paper as (A. § V. 4), (A 39), etc.

** Such a unified description of nuclear structure has also been discussed by HILL and WHEELER (1953) ("the collective nuclear model").

In Chapter II, the formulation of the coupled particle-collective model and its general dynamical features are considered. The subsequent three chapters discuss the properties of nuclear ground states (spins, magnetic moments, and quadrupole moments) which yield information on the nuclear coupling scheme. Chapter VI treats the level structure of the low energy region, resulting from the interplay of the particle and collective types of excitation. Important evidence on the interpretation of nuclear excitations is afforded by the analysis of gamma and beta transitions (Chapters VII and VIII). A summary of main conclusions is given in Chapter IX.

Some details, mostly of a mathematical nature, are deferred to appendices (Ap. I—IV). In Appendix V, a description of nuclear reactions is formulated, which embodies features of single-particle scattering as well as the formation of the compound nucleus, and which assumes the same couplings as those operating in the low energy phenomena. In Appendix VI, a discussion is given of the excitation of nuclei by the electrostatic field of an incident particle, which should be a valuable tool, especially in the study of collective types of excitation.

The present investigation has been carried out at the Institute for Theoretical Physics of the Copenhagen University*, and we have greatly benefited from numerous discussions with members and guests of the Institute, as well as with members of the Theoretical Study Group of CERN (European Council of Nuclear Research), which for the last year has been assembled at the Institute. Especially, we are indebted to Professor NIELS BOHR for his continued interest in this work and for many enlightening discussions on the combination of the evidence on nuclear collective and individual-particle motion in a consistent description of nuclear dynamics. We would also like to acknowledge our many stimulating contacts over a period of years with Professors V. F. WEISSKOPF and J. A. WHEELER, who have given valuable comments on many problems of nuclear structure.

* One of us (B.R.M.) wishes to acknowledge the grant of an A.E.C. postdoctoral fellowship, held during the years 1951—53.

II. The Coupled System of Particles and Collective Oscillations.

a) Formulation of the Model.

i. *Collective coordinates.*

The nuclear collective properties may be described by a set of coordinates α characterizing the spatial distribution of the nucleon density which, in turn, defines the nuclear field. Such collective coordinates are symmetric functions of the individual nucleon coordinates.

For a system with a small compressibility, the collective degrees of freedom which have the lowest energies are associated with deformations in shape with approximate preservation of volume. Assuming the system to have a sharp surface, the normal coordinates of these oscillations would be the expansion parameters $\alpha_{\lambda\mu}$ of the nuclear surface defined by (cf., e. g., (A. 1))

$$R(\vartheta, \varphi) = R_0 \left[1 + \sum_{\lambda\mu} \alpha_{\lambda\mu} Y_{\lambda\mu}(\vartheta, \varphi)\right], \tag{II.1}$$

where R_0 is the equilibrium radius, and $Y_{\lambda\mu}$ the normalized spherical harmonic, of order λ, μ. Such surface oscillations are associated with a collective flow with the same velocity field as for the oscillations of an incompressible classical liquid drop (cf., e. g., (A.31)). This leads to the expression

$$\alpha_{\lambda\mu} = \frac{4\pi}{3A} \sum_{p=1}^{A} \left(\frac{r_p}{R_0}\right)^{\lambda} Y^*_{\lambda\mu}(\vartheta_p, \varphi_p) \tag{II.2}$$

for the collective parameters in terms of the polar coordinates $(r_p, \vartheta_p, \varphi_p)$ of the individual particles.

The nuclear compressibility* implies a non-constant radial

* For estimates of the nuclear compressibility, cf. FEENBERG (1947) and SWIATECKI (1951).

density distribution, and the proper modes can no longer be characterized as pure surface oscillations, but are also accompanied by density changes in the nucleus. The degrees of freedom associated with the compressibility imply that, for a given angular dependence, there is a set of normal oscillations with different radial density variations. The lowest among these has no radial nodes and corresponds, in the limit of vanishing compressibility, to the surface oscillations. This mode is in general the most important for the low energy nuclear properties; its coordinates will be of the form (2)* with some modification of the radial function resulting from the compressibility.

For a small compressibility, one can obtain corrections to the proper oscillations by considering only first order terms in the deviation from a uniform density distribution (FLÜGGE and WOESTE, 1952; WOESTE, 1952). In the case of an essentially non-uniform radial equilibrium distribution, major modifications in the collective properties may be expected.

The existence of two kinds of nucleons implies additional types of oscillations in which neutrons and protons move with respect to each other (GOLDHABER and TELLER, 1948; STEINWEDEL and JENSEN, 1950). These oscillations are of special interest for the nuclear photo-effect but, because of their large frequencies, are in general of lesser importance for the low energy phenomena.

The types of collective motion considered correspond to an irrotational flow of nuclear matter, which is the collective response to variations in the nuclear field. Vorticity effects are already contained in the description of the particle structure for a fixed field and do not occur as collective phenomena provided the independent-particle approximation is adequate to describe this structure. It is also seen that vortex motion cannot be described in terms of parameters, such as the $\alpha_{\lambda\mu}$, which are symmetric functions of the particle coordinates and thus, due to the exclusion principle, cannot in a simple way be separated from the state of the particle structure.**

* A single number refers to an equation in the chapter in which the reference is made.

** For a discussion of the implications of the exclusion principle for the quantum rotations of a quasi-rigid system, cf. TELLER and WHEELER (1938).

ii. *Oscillations of a shell structure.*

The relationship of the particle and collective motion is especially simple if the frequencies ω_p for particle excitation are large compared with the frequencies ω_c of a collective type of motion. The nucleus can then be treated, in analogy to molecules, on the basis of the adiabatic approximation, and the appropriate wave function is of the type

$$\Psi_{n\nu}(x) = \Phi_\nu(\alpha)\,\psi_n(x, \alpha), \tag{II.3}$$

where x represents the coordinates, including spin variables, of all the particles in the nucleus. The wave function $\psi_n(x, \alpha)$, specified by a set of quantum numbers n, is the shell model wave function for a fixed field specified by the parameters α. The wave function $\Phi_\nu(\alpha)$ describes oscillations of the nucleus as a whole, characterized by additional quantum numbers, ν*.

In the approximation $\omega_p \gg \omega_c$ underlying (3), there corresponds to a state n of the particle structure a set of states with different quantum numbers ν, corresponding to a Hamiltonian of the form

$$H_c = T(\alpha) + E_n(\alpha), \tag{II.4}$$

where the potential energy $E_n(\alpha)$ is the energy of the particle structure n, calculated for fixed α. The existence of a collective kinetic energy T is contained in the implicit dependence of the wave function on x through α and may be obtained by writing the nucleon velocity as a sum of a velocity with respect to the nuclear field and a velocity of the collective flow. For small amplitudes of oscillation, T is a quadratic expression in the $\dot{\alpha}$.

If the particle structure prefers spherical symmetry, the deformation energy may be expanded around the equilibrium ($\alpha_{\lambda\mu} = 0$), and the surface Hamiltonian reduces to (cf. A.(2 and 3))

$$H_S = \sum_{\lambda\mu}{}' \left\{ \frac{1}{2} B_\lambda \left| \dot{\alpha}_{\lambda\mu} \right|^2 + \frac{1}{2} C_\lambda \left| \alpha_{\lambda\mu} \right|^2 \right\} \tag{II.5}$$

* A wave function describing the adiabatic oscillation of a shell structure has also been given by HILL and WHEELER (1953; eq. (5)), but this expression appears to differ essentially from (3) above. The procedure employed by these authors of incorporating the collective motion both through the exponential factor involving the velocity potential and in the oscillator function $h(\alpha)$ seems difficult to interpret; it appears that in the resultant wave function, obtained by integration over the α-variable, the function h does not directly represent the probability amplitude for a given deformation.

which represents a set of harmonic oscillators with frequencies

$$\omega_\lambda = \sqrt{\frac{C_\lambda}{B_\lambda}}. \tag{II.6}$$

The coefficient B_λ is associated with the mass transported by the collective flow and depends on the velocity field. For pure surface oscillations described by the coordinates (2), one obtains the classical hydrodynamical expression (cf., e. g., (A. 4)),

$$B_\lambda = \frac{1}{\lambda}\frac{3}{4\pi} A M R_0^2, \tag{II.6a}$$

where M is the nucleon mass. The coefficient C_λ represents the nuclear deformability; one may attempt to estimate C_λ from the empirically determined surface energy and the assumption of a uniform charge distribution. This leads to (cf., e. g., (A. 5))

$$C_\lambda = (\lambda-1)(\lambda+2) R_0^2 S - \frac{3}{2\pi}\frac{\lambda-1}{2\lambda+1}\frac{Z^2 e^2}{R_0} \tag{II.6b}$$

where S is the surface tension and Ze the nuclear charge. The analysis of nuclear binding energies leads to the estimate $4\pi R_0^2 S = 15.4\ A^{2/3}$ MeV (cf. ROSENFELD, 1948, p. 24).

While the form of (5) has a rather general validity, it must be stressed that the analogy with the hydrodynamics of a classical liquid drop is of limited scope, and characteristic effects of the quantum structure of the nucleus are to be expected. Thus, the deformability will depend on the particle state in question* and the value of C_λ will be especially large for closed-shell nuclei which owe their particular stability to their spherical form.** The nuclear compressibility may also have an important effect on the value of B_λ and on the relation (2) between $\alpha_{\lambda\mu}$ and the multipole moments.

When, in the following, we often make numerical estimates on the basis of the hydrodynamic approximation (2, 6a and 6b), it will be in order to gain a first orientation and to have a convenient reference with which to compare the evidence on the

* Features of the deformability of a quantum shell structure have been discussed by GALLONE and SALVETTI (1953) and by HILL and WHEELER (1953). Some comments on this problem from the point of view of the present formulation are given in Appendix I.

** We are indebted to Dr. W. J. SWIATECKI for valuable suggestions concerning this point.

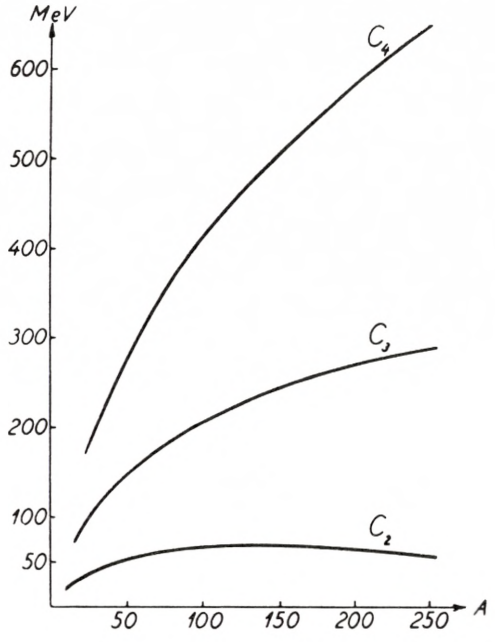

Fig. 1.

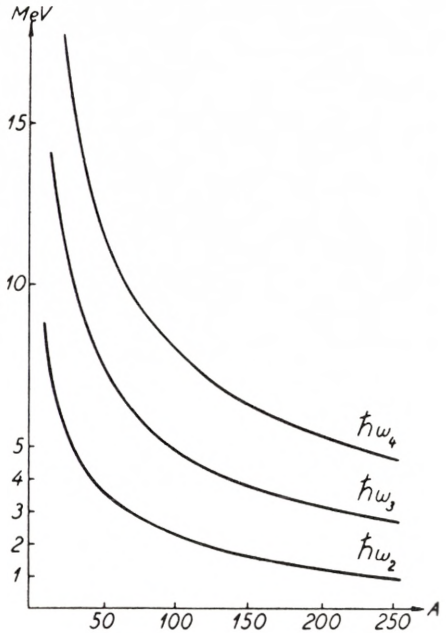

Fig. 2.

Fig. 1. *Nuclear deformability in the hydrodynamic approximation.* The deformability coefficients C_λ of the first three proper modes of the surface (cf. (5); $\lambda = 2$, 3, and 4) are plotted as a function of the atomic number A. The nuclear deformation energy is assumed to arise from a surface tension estimated from empirical binding energies and from the influence of a uniformly distributed electric charge (cf. (6b)).

Fig. 2. *Frequencies of surface oscillations in the hydrodynamic approximation.* The phonon energies $\hbar\omega_\lambda$ of the first three proper modes of the surface (cf. (6)) are plotted as a function of the atomic number A. The deformabilities C_λ of Fig. 1 are used, and the mass parameters B_λ are taken from (6a) which assumes a velocity field of the type associated with surface oscillations of an incompressible fluid.

nuclear collective properties deduced from empirical data. In Figs. 1 and 2 are plotted the hydrodynamical values of C_λ and of the phonon energies $\hbar\omega_\lambda$ for an assumed nuclear radius of

$$R_0 = 1.44 \times A^{1/3}\, 10^{-13} \text{ cm}. \tag{II.7}$$

iii. *Coupling to particle motion.*

The simple separation between collective and particle types of excitations, corresponding to stationary states of the type (3), is no longer possible if the particles possess modes of excitation

with frequencies smaller than, or comparable with, the collective frequencies. The particle structure may then be non-adiabatically excited by the collective oscillations, and the nucleus must be described in terms of a coupled system of collective and particle degrees of freedom.

The particle degrees of freedom represent the low frequency modes of excitation of the particle structure, associated with the particles in the last filled levels. The bulk of the nucleons, whose energies are well below the maximum for the occupied levels, manifest themselves at moderate nuclear excitations only through the collective properties of the nucleus.

For the coupled system of surface oscillators, with coordinates $\alpha_{\lambda\mu}$, and particle degrees of freedom, with appropriate coordinates x, the Hamiltonian may be written in the form

$$H = H_S(\alpha_{\lambda\mu}) + H_p(x) + H_{\text{int}}(x, \alpha_{\lambda\mu}), \tag{II.8}$$

where H_S is given by (5) and H_p represents the particle energy for a spherical nucleus. The coupling term H_{int} gives the energy dependence of the particles on the surface deformation.*, **

Expanding H_{int} in powers of $\alpha_{\lambda\mu}$ we get for the first term

$$H_{\text{int}} = -\sum_p k(r_p) \sum_{\lambda\mu} \alpha_{\lambda\mu} Y_{\lambda\mu}(\vartheta_p, \varphi_p), \tag{II.9}$$

where the sum p extends over the particles included in H_p.*** The assumption of a sharp nuclear boundary implies that $k(r_p)$ has the form of a delta function at the surface with matrix elements given by (cf. FEENBERG and HAMMACK, 1951)

$$< nl \,|\, k(r_p) \,|\, n'l' > = V_0 R_0^3 \Re_{nl}(R_0)\, \Re_{n'l'}(R_0), \tag{II.10}$$

where n and l label the radial and orbital angular momentum quantum numbers of the particle with radial wave function $\Re_{nl}$.

* The existence of an important coupling between particle motion and the nuclear deformation, associated with the centrifugal pressure exerted by the particle on the surface, was first recognized by RAINWATER (1950).

** It is interesting to note that a somewhat similar effect has been discussed for the atomic spectra where a small level shift for non-penetrating orbits has been ascribed to a polarization of the atomic core (BORN and HEISENBERG, 1924; cf. also DOUGLAS, 1953).

*** There may also be a contribution to H_{int} from the spin orbit force, but its dependence on $\alpha_{\lambda\mu}$ is more ambiguous (PFIRSCH, 1952; DAVIDSON and FEENBERG, 1953).

The nuclear potential is denoted by V_0. For binding energies in the region 5—10 MeV, the matrix elements of k are approximately independent of n and l and are of the order of 40 MeV, assuming a kinetic energy inside the nucleus of 25 MeV. In the following, we therefore treat k as a constant. If particles are replaced by holes in a closed-shell structure, the sign of k is reversed.

In the following paragraphs, we shall discuss some approximate solutions for the nuclear Hamiltonian (8) for various types of particle configurations. For most physical problems involving low nuclear excitations, the collective motion associated with surface deformations of quadrupole type ($\lambda = 2$) are of primary importance. We especially consider the effect of these deformations and usually drop the index λ.

The coupled system of particles, obeying Fermi statistics, and surface oscillators, which are equivalent to a Boson field, is in many respects analogous to the dynamical system considered, for instance, in electromagnetic theory. The coupling term (9) is of a similar form as in the electrodynamic system, with the coupling constant k playing the role of the charge e. Thus, many effects characteristic of field theories, such as the influence of the field on the motion of a particle in an external potential (Lamb-Retherford effect), the interaction of particles through the intermediate field, etc., have their counterpart in the unified nuclear model. The formal analogies also imply that many methods of solution are common to the two systems.

b) Coupling of Single Particle to Nuclear Surface.

An especially simple case of the coupled system occurs when the particle configuration can be described in terms of a single particle outside of a fairly stable structure of spherical symmetry. In this paragraph, we consider methods of treating this system, appropriate to different strengths of the coupling.

i. *Perturbation approximation.*

For sufficiently weak coupling, the motions of the particle and the surface are approximately independent. The state of the

particle is then characterized by the same quantum numbers as in the shell model. The surface oscillations* are described by the number of phonons, N, each having an angular momentum of two units, the total angular momentum of the surface R, and its z-component m_R. In general, two additional quantum numbers are required to specify completely the state of the surface, but, for small values of $N (N \leq 3)$, the above quantum numbers are sufficient.

The effect of the coupling implies a certain interweaving of particle and surface motion, which for weak coupling is conveniently treated by expanding the wave function in the representation of uncoupled motion**, ***

$$\Psi = |> = \sum_{jNR} |j;\ NR;\ IM> <j;\ NR;\ IM|>, \qquad \text{(II.11)}$$

where j stands for the particle quantum numbers, while the total nuclear angular momentum and its z-component are denoted by I and M.

In the absence of coupling, the ground state is given by $|j;\ 00;\ I = j,\ M>$ and, to first order, H_{int}, which is linear in α_μ (cf. (9)), only introduces the states $|j';\ 12;\ I, M>$, where the particle state j' has the same parity as the state j and differs by at most two units in the total angular momentum. The relevant matrix element for the creation of the one-phonon state is obtained from (9) and (A. § III.1), and is given by

$$\left.\begin{aligned} &<j;\ 00;\ I = j, M \,|\, H_{\text{int}} \,|\, j';\ 12;\ I, M> \\ &\qquad = -k \sqrt{\frac{\hbar\omega}{2C}} <j \,|\, h \,|\, j'> \end{aligned}\right\} \qquad \text{(II.12)}$$

in terms of the coupling constant k, and the surface frequency ω and deformability C. The coefficients $<j \,|\, h \,|\, j'>$ can be expressed in terms of Racah coefficients and are given in Appendix II.

These matrix elements determine to first order the nuclear

* The quantization of free surface waves has been discussed by Nogami (1948), A. Bohr (1952), and Jekeli (1952).

** The coupling between particle motion and surface oscillations has been considered in such a phonon representation by Foldy and Milford (1950).

*** We use the bracket notation of Dirac (1947). The proper vectors are given by $|\ j;\ NR;\ IM>$, while the expansion coefficients are $<j;\ NR;\ IM\,|>$.

wave function from which the various nuclear properties can be obtained. Thus, the coupling leads to a sharing of angular momentum between the particle and the surface, which is reflected in a reduction of the expectation value of j_z. If j remains a constant of the motion, we get

$$<j_z> = \left(1 - \frac{15}{128\,\pi}\,\frac{(2j-1)(2j+3)}{j^2(j+1)^2}\,\frac{k^2}{\hbar\omega C}\right) M. \qquad \text{(II.13)}$$

The more general case in which particle states having a different angular momentum are admixed is considered in Appendix II.

For the following, it will be convenient to introduce the dimensionless parameter

$$x = \sqrt{\frac{5}{16\,\pi}}\,\frac{1}{\sqrt{j}}\,\frac{k}{\sqrt{\hbar\omega C}} \qquad \text{(II.14)}$$

as a measure of the strength of the coupling. From (13) one sees that the validity of the perturbation approximation is essentially determined by the smallness of x. The relevant parameter for the perturbation expansion is actually $x\sqrt{j}$, which represents the order of magnitude of the amplitude of the one-phonon state.

ii. *Strong coupling approximation.*

For $x\sqrt{j} \gtrsim 1$, the perturbation treatment is no longer valid, but for $x \gg 1$ one can obtain another type of approximate solution to the coupled system (A. § V.3).* For such strong couplings, the nuclear surface acquires a large deformation and, therefore, a certain stability in its spatial orientation. One then obtains an approximate solution by considering, first, the relatively fast motion of the particle with respect to the deformed nuclear surface and, subsequently, the relatively slow vibration and rotation of the entire system.**

* Apart from factors involving j, the parameter x corresponds to the ratio of total nuclear deformation to zero point oscillation amplitude used in A to characterize the strength of the coupling (cf., e. g., (II. 22)).

** This solution of the coupled nuclear system is in some respects similar to the strong coupling treatment of the nucleon-meson coupling, the $\vec{j}$ of the particle playing the role of the nucleon spin, or isotopic spin (cf., e. g., Tomonaga, 1946). The nucleon isobars are the analogue of the nuclear rotational states.

The surface will in general acquire an axially symmetric shape under the influence of the centrifugal pressure exerted by the particle. The resulting nuclear coupling scheme (A. Bohr, 1951), illustrated in Fig. 3, is thus analogous to that of linear molecules.

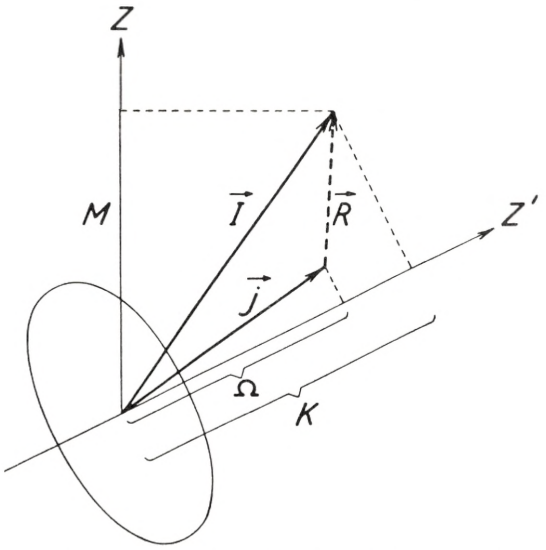

Fig. 3. *Coupling scheme for strong particle-surface interaction.* In strong coupling, the surface acquires an axially symmetric deformation. The angular momentum $\vec{j}$ of the particle precesses around the nuclear axis with a constant projection Ω. The total angular momentum $\vec{I}$ is the sum of $\vec{j}$ and the angular momentum $\vec{R}$ of the surface. The coupled system of particle and surface rotates like a symmetric top with quantum numbers I, K (projection of $\vec{I}$ on nuclear axis), and M (projection of $\vec{I}$ on space fixed axis).

The angular momentum vector $\vec{j}$ of the particle precesses rapidly around the nuclear symmetry axis z' with a constant projection Ω. The nuclear surface performs small vibrations, both with respect to magnitude and shape of the deformation. The rotational motion is like that of a symmetric top and is characterized by the three quantum numbers I, K, and M, representing the total nuclear angular momentum, its projection on the symmetry axis z' and on the fixed z-axis, respectively.

From the analysis which follows, one finds that the particle precession frequency is of order $x^2\omega$, while the vibrational frequencies are of order ω. The rotational frequencies about the

symmetry axis and an axis perpendicular to z' are of order ω and $x^{-2}\omega$, respectively. (Cf. also A. § V.3 and Appendix IV).

The strongly coupled system is conveniently described by introducing the Eulerian angles θ_i specifying a coordinate system fixed in the nucleus, and the two additional surface coordinates β and γ defining the nuclear shape (cf. A. § II.2). The total deformation parameter β is given by

$$\beta^2 = \sum_{\mu} |\alpha_\mu|^2, \tag{II.14a}$$

while γ is an angular coordinate characterizing the eccentricity of the nuclear shape. Thus, for $\gamma = 0$ and π, the deformation is symmetric about the z'-axis, and is of prolate and oblate shape, respectively (cf. A. Fig. 1).

The strong coupling wave function has the form (A. 118)

$$\left.\begin{aligned} &|\Omega;\ n_\beta n_\gamma;\ IKM> \\ &= \sqrt{\frac{2I+1}{16\pi^2}} \cdot \varphi_{n_\beta n_\gamma}(\beta, \gamma) \left\{ \chi_\Omega \mathfrak{D}^I_{MK}(\theta_i) + (-)^{I-j} \chi_{-\Omega} \mathfrak{D}^I_{M-K}(\theta_i) \right\} \end{aligned}\right\} \tag{II.15}$$

where χ_Ω describes the motion of the particle with respect to the deformed nucleus, while $\varphi_{n_\beta, n_\gamma}$ represents vibrations in β and γ characterized by the quantum numbers n_β and n_γ. Finally, the $\mathfrak{D}^I_{MK}$ are the proper functions for the symmetric top, and describe the nuclear rotations. The normalization is such that $\mathfrak{D}$ gives the unitary transformation from the fixed coordinate system to the nuclear coordinate system (cf. WIGNER, 1931). The simultaneous occurrence in (15) of both signs for Ω and K reflects the invariance of the surface with respect to a rotation of 180° about an axis perpendicular to z',* and is similar to the symmetrization of wave functions for homonuclear molecules (cf. HERZBERG, 1950, p. 128 ff.). The symmetrization ensures that the total parity of the strong coupling wave function equals the parity of the particle state. The sign of the symmetrization term in (15) depends on j, and if j is not a good quantum number, each part of χ must be symmetrized with the appropriate sign.

The wave function (15), apart from the symmetrization, is actually of the form (3), corresponding to the fact that the pre-

* Cf. A. § V.2 for a discussion of the symmetry requirements for the strong coupling wave function.

cession frequency of the particle is large compared to the collective frequencies of the system. This contrasts with the weak coupling situation where the degeneracy with respect to spatial orientation of $\vec{j}$ provides a very easily excitable degree of freedom. Thus, (11) is in general not of the type (3).

The sharing of angular momentum between particle and surface approaches a definite limit with the realization of the strong coupling scheme of Fig. 3. The expectation value of $\vec{j}$ is given by

$$<\vec{j}> = \frac{<\vec{j}\cdot\vec{I}>}{I(I+1)}<\vec{I}>, \tag{II.16}$$

and for $\vec{j}\cdot\vec{I}$ we may write

$$\vec{j}\cdot\vec{I} = j_1 I_1 + j_2 I_2 + j_3 I_3, \tag{II.17}$$

where the components of the two vectors refer to the coordinate system fixed in the nucleus. One thus finds, for the state (15),

$$<\vec{j}\cdot\vec{I}> = \Omega K + (-)^{I-j}\frac{1}{2}\left(j+\frac{1}{2}\right)\left(I+\frac{1}{2}\right)\delta_{\Omega,\frac{1}{2}}\,\delta_{K,\frac{1}{2}} \tag{II.18}$$

where the last term arises from the symmetrization and only contributes for $\Omega = K = \frac{1}{2}$ (cf. also DAVIDSON and FEENBERG, 1953). Therefore, from (16),

$$<j_z> = \frac{\Omega K M}{I(I+1)}\left\{1 + (-)^{I-j}\,2\left(j+\frac{1}{2}\right)\left(I+\frac{1}{2}\right)\delta_{\Omega,\frac{1}{2}}\,\delta_{K,\frac{1}{2}}\right\}. \tag{II.19}$$

For the ground state we have $I = K = \Omega$, except for $K = \Omega = \frac{1}{2}$ (cf. below), and thus

$$<j_z> = \frac{I}{I+1}M. \tag{II.20}$$

For each particle state Ω, we have a spectrum of vibrational and rotational states, as in the case of molecules (cf. (3)). The nuclear potential energy is a sum of the surface energy and of the particle energy as a function of the deformation and, if j is a good quantum number, is given by (cf. A. 77 and 98)

$$W_{\text{pot}}(\beta, \gamma) = \left. \begin{aligned} & \\ H_p + \frac{1}{2} C \beta^2 + \sqrt{\frac{5}{4\pi}} k \beta \cos \gamma \frac{1}{4j(j+1)} (3\Omega^2 - j(j+1)), \end{aligned} \right\} \quad \text{(II.21)}$$

where H_p is the particle energy for an undeformed nucleus.

It is seen from (21) that, for $j > 3/2$, the lowest minimum of W_{pot} and, therefore, the lowest state of the nucleus, occurs for $\Omega = j$ and a cylindrically symmetric equilibrium deformation with $\gamma = \pi$ (oblate shape). The equilibrium value of β is given by

$$\beta = \sqrt{\frac{5}{4\pi}} \frac{k}{C} \frac{2j-1}{4(j+1)} = x \sqrt{j} \frac{2j-1}{2(j+1)} \sqrt{\frac{\hbar\omega}{C}} \quad \text{(II.22)}$$

in terms of the coupling parameter x (cf. (14)).

The kinetic energy of the surface motion consists of a vibrational and a rotational part. For strong coupling, the dominant term is the vibrational energy (A. 48)

$$T_{\text{vib}} = -\frac{\hbar^2}{2B} \left\{ \frac{1}{\beta^4} \frac{\partial}{\partial \beta} \beta^4 \frac{\partial}{\partial \beta} + \frac{1}{\beta^2} \frac{1}{\sin 3\gamma} \frac{\partial}{\partial \gamma} \sin 3\gamma \frac{\partial}{\partial \gamma} \right\}. \quad \text{(II.23)}$$

The Hamiltonian obtained by adding (23) to (21) describes oscillations around the equilibrium positions of β and γ (cf. (4)). Since the zero point amplitude of β is of order $(\hbar\omega/C)^{1/2}$, which is small compared to (22) for $x > 1$, one obtains approximately independent harmonic oscillations in the β and γ variables with states labeled by n_β, n_γ.

The rotational energy can be expressed in terms of the angular momentum quantum numbers, and is given by*

$$W_{\text{rot}} = \left. \begin{aligned} & \frac{\hbar^2}{2\Im_3} (K-\Omega)^2 + \left(\frac{\hbar^2}{4\Im_1} + \frac{\hbar^2}{4\Im_2} \right) \left\{ I(I+1) - K^2 \right. \\ & \left. + j(j+1) - \Omega^2 - (-)^{I-j} \left(j + \frac{1}{2} \right) \left(I + \frac{1}{2} \right) \delta_{\Omega, \frac{1}{2}} \delta_{K, \frac{1}{2}} \right\} \end{aligned} \right\} \quad \text{(II.24)}$$

where the moments of inertia are given by (A. 27)

$$\Im_\varkappa = 4B\beta^2 \sin^2 \left(\gamma - \varkappa \frac{2\pi}{3} \right) \qquad \varkappa = 1, 2, 3. \quad \text{(II.25)}$$

* Cf. (A. 98); the last term in (24) arises from U_1 (cf. A. 96) which contributes a diagonal term in the special case of $\Omega = K = 1/2$ (cf. also DAVIDSON and FEENBERG, 1953).

For $\Omega = j$, the lowest rotational state occurs, according to (24), for $I = K = \Omega = j$.

The case of $j = 3/2$ requires special consideration, since the last term in (21) has the same value for $\Omega = 3/2$ and $\gamma = \pi$ as for $\Omega = 1/2$ and $\gamma = 0$. In this case, the potential surface has no pronounced minimum in γ, which has the consequence that there is no exact limiting solution of the type (15). The strong coupling wave function has then a somewhat more complex form and requires the solution of a set of coupled differential equations. Still, it can be shown that the ground state is always $I = 3/2$ (cf. Appendix III.ii).

For $j = 1/2$ there is no coupling between particle and surface. Actually, in this case, the strong coupling wave function (15) reduces to the uncoupled wave function.

The Hamiltonian consisting of the three terms (21), (23), and (24) does not represent the total energy of the nucleus. There are additional terms (cf. A. 96) which are non-diagonal in the representation (15) and which cause the breakdown of the strong coupling solution for $x \lesssim 1$. An estimate of these perturbation terms provides a measure of the accuracy of the strong coupling solution and can be used to obtain correction terms when x has intermediate values (A. § V.4; FORD, 1953; cf. also Appendix III.ii).

The non-spherical character of the nuclear field implies that the j of the particle is not an exact constant of the motion. Major modifications in χ_Ω may occur if there are close-lying single-particle levels which are coupled by the surface. In such cases, χ_Ω may be considered as a superposition of particle states with different j, however all with the same Ω. The last term in the potential energy (21) is then to be replaced by (cf. (9) and (A.12))

$$W_{\text{coupl}} = -k\beta \cos\gamma Y_0(\vartheta'), \tag{II.26}$$

which is a non-diagonal matrix in the particle quantum numbers j whose elements are given in Appendix III.i. The coordinate ϑ' of the particle is referred to the nuclear z'-axis. The rotational energy remains of the form (24), which is diagonal in j.

The potential energy matrix must now be diagonalized and its proper values determined as a function of the deformation.

The minimum of the lowest potential energy surface corresponds to the ground state equilibrium and the ground state χ_Ω is determined as the proper vector of W at equilibrium.

Such effects are of importance in causing a partial decoupling of the particle $\vec{l}$ and $\vec{s}$ and also occur in regions where there are near-lying levels of the same parity (e. g. $s_{1/2}-d_{3/2}$; $p_{3/2}-f_{5/2}$). In the case of $j = 1/2$ states, the non-diagonal terms are of special interest in making possible a strong coupling to the surface. Calculations of this type are employed in particular in the Addendum to Chapters IV and V.

iii. *Intermediate coupling.*

The treatments of the coupled system discussed above apply in the limiting cases of weak and strong coupling. It is of interest, however, to follow the transition between the two coupling regions. This is of special importance for large j, since the perturbation approximation is valid for $x\sqrt{j} \ll 1$, while the strong coupling approximation demands $x \gg 1$. This gap between the regions of validity of the two solutions reflects the increasing number of phonons necessary to achieve the strong coupling situation for increasing j.

In the intermediate coupling region, one may employ the weak coupling representation (11), carrying the expansion sufficiently far to give an adequate representation of the nuclear state. The determination of the coefficients of the wave function requires the solution of the corresponding secular determinant.*

As an illustration of this procedure, the solution has been worked out for the case of $I = j = 3/2$, including all states with phonon number N up to 4. The expansion coefficients are plotted in Fig. 4 as a function of x.**

Further information about the intermediate coupling region can be obtained by considering the case of very large j for which one can obtain a semi-classical solution valid for all x. (Cf. Appendix IV). From this solution, one can calculate (Ap. IV.10)

* Cf. the non-adiabatic treatment of the meson-nucleon system discussed by TAMM (1945) and DANCOFF (1950).

** Note added in proof: The intermediate coupling treatment, based on the uncoupled representation, has been extended by D. C. CHOUDHURY (cf. forthcoming publication), who has studied level structures, as well as magnetic moments and quadrupole moments, for a number of configurations.

$$< j_z > = \left(1 - \frac{1}{I+1} \frac{x^2}{\sqrt{x^4 + 4/9}}\right) M \qquad \text{(II.27)}$$

correct to terms of order M/I. To this order, (27) coincides for small x with the perturbation result (13); for large x, the value of (27) equals the strong coupling result (20).

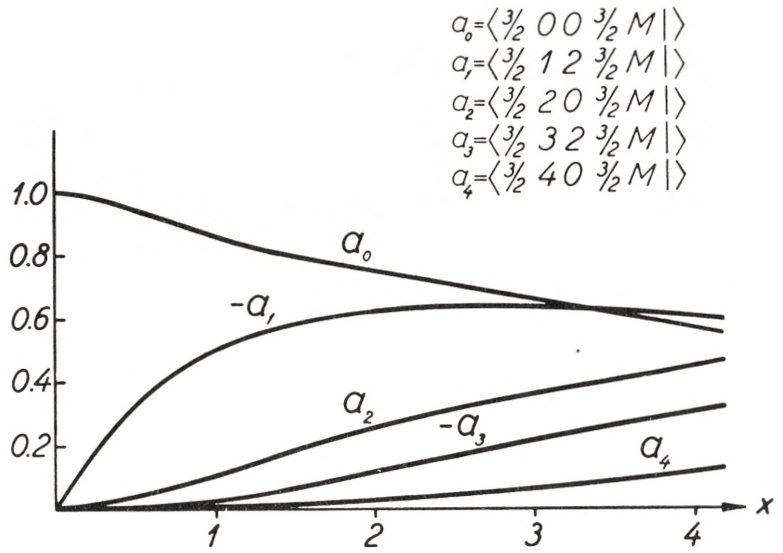

Fig. 4. *Wave function in intermediate coupling for* $I = j = 3/2$. The wave function for the ground state ($I = 3/2$) of the system consisting of a $j = 3/2$ particle coupled to the nuclear surface oscillations is expanded in the representation of uncoupled motion (11). The Hamiltonian is diagonalized including all states with up to four phonons, and the probability amplitudes are plotted as functions of the coupling parameter x (cf. (14)). In the particular case considered, only a single state occurs for each value of the phonon number.

The process of transfer of angular momentum to the surface, as a function of x, is illustrated in Fig. 5 for the various solutions considered in this chapter.

In the hydrodynamic approximation (cf. Figs. 1 and 2), one obtains from (14), assuming $k = 40$ MeV, a coupling strength of $x = 0.9\, j^{-1/2}$ for $A = 20$ increasing rather slowly with A to a value of $x = 1.4\, j^{-1/2}$ for $A = 200$. From Fig. 5 one sees that this would correspond to an intermediate region in which neither the perturbation nor the strong coupling approximation would be very reliable.* Besides the contribution of H_{int} that is diagonal

* Similar conclusions have been drawn (Davidson and Feenberg, 1953;

in j, there is also in general a contribution to the coupling energy from the interaction between states of different j. In some cases, this latter coupling may considerably increase the effective value of x.

For a single particle moving with respect to a closed-shell core of great stability, the expected large value of C, as compared with the hydrodynamic estimate (cf. § II a.ii and Ap. I), may

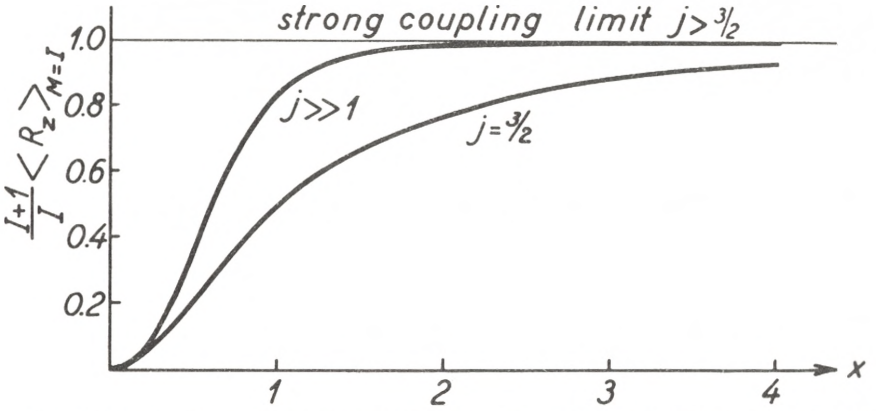

Fig. 5. *Sharing of angular momentum between particle and surface motion.* The particle-surface coupling implies a transfer of angular momentum from the particle motion to the surface oscillators, which, in the limit of strong coupling, approaches the value (20) for $j > 3/2$. For $j = 3/2$, the limiting ordinate in the figure is somewhat in excess of unity (cf. Ap. III.8). The gradual transfer of angular momentum as a function of the coupling parameter x (14) is shown for the case of $j = 3/2$ (obtained from Fig. 4) and $j \gg 1$ (cf. (27) and Ap. IV).

lead to a considerable reduction in the value of x. In such a situation, the particle-surface coupling may have only a minor effect on the properties of the system.

c) Many-Particle Configurations.

In the case of configurations involving several particles, the coupled system can be treated by methods similar to those discussed in the previous paragraph. While the surface coupling effects considered there may be described as nucleon self-energy

Ford, 1953) from a comparison of the proper values of the strong coupling Hamiltonian with those of the uncoupled system. In the procedure employed, however, corrections to the vibrational energy (A. 108 and 113) of the same order as the rotational energies have been neglected. If these are included, the comparison is somewhat more favourable to the strong coupling solution.

effects arising from the coupling to the phonon field, this coupling also produces mutual interactions between particles.

An additional feature which may affect the coupling scheme arises from the nuclear forces acting between the particles. The resultant coupling scheme will in general depend on a competition between the two effects. We first consider the surface coupling in the absence of direct forces between the particles.

i. *Weak surface coupling.*

For sufficiently weak coupling, one can employ the usual perturbation procedure of field theory to obtain effective two-particle interactions, resulting from the surface coupling. These interactions remove the degeneracy of many-particle configurations and may thus be important in determining the ground state spin.

If j_1 and j_2 of the particles are constants of motion, one may use a simplified form of H_{int} in terms of the operators $\vec{j}_1$ and $\vec{j}_2$ (A. 76, 77, 78), and one finds the two-body potential

$$\left.\begin{aligned} V(1,2) = -\frac{5}{64\pi}\frac{k^2}{C}\frac{1}{j_1(j_1+1)\,j_2(j_2+1)}\,[6(\vec{j}_1\vec{j}_2)^2 \\ +3(\vec{j}_1\vec{j}_2)-2j_1(j_1+1)\,j_2(j_2+1)]\,. \end{aligned}\right\} \quad \text{(II.28)}$$

More general expressions may be derived if the surface introduces states with other j values. The interaction (28) is of the type well known from quadrupole couplings in atoms and molecules and is attractive if the two particles have parallel or antiparallel angular momenta and repulsive for perpendicular orientations. Since the coupling constant for a hole has opposite sign to that for a particle, two holes interact as given by (28), while a particle and a hole have an interaction with opposite sign.

ii. *Strong surface coupling.*

For increasing coupling strengths, one obtains more complicated two-body interactions in addition to many-particle interactions. However, for strong coupling, the surface effect again becomes simple if viewed in the appropriate coordinate system. Under the combined action of the particles, the surface in general

acquires an equilibrium deformation of cylindrically symmetric character*; and, relatively to the deformed nucleus, the particles move independently of each other as long as the direct nuclear forces can be neglected.**

The wave function is of the type (15), where the particle state χ_Ω now stands for an appropriately antisymmetrized product of individual particle wave functions, each characterized by a quantum number Ω_p. The total Ω equals the sum of the individual Ω_p (cf. Fig. 6a). The symmetrization of the wave function follows the same lines as (15), except that the exponent j in the phase of the symmetrization term is replaced by $\sum_p j_p$.

Corresponding to (21) and (26), the potential energy is given by

$$W_{\text{pot}}(\beta, \gamma) = \sum_p H_p + \frac{1}{2} C \beta^2 - \beta \cos \gamma \sum_p k_p Y_0(\vartheta'_p). \qquad \text{(II.29)}$$

If not only the Ω_p, but also the j_p, are good quantum numbers, simpler interaction terms of the type used in (21) replace the last term in (29).

We first consider a group of n equivalent particles with a definite j. If n is smaller than half the number of states in the shell, the equilibrium shape of the nucleus has $\gamma = \pi$. The part-

* In special cases, an asymmetric equilibrium deformation may be favoured, or the potential energy surface may have no pronounced minimum in γ. The quantities Ω_p and K are then no longer constants of the motion, and a more complex rotational spectrum arises (cf. the case of asymmetric molecules; cf. also Ap. III.ii).

** The strong coupling solution for many-particle configurations has also been considered by FORD (1953).

Fig. 6. *Coupling schemes for many-particle configurations.* In many-particle configurations, the coupling scheme results from a competition between surface coupling and particle forces. Two extreme cases are shown.

a) Surface coupling dominates over particle forces. The particles move independently of each other in the deformed nucleus, each having a constant component Ω_p of angular momentum along the symmetry axis. The total Ω equals $\sum_p \Omega_p$ and the nuclear ground state has $I = K = \Omega$. The figure illustrates the coupling scheme for a $(j)^3$ configuration. The three lowest particle states have $\Omega_p = j, -j, j-1$, leading to $I = \Omega = j - 1$.

b) Particle forces dominate over surface coupling. The particles are coupled to a resultant $\vec{J}$ which is then coupled to the surface as a single particle (cf. Fig. 3). The figure refers to a $(j)^3$ configuration, where the particle forces in general favour the state $J = j$ (cf. p. 34). The resultant ground state has $I = \Omega = J = j$.

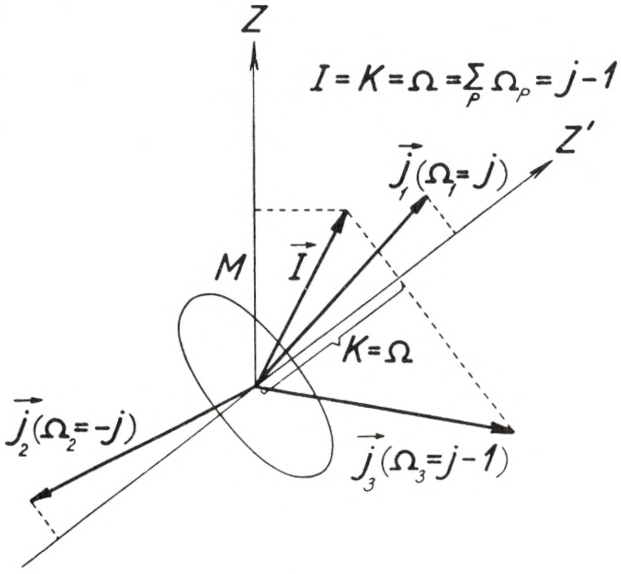
Z
$I = K = \Omega = \sum_p \Omega_p = j-1$
Z'
$\vec{j}_1(\Omega_1 = j)$
M
$\vec{I}$
$K = \Omega$
$\vec{j}_2(\Omega_2 = -j)$
$\vec{j}_3(\Omega_3 = j-1)$

Fig. 6 a.

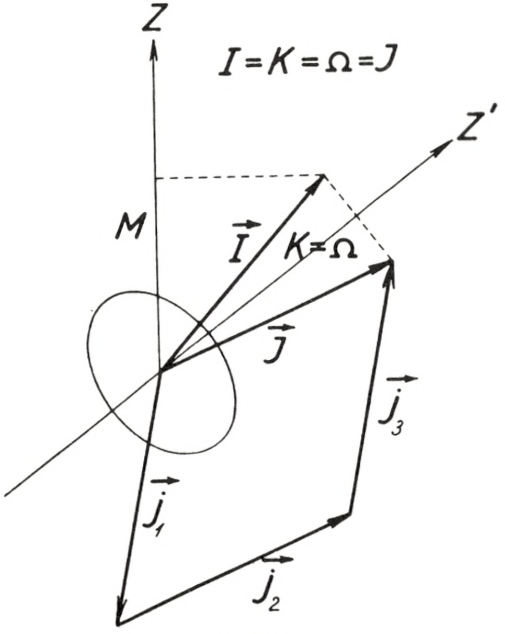
Z
$I = K = \Omega = J$
Z'
M
$\vec{I}$
$K = \Omega$
$\vec{J}$
$\vec{j}_3$
$\vec{j}_1$
$\vec{j}_2$

Fig. 6 b.

icles fill pairwise in states of opposite Ω_p; for n even, the ground state has $\Omega = 0$, while, for n odd, we get $\Omega = j - 1/2$ $(n-1)$. If n is greater than $j + 1/2$, it is more convenient to consider the holes in the shell. The preferred shape now has $\gamma = 0$, and one gets the same rules for Ω of the ground state if n is replaced by the number of holes. In the special case of a half filled shell, the nucleus spends equal time around the positions $\gamma = 0$ and $\gamma = \pi$. For nuclei of this type, the total Hamiltonian is invariant with respect to a replacement of particles by holes together with the substitution $k \to -k$ or $\gamma \to \gamma + \pi$ (self charge conjugate configurations).

If we have two groups a and b of equivalent particles, there is again in general a definite preference for either $\gamma = 0$ or $\gamma = \pi$. For an even group, the states are occupied pairwise with a resultant $\Omega_a = 0$, while an odd group contributes a finite Ω_a. If both groups are odd, the energy (29) is degenerate, corresponding to $\Omega = |\Omega_a \pm \Omega_b|$. In special cases, such as when one group is obtained from the other by replacing particles by holes, the positions $\gamma = 0$ and $\gamma = \pi$ may be equally preferred and the Hamiltonian possesses the same symmetry as discussed above.

The rotational contribution to W has the form

$$\left.\begin{aligned} W_{\text{rot}} = \frac{\hbar^2}{2\,\Im_3}(K-\Omega)^2 + \left(\frac{\hbar^2}{4\,\Im_1} + \frac{\hbar^2}{4\,\Im_2}\right)[I(I+1) - K^2 \\ + D\vec{J}^2 - \Omega^2 - 2D(J_1 I_1 + J_2 I_2)], \end{aligned}\right\} \quad \text{(II.30)}$$

where $\vec{J} = \sum_p \vec{j}_p$ and where the operator D picks out the part which is diagonal in the strong coupling representation (cf. FORD, 1953). The last term in (30) contributes only for configurations with $\Omega = K = 1/2$ and if equivalent particles are filled pairwise with opposite Ω_p; the term is then equal to the last term of (24) for the remaining odd particle. Apart from this special case of $\Omega = 1/2$ the nuclear ground state has $I = K = \Omega$.

In odd-odd nuclei, there are, as mentioned above, two families of states with $\Omega = |\Omega_a \pm \Omega_b|$, whose energies are degenerate in first order. This degeneracy is removed by the rotational terms (30), and the ground state has $I = K = \Omega = |\Omega_a - \Omega_b|$ in the limit of strong coupling.

The validity of the strong coupling approximation depends on the magnitude of the total deformation, as compared with the zero point oscillations. Since the particles act coherently in producing the deformation, the effective coupling increases with the addition of particles until the next closed-shell configuration is approached. Thus, for two equivalent particles, the relevant parameter measuring the strength of the coupling is $2x$ rather than x. The hydrodynamic estimate of the coupling strength for a single particle, given on p. 25, therefore implies a rather fully developed strong coupling situation in regions removed from closed shells.*

iii. *Influence of particle forces.*

The influence of nuclear two-body forces, with the neglect of surface coupling, has been considered for the (*jj*) coupling scheme along lines similar to those employed in atomic spectra (MAYER, 1950a; KURATH, 1950, 1952, 1953; FLOWERS, 1952, 1952a, 1952b; EDMONDS and FLOWERS, 1952, 1952a; TALMI, 1952; HITCHCOCK, 1952, 1952a; RACAH and TALMI, 1952). The choice of the forces is somewhat uncertain, since the present knowledge of the nuclear two-body system only partially defines the interaction. Moreover, the problem of nuclear saturation as well as the existence of shell regularities has raised the question whether these forces are appropriate to the description of interactions of nucleons in nuclei (cf., e. g., WEISSKOPF, 1952). The analysis of coupling schemes for nuclear many-particle configurations may provide evidence on these important questions.

The competition between the particle forces and the surface interactions determines the resultant nuclear coupling scheme. If the forces are weak compared to the coupling of the individual particles to the nuclear axis of deformation, the coupling scheme is that discussed in § II c.ii and illustrated by Fig. 6a. The effect of the particle forces is then to contribute a small energy shift which depends on the Ω_p quantum numbers. Such effects may be significant if there are near-lying states of different Ω, such as in odd-odd nuclei.

* Numerical examples illustrating the improvement of the strong coupling approximation for several particles have been given by FORD (1953) (cf. also the footnote on p. 25—26).

With increasing strength, the particle forces tend to destroy the above type of strong coupling solution by introducing non-diagonal terms in the Ω_p and, if the particle forces and the surface coupling are comparable, a rather complex situation may arise. For very strong forces, the particle structure is coupled to a resultant angular momentum $\vec{J}$. This vector is then coupled to the surface in the same manner as a single particle (cf. Fig. 6b) with an effective coupling constant (cf. Table VIII)

$$k_J = \frac{2(J+1)}{2J-1} \sum_p k_p < 3\cos^2\vartheta_p - 1 >_{J_z = J}. \qquad \text{(II.31)}$$

In this case, the nuclear ground state spin $I = J$ is determined by the particle forces.

A simple comparison of the strength of the surface coupling relative to that of the particle forces is obtained by considering that the former results from the interaction of the nucleons with the total displaced matter of the nuclear deformation. While the particle forces may play an important role in light nuclei, the surface coupling should thus become increasingly dominant in heavier nuclei and especially for the large deformations encountered in regions removed from closed shells.

III. Ground State Spins.

The interpretation of ground state spins and parities is most unambiguous in regions with large separations between neighbouring single-particle levels, where the lowest particle configuration can be uniquely assigned. The ordering of levels within this configuration is determined by the forces acting between the particles and by their coupling to the surface (cf. § IIc), and the observed ground state spin may give evidence on the resulting coupling scheme. The parity follows directly from the configuration.

In regions with close-lying particle levels, the lowest state of the system may be affected by relatively small shifts in the configuration energies, arising from surface or particle interactions,* as well as by configuration mixings produced by these interactions.

In the present chapter, we restrict ourselves to the problem of the lowest state for a given configuration. Some aspects of the configuration interactions are considered in connection with magnetic moments (cf. Addendum to Chapters IV and V) and level structures (§ VIb).

i. *Single-particle configurations.*

For a single-particle configuration, it follows from the considerations in § IIb that, for the lowest state, I equals j of the particle, irrespective of the strength of the surface coupling. Indeed, for this important class of nuclei, the observed spins and parities are successfully accounted for by the strong spin orbit coupling shell model (MAYER, 1950; HAXEL, JENSEN and SUESS, 1950).

* Cf., e. g., the shell model pairing energy (MAYER, 1950a).

ii. *Configurations of two equivalent particles. Even structures.*

The calculations based on the assumption of attractive two-body forces have shown that such forces will couple two equivalent particles to a ground state of spin zero (MAYER, 1950a; FLOWERS, 1952b; EDMONDS and FLOWERS, 1952a; RACAH and TALMI, 1952).

The same result is obtained for the influence of the surface coupling. In weak coupling, this effect may be considered in terms of equivalent two-body interactions given by (II.28), which favour the state $I = 0$. In strong coupling, the particles fill pairwise in states of opposite Ω_p and the ground state has $I = K = \Omega = 0$.

Empirically, one has always found $I = 0$ for these configurations, but the rule is far more general, applying to all even-even nuclei. For configurations involving only protons or neutrons, this result can be obtained for short range attractive forces (MAYER, 1950a; FLOWERS, 1952b). It is apparent that the surface, in strong coupling, leads to $I = 0$ quite generally for even-even nuclei (cf. § II.ii).

Since, in the strong coupling picture, an even group of equivalent particles has no influence on the angular momentum properties of the nuclear ground state, aside from the tendency to favour prolate or oblate deformations, one has a certain basis for treating any odd-A nucleus in terms of the odd group of particles alone. Thus, if the odd group contains only a single particle (or hole) with an angular momentum j, one obtains the same ground state spin ($I = j$) as for a single-particle configuration (cf. § III.i). The observed spins of these nuclei have been found to be consistent with such a simplification of the model (MAYER, 1950; HAXEL, JENSEN and SUESS, 1950). The possibility exists, however, that the even group of particles produces a deformation of the opposite shape to that preferred by the odd group and thereby affects the ground state spin.

iii. *Configurations of three equivalent particles.*

Several calculations have been carried out to determine the ground state spin resulting from two-body forces acting in $(j)^{\pm 3}$ configurations (MAYER, 1950a; KURATH, 1950; TALMI, 1952;

Edmonds and Flowers, 1952a; Flowers, 1952a; Racah and Talmi, 1952). These calculations have shown that, for sufficiently short range attractive forces, one obtains $I = j$ for the ground state; when the range is no longer negligible compared to the nuclear radius, the ground state may have other spin values. The range at which cross-overs occur depends somewhat on the shape and exchange nature of the two-body potential.

For the $(5/2)^3$ and $(7/2)^3$ configurations, the state $I = j - 1$ will, for sufficiently long range forces, become the ground state, but the necessary range seems to be considerably in excess of that deduced from two-body data. For the $(9/2)^3$ configurations, a ground state of $I = 7/2$ not only requires an excessively long range, but also a rather implausible exchange nature of the potential.

Thus, it appears that, for forces consistent with the known properties of the two-body system, the state $I = j$ remains the ground state. It may be added that particle forces of sufficiently long range to produce cross-overs in the $(j)^3$ configurations would also strongly affect the predicted ground state spins of other configurations. In particular, high ground state spins may result for even-even nuclei, and the even group of particles no longer remains inert with respect to the spins of odd-A nuclei (Edmonds and Flowers, 1952a).

The effect of the surface coupling on the splitting of the $(j)^{\pm 3}$ configuration may be treated in weak and strong coupling. In the former case, the effective two-body interaction (II.28) can be shown to lead to a ground state spin of $I = j$ for $j = 5/2$, $7/2$, and $9/2$.

In strong coupling, however, three particles produce an oblate deformation and fill the three lowest levels $\Omega_p = j$, $-j$, $j - 1$, with a resultant $\Omega = j - 1$ and $I = K = \Omega = j - 1$ for the ground state (cf. Fig. 6a). For a $(j)^{-3}$ configuration, a prolate deformation results with the same angular momentum quantum numbers as for $(j)^3$. The special case of three $j = 5/2$ particles, which constitute a half filled shell, possesses the symmetry in γ discussed in § IIc.ii, aside from the stabilizing influence of an even non-closed configuration.

Evidence on the level order for $(j)^{\pm 3}$ configurations has been obtained from spectroscopic measurements of ground state spins

and from the analysis of nuclear disintegration schemes. The observed spin for the lowest state within these configurations is given in Table I which shows that the values $I = j$ and $I = j - 1$ occur about equally frequently.

TABLE I. Lowest spins of $(j)^{\pm 3}$ configurations.

Nucleus	Configuration	I_{lowest}
$_{10}Ne^{21}$	$(d_{5/2})^3$	3/2 *g*
$_{11}Na^{23}$	,,	3/2 *g*
$_{20}Ca^{43}$	$(f_{7/2})^3$	7/2 *g**
$_{23}V^{51}$	,,	7/2 *g*
$_{25}Mn^{55}$	$(f_{7/2})^{-3}$	5/2 *g*
$_{32}Ge^{75}$	$(g_{9/2})^3$	7/2 **
$_{34}Se^{77}$	,,	7/2
$_{36}Kr^{79}$	,,	7/2 *g*
$_{34}Se^{81}$	$(g_{9/2})^{-3}$	7/2
$_{36}Kr^{83}$	,,	9/2 *g*
$_{38}Sr^{85}$	,,	9/2 *g*
$_{43}Tc^{95}$	$(g_{9/2})^3$	9/2 *g*
$_{43}Tc^{97}$	,,	9/2 *g*
$_{43}Tc^{99}$	,,	9/2 *g*
$_{47}Ag^{107}$	$(g_{9/2})^{-3}$	7/2
$_{47}Ag^{109}$	,,	7/2

The table includes available evidence on the spin of the lowest state in $(j)^{\pm 3}$ configurations in those regions where the configuration assignment is relatively unambiguous. This assignment, for the odd group of particles, is given in the second column, while the third column gives the observed spin of the lowest state of the configuration. The letter *g* indicates ground state of the nucleus. The spin values come from spectroscopic data (MACK, 1950) and from the analysis of decay schemes (GOLDHABER and HILL, 1952), except where otherwise noted.

* JEFFRIES (1953) (added in proof). ** SMITH et. al. (1952).

The empirical data may be interpreted in a straightforward manner by assuming that the surface coupling dominates over the particle interactions and produces a lowest spin $I = j$ or $I = j - 1$, depending on the strength of the coupling. It is also possible that the occurrence of $I = j$ reveals a significant influence of the particle forces (cf. Fig. 6b).

This interpretation would imply that $I = j$ is more likely in regions near a closed shell in the even structure, while $I = j - 1$

would be preferred for more deformed nuclei. Such a trend is indeed discernible in the data. Thus, in the $f_{7/2}$ shell, $I = 7/2$ is observed for $_{20}Ca^{43}$ and $_{23}V^{51}$ with the closed-shell even structures, while the more deformed $_{25}Mn^{55}$ gives $I = 5/2$. In the $g_{9/2}$ shell, $I = 7/2$ is, for the odd-neutron nuclei, favoured for $Z = 32$, 34, and 36, while $I = 9/2$ lies lowest for $Z = 36$ and 38, corresponding to the approach to the closed subshell at 38. For the odd-proton nuclei, $I = 9/2$ is favoured for $N = 52$, 54, and 56 in the region of the closed shell at 50, while the more deformed nuclei with $N = 60$ and 62 have $I = 7/2$. Such trends could be tested in more detail if the separation between the $I = 7/2$ and $I = 9/2$ levels were known for a sequence of isotopes or isotones.

In this discussion, the even structure has been considered only in its influence on the magnitude of the nuclear deformation. As mentioned on p. 34, more specific effects may occur if the even structure has a strong preference for a shape opposite to that produced by the odd structure. In those cases in Table I where the even configurations are sufficiently well known for such considerations, it is verified that no such anomalies are expected.

Evidence is also available on the level order for $(g_{9/2})^5$ configurations which are expected to occur for 45 particles. For the known nuclei of this type, the lowest state of the configuration has been found to be $I = 7/2$. No calculations have been reported on the effect of particle forces in these configurations. The weak coupling approximation of the effect of surface coupling has not been worked out either but, in the limit of strong coupling, the state $I = 5/2$ would be favoured. It seems not implausible that $I = 7/2$ could result from an intermediate coupling. Considerable interest would attach to the location of the lowest $(5/2+)$ state.

iv. *Odd-odd nuclei.*

The ground state spins resulting from two-body forces have been considered for various types of odd-odd nuclei (Kurath, 1952, 1953; Hitchcock, 1952, 1952a; Edmonds and Flowers, 1952a). The results appear to be more sensitive to the range and exchange nature of the forces than in the case of odd-A nuclei.

The coupling scheme arising from the surface interaction can be derived from (II.28) for weak coupling and from the considerations in § IIc.ii for strong surface coupling. In the latter case, there are two families with $\Omega = |\Omega_{\text{prot}} \pm \Omega_{\text{neut}}|$, whose energies differ only by amounts of the order of rotational energies. In the strong coupling limit, the ground state corresponds to the lower value, but the order may be altered by deviations from strong coupling or by even a minor influence of particle forces.

TABLE II. Spins of simple odd-odd nuclei.

Nucleus	Configuration		I_{obs}	$I\binom{\text{weak}}{\text{coupl.}}$	$I\binom{\text{strong}}{\text{coupl.}}$
	protons	neutrons			
$_5B^{10}$	$(p_{3/2})^{-1}$	$(p_{3/2})^{-1}$	3	0	0,3
$_{17}Cl^{36}$	$d_{3/2}$	$(d_{3/2})^{-1}$	2	2	1,2
$_{17}Cl^{38}$	$d_{3/2}$	$f_{7/2}$	2	2	2,5
$_{19}K^{40}$	$(d_{3/2})^{-1}$	$f_{7/2}$	4	4	3,4
$_{37}Rb^{86}$	$(f_{5/2})^{-1}$	$(g_{9/2})^{-1}$	2	2	2,7

The table lists odd-odd nuclei whose proton and neutron configurations may be described in terms of a single particle or hole with $j > 1/2$. The observed spins, in column four, are taken from the references in Table XXI, except for Cl^{38} whose spin is derived from its observed beta spectrum (cf. Table XXXII).

The spins expected for weak and strong surface coupling are given in the two last columns. The weak coupling results coincide with those obtained for attractive spin-independent particle forces of zero range. For strong coupling, two values are listed, corresponding to the degenerate Ω-values implied by (II.29) ($\Omega = |\Omega_{\text{prot}} \pm \Omega_{\text{neut}}|$). The rotational energy (II.30) favours the smaller of the two spin values, but the relative position of the two states may be shifted by deviations from strong coupling or by even rather weak particle forces.

The measured spins of odd-odd nuclei with simple two-particle configurations are listed in Table II, which also gives the calculated values for weak and strong surface coupling.* We have confined ourselves to regions of relatively pure configurations and have omitted nuclei for which one or both of the odd particles have $j = 1/2$. These latter particle states are affected by the sur-

* In the present discussion, we restrict ourselves to nuclei with $A > 8$, since the division into particle and collective degrees of freedom loses its significance for the very lightest nuclei. Moreover, for the light nuclei, the analysis is complicated by the fact that the particle forces in general lead to a situation intermediate between (jj) and (LS) coupling (cf. INGLIS, 1952).

face only through their coupling to neighbouring states, and are also somewhat special as regards the effect of particle forces, since spin dependent interactions become decisive. For the cases in Table II, the ground state spin resulting from spin independent interactions of zero range (KURATH, 1952) coincide with the weak coupling values in column five. Results of other forces have been considered by the above mentioned authors.

It appears that both particle forces and surface interactions are capable of accounting for the data in Table II.* An interesting feature is the empirical evidence for a different coupling of particle-particle from that of particle-hole. This can be understood in terms of two-body forces of the Wigner or Majorana type (KURATH, 1953) and also follows from the opposite signs of the surface coupling associated with particles and holes.

The coupling scheme in some more complex odd-odd nuclei is considered in the Addendum to Chapters IV and V, in connection with a discussion of nuclear moments.

v. *Summary.*

The ground state spin is determined in general by a competition between particle forces and surface coupling. Often the two effects favour the same value of I, but, especially in the case of $(j)^3$ configurations, the predictions are different and the empirical evidence can be used to obtain information about the nuclear coupling scheme (cf. also footnote below).

The available data can be interpreted in a consistent manner in terms of the expected dominance of the surface coupling over the direct particle forces (cf. p. 32). The observed spins confirm the approach to the strong coupling scheme in regions removed

* Note added in proof: A level scheme for $_{17}Cl^{34}$ has recently been given (ARBER and STÄHELIN, 1953), in which the ground state has $I = 0$ (even parity) and in which there appears an isomeric level at 145 keV with $I = 3$ (even parity). For weak surface coupling the lowest state of this $(d_{3/2}; d_{3/2})$ configuration has $I = 0$, while for strong coupling one finds two states $I = 0,3$ with the former favoured by the rotational energy. Attractive particle forces of the expected range yield $I = 3$ for the ground state (KURATH, 1953).

Additional evidence on the ground state spins of self-mirrored odd-odd nuclei could provide further information on the competition between the direct particle forces and the coupling to the surface deformations, since the former in general favour $I = 2j$, while the latter gives $I = 0$ (cf., especially, $_{13}Al^{26}$, $_{19}K^{38}$, $_{21}Sc^{42}$, and $_{27}Co^{54}$).

from closed shells, with a relatively weaker coupling acting in the neighbourhood of closed shells.

In the immediate vicinity of major closed shells, the expected weak surface coupling implies the most favourable conditions for the study of particle forces. Important evidence on the strength and nature of these forces could be provided by further experimental data on ground state spins and moments in this region, especially when combined with a knowledge of the excitation spectrum and lifetimes of excited states (cf. § VIb).

IV. Magnetic Moments.

The sharing of angular momentum between particles and surface implies that both particle and surface motion contribute to the nuclear magnetic moment. Because of the large intrinsic moment of the nucleons, the particle aspect of nuclear moments is in general the more conspicuous, and indeed the empirical moments have provided a valuable guide in the formulation of the shell model (SCHMIDT, 1937; FEENBERG and HAMMACK, 1949; NORDHEIM, 1949; MAYER, 1950; HAXEL, JENSEN and SUESS, 1950).

In a more quantitative analysis, however, the surface coupling plays an important role. Appreciable shifts from the single-particle values can arise from the modified nuclear coupling scheme produced by the surface interaction; additional effects result from the tendency of the surface coupling to admix near-lying particle states, which may have very different magnetic properties (FOLDY and MILFORD, 1950; A. BOHR, 1951; DAVIDSON and FEENBERG, 1953).

The analysis of magnetic moments may also provide evidence on the extent to which the magnetic properties of nucleons may be affected by their interaction with nuclear matter (cf., e. g., VILLARS, 1947; SACHS, 1948; MIYAZAWA, 1951 a).

a) Shell Model Moments.

For a single particle moving in a spherical potential, the magnetic moment is given by

$$\mu = j g_j = j\left(g_l \pm \frac{1}{2\,l+1}\,(g_s - g_l)\right) \qquad j = l \pm 1/2, \qquad \text{(IV.1)}$$

where g_j is the total g-factor and

$$g_s = \left\{ \begin{matrix} 5.585 \\ -3.826 \end{matrix} \right\} \quad \text{and} \quad g_l = \left\{ \begin{matrix} 1 \\ 0 \end{matrix} \right\} \qquad \text{(IV.2)}$$

the intrinsic and orbital g-factors in units of nuclear magnetons. In the bracket, the upper values refer to a proton, the lower to a neutron.

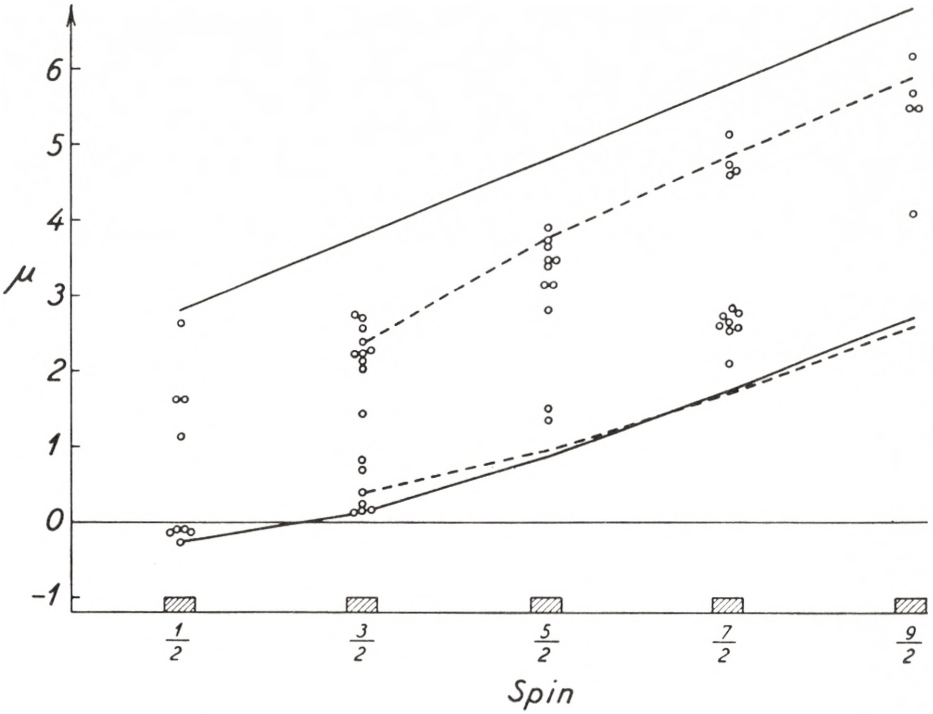

Fig. 7. *Magnetic moments of odd-proton nuclei.* The moments of odd-proton nuclei with $A > 8$ are plotted against the nuclear spin. This type of diagram was first used by SCHMIDT (1937). The experimental values are taken from the references given in the Addendum. The full-drawn curves give the single-particle values (1 and 2), while the dotted curves give the moment values obtained in the limit of strong surface coupling, assuming the particle j to remain a constant of the motion (cf. (6) and Ap. III.9). The surface coupling may further influence the magnetic moment through the tendency to admix neighbouring particle orbitals. This effect, however, depends sensitively on the level order and the shape and magnitude of the deformation, and must therefore be considered separately for the individual nuclei (cf. Table VII and the Addendum).

The empirical moments for odd-A nuclei are plotted in Figs. 7 and 8, in which also the single-particle values (1 and 2) are shown by the solid lines. In spite of the appreciable scatter of the empirical moments, they show a tendency to cluster in two groups, for given I, which can be related to the single-particle values. This correlation has been successfully employed in the

determination of nuclear parities (cf., e. g., MAYER, MOSZKOWSKI and NORDHEIM, 1951). Also the trends of the moments with I give support to the value (2) for the orbital g-factor.

For many-particle configurations, the magnetic moment depends on the coupling scheme which leads to the total angular momentum J. For a group of equivalent particles, one has, in

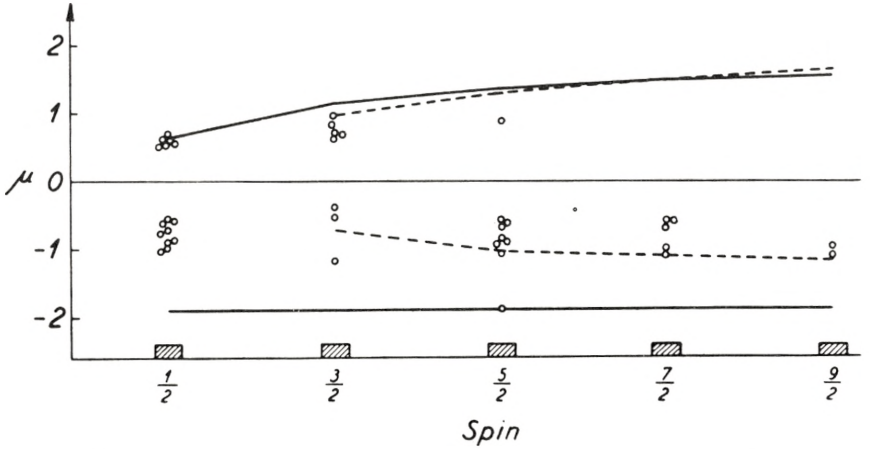

Fig. 8. *Magnetic moments of odd-neutron nuclei.* The moments of odd-neutron nuclei with $A > 8$ are plotted against the nuclear spin (cf. also the caption to Fig. 7).

the (jj) coupling model, $g_J = g_j$, but changes in the g-factor may arise for odd-A nuclei when the even structure is not a closed shell. In such cases, the nuclear state for a given J will in general depend on the interparticle forces; for three or five nucleons in $j = 3/2$ orbitals, the assumption of charge independent forces, however, suffices to determine the nuclear wave function. The magnetic moments for these cases are listed in Table III. For odd-odd nuclei, the magnetic moment is in general unique only when the proton—as well as the neutron—configuration is that of a single particle. By making more explicit assumptions about the character of the forces, one can obtain magnetic moments for more complicated many-particle configurations (HITCHCOCK, 1952; FLOWERS, 1952c).

A comparison of the shell model magnetic moments with the empirical data is given in Table IV. Nuclei are listed for which magnetic moments are known, and for which the (jj) coupling

TABLE III. Properties of charge symmetrized states of type $(j = 3/2)^3_{J=3/2}$ with $T = 1/2$.

Configuration		Magnetic moments		Quadrupole moments	Mirror β-decay
protons	neutrons	μ_j	μ_J	$Q_J/\lvert Q_j \rvert$	$(D_{GT})_J/(D_{GT})_j$
$(p_{3/2})^{\pm 1}$	$(p_{3/2})^2$	3.79	3.03	$\mp$ 11/15	121/225
$(p_{3/2})^2$	$(p_{3/2})^{\pm 1}$	— 1.91	—.1.15	$\mp$ 2/3	121/225
$(d_{3/2})^{\pm 1}$	$(d_{3/2})^2$	0.12	0.26	$\mp$ 11/15	121/225
$(d_{3/2})^2$	$(d_{3/2})^{\pm 1}$	1.15	1.01	$\mp$ 2/3	121/225

The table compares magnetic moments, quadrupole moments, and β-decay transition probabilities for the charge symmetrized state J with the corresponding quantities for the single-particle state j. Magnetic moments have been given by MIZUSHIMA and UMEZAWA (1952), quadrupole moments by HORIE and YOSHIDA (1951) and FLOWERS (1952c), and β-decay matrix elements by KOFOED-HANSEN and WINTHER (1952).

shell model provides a unique prediction μ_p. It is seen that, in most cases, the deviations from μ_p are of the order of a half to one magneton. The cases of agreement between μ_p and μ_{obs} are principally the $p_{1/2}$-nuclei and the self-mirrored odd-odd nuclei (cf. pp. 67 and 81).

b) Moments of the Coupled System.

For the coupled system consisting of a single particle and the nuclear surface, the magnetic moment is given by

$$\mu = < g_s s_z + g_l l_z + g_R R_z >_{M=I} \qquad \text{(IV.3)}$$

where g_R is the g-factor for the angular momentum carried by the surface. For a uniformly charged nucleus, we have*

$$g_R = Z/A. \qquad \text{(IV.4)}$$

If j remains a good quantum number, (3) reduces to

$$\left.\begin{aligned} \mu &= < g_j j_z + g_R R_z >_{M=I} \\ &= g_j I - (g_j - g_R) < R_z >_{M=I}. \end{aligned}\right\} \qquad \text{(IV.5)}$$

* In the discussion of the empirical data we employ for simplicity the fixed value $g_R = 0.45$, except for the self-mirrored odd-odd nuclei for which $g_R = 0.5$.

TABLE IV. Comparison of magnetic moments with shell model values.

Nucleus	Configurations		I	μ_{obs}	μ_p
	protons	neutrons			
$_4Be^9$	$(p_{3/2})^2$	$(p_{3/2})^{-1}$	3/2	−1.18	−1.15
$_5B^{10}$	$(p_{3/2})^{-1}$	$(p_{3/2})^{-1}$	3	1.80	1.88
$_5B^{11}$	$(p_{3/2})^{-1}$	—	3/2	2.69	3.79
$_6C^{13}$	—	$p_{1/2}$	1/2	0.70	0.64
$_7N^{14}$	$p_{1/2}$	$p_{1/2}$	1	0.40	0.37
$_7N^{15}$	$p_{1/2}$	—	1/2	−0.28	−0.26
$_8O^{17}$	—	$d_{5/2}$	5/2	−1.89	−1.91
$_9F^{19}$	$s_{1/2}$	—	1/2	2.63	2.79
$_{11}Na^{22}$	$(d_{5/2})^3$	$(d_{5/2})^3$	3	1.75	1.73
$_{13}Al^{27}$	$(d_{5/2})^{-1}$	—	5/2	3.64	4.79
$_{14}Si^{29}$	—	$s_{1/2}$	1/2	−0.56	−1.91
$_{15}P^{31}$	$s_{1/2}$	—	1/2	1.13	2.79
$_{16}S^{33}$	—	$d_{3/2}$	3/2	0.64	1.15
$_{17}Cl^{35}$	$d_{3/2}$	$(d_{3/2})^2$	3/2	0.82	0.26
$_{17}Cl^{37}$	$d_{3/2}$	—	3/2	0.68	0.12
$_{19}K^{39}$	$(d_{3/2})^{-1}$	—	3/2	0.39	0.12
$_{19}K^{40}$	$(d_{3/2})^{-1}$	$f_{7/2}$	4	−1.30	−1.68
$_{23}V^{51}$	$(f_{7/2})^3$	—	7/2	5.15	5.79
$_{37}Rb^{86}$	$(f_{5/2})^{-1}$	$(g_{9/2})^{-1}$	2	−1.69	−2.13
$_{37}Rb^{87}$	$(p_{3/2})^{-1}$	—	3/2	2.75	3.79
$_{38}Sr^{87}$	—	$(g_{9/2})^{-1}$	9/2	−1.1	−1.91
$_{39}Y^{89}$	$p_{1/2}$	—	1/2	−0.14	−0.26
$_{40}Zr^{91}$	—	$d_{5/2}$	5/2	−1.1	−1.91
$_{82}Pb^{207}$	—	$p_{1/2}$	1/2	0.59	0.64
$_{83}Bi^{209}$	$h_{9/2}$	—	9/2	4.08	2.62

The table lists the nuclei with measured magnetic moments, for which the shell model yields unique μ-values, without specific assumptions about the nuclear forces other than charge independence. For references to the empirical data, cf. Addendum to Chapters IV and V. The odd-A nuclei are single-particle configurations, except for Be^9 and Cl^{35} for which cf. Table III. The odd-odd nuclei mostly have two-particle configurations, in which case the measured spin uniquely determines the state. For Na^{22} the total g-factor follows from the symmetry of the configuration, even though the state is not unique.

For the ground state with $I = j$, the dependence of $< R_z >$ on the coupling strength has been discussed in § IIb and is illustrated in Fig. 5. In the limit of large x, we get from (II.20), for $I = j > 3/2$, the strong coupling value (cf. A. BOHR, 1951)

$$\mu_c = \mu_{sp} - (g_j - g_R) \frac{I}{I+1}. \qquad \text{(IV.6)}$$

For $I = j = 3/2$, the limiting value μ_c differs somewhat from (6) (cf. Ap. III.9); for $I = j = 1/2$, there is no coupling to the surface and $\mu = \mu_{sp}$.

The values of μ_c for j a constant ($j = I$) are plotted as dotted lines in Figs. 7 and 8.

If there are neighbouring single-particle states j', which are admixed by the surface coupling, the magnetic moment may be strongly influenced. In the perturbation approximation, one obtains from (Ap. II.3 and 4)

$$\left.\begin{aligned} \mu &= \mu_{sp} \\ &+ x^2 \sum_{j'} \{ -\alpha_{jj'} (g_j - g_R) + \beta_{jj'} (g_{j'} - g_R) \} \left(\frac{\hbar\omega}{\hbar\omega + \Delta_{jj'}} \right)^2, \end{aligned} \right\} \quad \text{(IV.7)}$$

where the coefficients α and β are given in Table V, and where $\Delta_{jj'}$ represents the spacing between the particle states j and j'.

TABLE V. Coefficients in magnetic moment shifts produced by weak surface coupling.

I	$j' = j-2$		$j' = j-1$		$j' = j$		$j' = j+1$		$j' = j+2$	
	α	β	α	β	α	β	α	β	α	β
1/2	—	—	—	—	—	—	$\frac{1}{5}$	$-\frac{1}{5}$	$\frac{3}{10}$	$\frac{7}{10}$
3/2	—	—	$\frac{9}{10}$	$\frac{9}{50}$	$\frac{18}{25}$	—	$\frac{27}{70}$	$\frac{117}{350}$	$\frac{81}{35}$	$\frac{729}{175}$
5/2	$\frac{5}{2}$	$\frac{1}{2}$	$\frac{5}{7}$	$\frac{13}{49}$	$\frac{48}{49}$	—	$\frac{10}{21}$	$\frac{74}{147}$	$\frac{125}{21}$	$\frac{1375}{147}$
7/2	$\frac{63}{10}$	$\frac{27}{10}$	$\frac{7}{10}$	$\frac{37}{90}$	$\frac{10}{9}$	—	$\frac{35}{66}$	$\frac{115}{198}$	$\frac{245}{22}$	$\frac{3185}{198}$
9/2	$\frac{81}{7}$	$\frac{45}{7}$	$\frac{54}{77}$	$\frac{414}{847}$	$\frac{144}{121}$	—	$\frac{81}{143}$	$\frac{981}{1573}$	$\frac{5103}{286}$	$\frac{76545}{3146}$

The magnetic moment shift in a state $I = j$, arising from the sharing of angular momentum between the particle and the surface, and from the admixture of neighbouring orbitals j', is given in the weak coupling region by (IV.7). The table lists the coefficients $\alpha_{jj'}$, and $\beta_{jj'}$, occurring in this equation.

If the surface admixes the spin orbit partner, there is an additional contribution to μ from cross terms in j, j' giving (cf. Ap. II.5)

$$\left.\begin{aligned}\delta\mu = \pm x^2 (g_s - g_l) \frac{3}{4(2l+1)} \frac{(2j-1)(2j+3)}{(j+1)^2} \\ \left(\frac{\hbar\omega}{\hbar\omega + \Delta_{jj'}}\right),\end{aligned}\right\} \quad \text{(IV.8)}$$

where the upper and lower signs refer to the cases of a particle and a hole, respectively.

In strong coupling, the magnetic moment of a state with $I = K = \Omega \geqslant 3/2$ is given by

$$\mu_c = \frac{I^2}{I+1} g_\Omega + \frac{I}{I+1} g_R, \quad \text{(IV.9)}$$

where

$$g_\Omega = \frac{1}{\Omega} < g_s s_3 + g_l l_3 > \quad \text{(IV.10)}$$

is the g-factor associated with the particle motion in the deformed nucleus and can be evaluated for wave functions χ_Ω of the type discussed in § IIb.

For the special case of $\Omega = K = 1/2$, the value of μ_c is most easily obtained from (3) by means of the expectation values of j_z, given by (II.19), and of s_z given by (Ap. III.2).

For many-particle configurations, magnetic moments can be derived for the different coupling schemes discussed in § IIc. In the strong coupling scheme, in which the state is characterized by the Ω_p of the individual particles (cf. Fig. 6a), formula (9) still holds where, for odd-A nuclei, g_Ω is the g-factor for the last odd particle. For odd-odd nuclei, we have

$$g_\Omega = \frac{1}{\Omega} (\Omega_a g_a + \Omega_b g_b). \quad \text{(IV.11)}$$

If the nuclear forces first couple the particle to a resultant J (cf. Fig. 6b), the magnetic moment is obtained as for a single particle with a g-factor equal to g_J.

c) Comparison with Empirical Data.

A detailed application of the coupled model to the interpretation of moments of individual nuclei is given in the Ad-

dendum to Chapters IV and V. In the present section, we consider some of the general trends of the empirical data and summarize the conclusions that can be drawn from the more detailed analysis.

The surface coupling may affect the magnetic moment in two ways, by the transfer of angular momentum to the surface

TABLE VI. Magnetic moments in strong coupling.

Nucleus	Configuration		I	μ_{obs}	μ_c	μ_p
	protons	neutrons				
$_4Be^9$	$(p_{3/2})^2$	$(p_{3/2})^{-1}$	3/2	−1.18	−0.73	−1.15
$_5B^{11}$	$(p_{3/2})^{-1}$	—	3/2	2.69	2.37	3.79
$_8O^{17}$	—	$d_{5/2}$	5/2	−1.89	−1.04	−1.91
$_{12}Mg^{25}$	$(d_{5/2})^{-2}$	$(d_{5/2})^{-1}$	5/2	−0.86	−1.04	
$_{13}Al^{27}$	$(d_{5/2})^{-1}$	—	5/2	3.64	3.75	4.79
$_{21}Sc^{45}$	$f_{7/2}$	$(f_{7/2})^4$	7/2	4.76	4.86	
$_{22}Ti^{49}$	$(f_{7/2})^2$	$(f_{7/2})^{-1}$	7/2	−1.10	−1.14	
$_{27}Co^{57}$	$(f_{7/2})^{-1}$	$(p_{3/2}, f_{5/2})^2$	7/2	4.6	4.86	
$_{27}Co^{59}$	$(f_{7/2})^{-1}$	$(p_{3/2}, f_{5/2})^4$	7/2	4.65	4.86	
$_{38}Sr^{87}$	—	$(g_{9/2})^{-1}$	9/2	−1.1	−1.20	−1.91
$_{41}Nb^{93}$	$g_{9/2}$	$(d_{5/2}, g_{7/2})^2$	9/2	6.17	5.93	
$_{49}In^{113}$	$(g_{9/2})^{-1}$	$(d_{5/2}, g_{7/2}, h_{11/2})^{14}$	9/2	5.49	5.93	
$_{49}In^{115}$	$(g_{9/2})^{-1}$	$(d_{5/2}, g_{7/2}, h_{11/2})^{16}$	9/2	5.50	5.93	

The table lists the relatively simple nuclei whose odd structure is of $(j)^{\pm 1}$ type with a j larger than that of neighbouring orbitals. The last three columns give the observed moments, those calculated for strong surface coupling, and those resulting from particle forces with the neglect of surface coupling. The latter are only listed where the particle forces lead to a unique coupling scheme. For reference to experimental data, cf. the Addendum.

and by the admixture of near-lying particle orbitals. In a special class of nuclei, the former effect can be studied alone, provided the coupling is strong. Thus, if the odd-particle j is the largest in the corresponding shell, the strong coupling solution with $\Omega = j$ will have no other orbitals admixed.

Nuclei of this type, whose odd configuration consists of a single particle or a single hole, are listed in Table VI. The three last columns give the empirical moments and those calculated for strong and vanishing surface coupling.

It is seen that the assumption of a rather strong surface coupling makes possible an approximate interpretation of these moments. The principal exception is ${}_8O^{17}$, for which many properties attest the expected undeformability of the very stable ${}_8O^{16}$ core (cf. § Vc). In some cases, the magnitude of μ_{obs} is a few tenths of a magneton below that of μ_c, which may possibly arise from an interaction effect on the nucleon moment (cf. p. 51).

The rather fully developed strong coupling situation indicated by the empirical values in Table VI implies, according to (5) and Fig. 5, that coupling strengths of $x \geqslant 1.5$ are required if the nuclei are described in terms of a single particle coupled to the surface. Such values of x are somewhat larger, by about a factor two, than those estimated for a single particle in the hydrodynamic approximation (cf. p. 25), but may be understood in terms of the increased coupling expected from the influence of the even structures (cf. p. 31). In cases where an even structure, for a spherical nucleus, would form a closed sub-shell, it may still be active, provided the energy gap to the next higher levels is not too large (cf. Ap. I).

A similar effect on the magnetic moment is expected for all nuclei with $I \geqslant 3/2$, and the strong coupling value μ_c (cf. 6 and Ap. III.9) corresponding to $j = I$ is plotted in Figs. 7 and 8 as broken lines. However, for nuclei other than those listed in Table VI, there are additional contributions to μ, arising from the interaction between neighbouring particle orbitals.

This effect is of special interest for $I = 1/2$ nuclei, where it provides a mechanism for strong surface coupling. Thus, for $(1/2+)$ nuclei, the strong interaction between $s_{1/2}$ and the $d_{5/2}$ and $d_{3/2}$ states may lead to a large deformation. The effect on the moment depends especially on the sign of the deformation (cf. Fig. 11). Thus, the expected prolate shape of F^{19} leads to a very small moment shift, while the expected oblate shape of Si^{29} and P^{31} explains the observed large deviations of the moment from that of a single-particle $s_{1/2}$ state (cf. Ad. i).

For the $(1/2-)$ nuclei, the admixed states have relatively little effect on the moment. In the first p-shell, the large $p_{1/2}$ —$p_{3/2}$ splitting in addition leads to rather small amplitudes of admixture. In higher p-shells, there is a considerable tendency for the moment deviations, caused by the $p_{3/2}$ and $f_{5/2}$ admixtures, to

cancel, which provides an understanding of the strikingly small spread of the moments of this group (cf. Ad. ii).

Another effect of the interconfiguration admixtures can be studied for the (3/2+) nuclei. Due to the $d_{3/2} - d_{5/2}$ interference, the magnetic moment depends, as for the (1/2+) nuclei, on the sign of the deformation (cf. Fig. 12) and thus distinguishes be-

TABLE VII. Summary of magnetic moments for $A < 50$.

Nucleus	Configurations		I	μ_{obs}	μ_p	μ_c
	protons	neutrons				
$_4Be^9$	$(p_{3/2})^2$	$(p_{3/2})^{-1}$	3/2	−1.18	−1.15	−0.7
$_5B^{10}$	$(p_{3/2})^{-1}$	$(p_{3/2})^{-1}$	3	1.80	1.88	1.79
$_5B^{11}$	$(p_{3/2})^{-1}$	—	3/2	2.69	3.79	2.3
$_6C^{13}$	—	$p_{1/2}$	1/2	0.70	0.64	0.64 to 0.75
$_7N^{14}$	$p_{1/2}$	$p_{1/2}$	1	0.40	0.37	0.40 to 0.47
$_7N^{15}$	$p_{1/2}$	—	1/2	−0.28	−0.26	−0.27 to −0.41
$_8O^{17}$	—	$d_{5/2}$	5/2	−1.89	−1.91	−1.04
$_9F^{19}$	$s_{1/2}$	—	1/2	2.63	2.79	2.5 to 2.8
$_{11}Na^{22}$	$(d_{5/2})^3$	$(d_{5/2})^3$	3	1.75	1.73	1.71 to 1.78
$_{11}Na^{23}$	$(d_{5/2})^3$	$(d_{5/2})^{-2}$	3/2	2.22		2.2 to 2.5
$_{11}Na^{24}$	$(d_{5/2})^3$	$(d_{5/2})^{-1}$	4	1.69		1.4 to 1.8
$_{12}Mg^{25}$	$(d_{5/2})^{-2}$	$(d_{5/2})^{-1}$	5/2	−0.86		−1.04
$_{13}Al^{27}$	$(d_{5/2})^{-1}$	—	5/2	3.64	4.79	3.75
$_{14}Si^{29}$	—	$s_{1/2}$	1/2	−0.56	−1.91	−1.2 to −0.6
$_{15}P^{31}$	$s_{1/2}$	—	1/2	1.13	2.79	1.9 to 1.2
$_{16}S^{33}$	—	$d_{3/2}$	3/2	0.64	1.15	0.8 to 0.2
$_{17}Cl^{35}$	$d_{3/2}$	$(d_{3/2})^2$	3/2	0.82	0.26	0.5 to 1.2
$_{17}Cl^{37}$	$d_{3/2}$	—	3/2	0.68	0.12	0.5 to 1.2
$_{19}K^{39}$	$(d_{3/2})^{-1}$	—	3/2	0.39	0.12	0.3 to −0.1
$_{19}K^{40}$	$(d_{3/2})^{-1}$	$f_{7/2}$	4	−1.30	−1.68	−1.0 to −0.3
$_{19}K^{41}$	$(d_{3/2})^{-1}$	$(f_{7/2})^2$	3/2	0.22		0.3 to −0.1
$_{19}K^{42}$	$(d_{3/2})^{-1}$	$(f_{7/2})^3$	2	−1.14		−0.7 to −0.9
$_{21}Sc^{45}$	$f_{7/2}$	$(f_{7/2})^4$	7/2	4.76		4.86
$_{22}Ti^{49}$	$(f_{7/2})^2$	$(f_{7/2})^{-1}$	7/2	−1.10		−1.14

The table compares the observed magnetic moment μ_{obs} with the moment μ_p given by the shell model, with neglect of surface coupling, and the moment μ_c obtained for strong surface coupling. The value of μ_p is given only where it is independent of special assumptions about the nuclear forces. In cases where the strong coupling state contains several values of j, the moment may be rather sensitive to the equilibrium value of β, and the values given for μ_c correspond to deformations in the range $0.1 < \beta < 0.4$. For a more detailed discussion of μ_c, and for references to the empirical data, cf. the Addendum.

tween particles and holes. Such differences are indeed apparent in the empirical data (cf. Table XIV).

Further effects of the interaction of neighbouring particle states are discussed in the Addendum. The states often have very different magnetic moments, and their interaction may lead to large moment shifts.

The analysis of magnetic moments for nuclei with $A < 50$ is summarized in Table VII. The table compares the observed moments with those calculated for vanishing and strong surface coupling (columns six and seven, respectively). In those cases where the strong coupling state contains particle orbitals of different j, the magnetic moment may depend rather sensitively on the magnitude of the deformation, and the table lists moments appropriate to deformations in the range $0.1 < \beta < 0.4$. The expected values of β vary considerably from nucleus to nucleus, and estimates of values appropriate to the individual nuclei are given in the Addendum.

It is seen from the data collected in Tables VI and VII, and from the discussion in the Addendum, that the unified description of the nucleus, in terms of the coupled system of particles and collective oscillations, makes possible a rather systematic interpretation of the magnetic moments of nuclei with sufficiently simple configurations. The empirical data give evidence for the expected approach to the strong coupling scheme, except in the immediate vicinity of major closed shells.

An interpretation is also possible of the moments of many heavier nuclei not included in Tables VI and VII, wherever the configurations are sufficiently well known (cf. the Addendum). An important anomaly is the as yet unexplained large moment shift of $_{83}Bi^{209}$ with its single-particle configuration. The stability of the $_{82}Pb^{208}$ core with its closed-shell structure implies a rather negligible effect of the surface coupling, as confirmed by the small quadrupole moment. The observed moment shift thus probably reflects some unexpected feature of the particle structure.

Besides the contributions to the nuclear magnetic moment from the individual particles and from the surface, there may be an additional effect arising from the interaction of the nucleons. Such interaction effects have been described as exchange magnetic moments, and have sometimes been considered as a partial

quenching of the meson cloud responsible for the nucleon moments (Villars, 1947; Sachs, 1948; Osborn and Foldy, 1950; Spruch, 1950; Miyazawa, 1951, 1951a; Bloch, 1951; de-Shalit, 1951; Schiff, 1951; Jensen and Mayer, 1952; Russek and Spruch, 1952; Ross, 1952).

It is of interest to employ the analysis of the empirical moments to obtain evidence on the possible magnitude of these phenomena. In the $j = l - 1/2$ nuclei, there are small residual moment shifts which may perhaps be interpreted as arising from interaction effects. For the $p_{1/2}$ and $d_{3/2}$ configurations, the data are consistent with a reduction of the intrinsic nucleon moment by about 0.3 magnetons (cf. pp. 69 and 74). Somewhat larger effects may be present in the $f_{5/2}$ and possibly also in the $g_{7/2}$ nuclei (cf. pp. 78 og 79). It seems somewhat difficult, however, to interpret the moment shift of Bi^{209} ($h_{9/2}$) in this way, since an effect five times larger would be required (cf. p. 81). The moments of the $j = l + 1/2$ nuclei, with the exception of O^{17}, do not seem inconsistent with a reduction of the nucleon moment by a few tenths of a magneton (cf. Table VI).

That interaction contributions to the moment are in general small compared to the effects of the surface coupling is further supported by the correlations of magnetic moments with quadrupole moments (cf. p. 70) and especially with beta decay *ft*-values. Thus, for all the nuclei in Table VII with $Z = N - 1$, for which there are major discrepancies between μ_{obs} and μ_p, the *ft*-values of the corresponding mirror transitions give strong evidence that these discrepancies are associated with modifications in the nuclear coupling scheme rather than in the intrinsic nucleon moments (cf. § VIIIc.i). In these cases, the coupled model simultaneously improves the agreement with both the magnetic moments and the beta decay data (cf. Table XXIX).

V. Quadrupole Moments.

The magnitude of the electric quadrupole moments reveals directly their collective origin (CASIMIR, 1936). At the same time, the trends are strongly correlated with the nuclear shell structure (GORDY, 1949; HILL, 1949; TOWNES, FOLEY and LOW, 1949; ROSENFELD, 1951). These dual aspects of the quadrupole moments find their explanation in the coupling between the particle motion and the surface deformations (RAINWATER, 1950).

The importance of the deformations for the whole dynamics of nuclear states implies intimate correlations between quadrupole moments and many other nuclear properties.

a) Shell Model Moments.

A single proton contributes a quadrupole moment

$$Q_j = < r^2 \, (3 \cos^2 \vartheta - 1) >_{m=j} = - \frac{2j-1}{2\,(j+1)} < r^2 >, \qquad \text{(V.1)}$$

where the mean value of r^2, although depending somewhat on n and l, is of the order of $3/5\, R_0^2$. A single hole in a proton shell yields a quadrupole moment equal to (1), but of opposite sign. For a single-neutron state, the quadrupole moment comes only from the recoil and is Z/A^2 times the above value.

For configurations with several equivalent protons coupling to a total J, the quadrupole moment is usually somewhat smaller than the single-particle value. Examples of such configurations are listed in Table VIII. For configurations involving both neutrons and protons, the values of Q_J are given in Table III for those configurations which lead to unique charge symmetrized wave functions.

TABLE VIII. Quadrupole moments for $(j)^3$ proton configurations.

J \ $(j)^3$	$(5/2)^3$	$(7/2)^3$	$(9/2)^3$
3/2	0	−3/5	−1/5
5/2	0	13/14	−1/42
7/2		1/3	121/90
9/2	0	−5/11	+0.58 −0.73
11/2		5/49	2/39
13/2			11/60
15/2		5/7	−7/102
17/2			7/15
21/2			7/6

The table lists the ratio of the quadrupole moment Q_J of the state $(j)^3_J$ to the value of Q_j (cf. V.1). The configuration $(9/2)^3$ has two states with $J = 9/2$ and the quadrupole moments listed are the extreme values obtainable by combination of the two states. From the values of Q_J one can also calculate the effective particle-surface coupling constants k_J given by (II.31).

In Fig. 9 are plotted the measured quadrupole moments of odd-A nuclei in units of $|Q_j|$. In the case of odd-neutron nuclei, the value of $|Q_j|$ for a corresponding proton is used as a unit. The most conspicuous feature of the figure is the magnitude of $|Q/Q_j|$ which, in most cases, exceeds 2 and which, in some regions, reaches values of 20 or more. Moreover, odd-neutron nuclei have Q-values comparable to those of corresponding odd-proton nuclei. Shell structure is also apparent in Fig. 9, especially in the expected change from positive to negative Q at the major shell closings.

b) Moments of the Coupled System.

In the coupled model, the total nuclear quadrupole moment becomes

$$Q = Q_p + Q_S \tag{V.2}$$

of which the first part is associated with the particle structure. The second part is due to the surface deformation and is given by (cf. II.2)

$$Q_S = \frac{3}{\sqrt{5\pi}} Z R_0^2 < \alpha_0 >_{M=I} \tag{V.3}$$

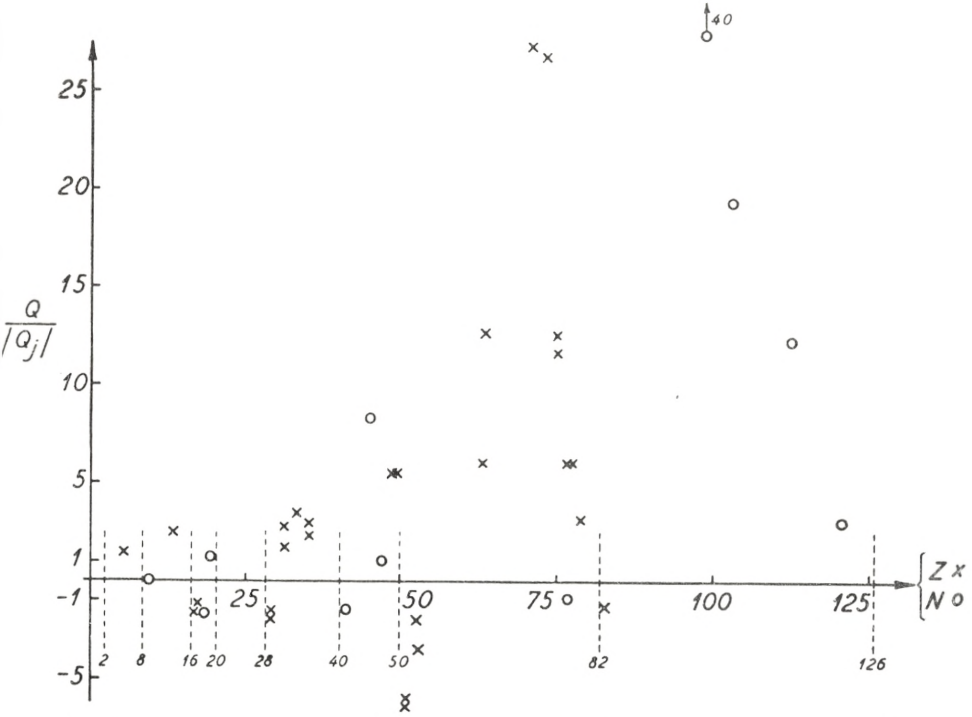

Fig. 9. *Quadrupole moments of odd-A nuclei.* Quadrupole moments, measured in units of the moment Q_j of a single-proton state with $j = I$ (cf. (1)), are plotted for odd-A nuclei with $A > 8$ as a function of Z (odd-proton nuclei) or N (odd-neutron nuclei). Similar diagrams have been given by GORDY (1949) and by TOWNES, FOLEY and LOW (1949). The experimental data are taken from the references given in the Addendum.

in the hydrodynamic approximation, where the nucleus is considered as an incompressible uniformly charged structure.

Quadrupole moments can be obtained from the various solutions of the coupled system considered in § IIb and § IIc. Thus, in first order perturbation approximation, the value of Q_S induced by a single particle may be found from (II.9) and (V.3) by considering only the α_0-part of the interaction. The matrix elements of α_0 and Y_0 are given by (A.38, 76, 77, and 78) and one obtains

$$Q_S = -\frac{3}{4\pi}\frac{2I-1}{2(I+1)}\frac{k}{C}ZR_0^2. \qquad \text{(V.4)}$$

The presence of near-lying single-particle levels does not influence this result to first order in k.

In strong coupling, we have (cf. A. 11 and 12)

$$\alpha_0 = \beta \cos\gamma \left(\frac{3}{2}\cos^2\theta - \frac{1}{2}\right) + \frac{\sqrt{3}}{2}\beta \sin\gamma \sin^2\theta \cos 2\psi. \qquad \text{(V.5)}$$

For the wave function (II.15), only the first term in (5) contributes to Q_S, and one obtains

$$Q_S = \frac{3K^2 - I(I+1)}{(I+1)(2I+3)} Q_0, \qquad \text{(V.6)}$$

where

$$Q_0 = \frac{3}{\sqrt{5\pi}} ZR_0^2 < \beta \cos\gamma > \qquad \text{(V.7)}$$

gives the intrinsic quadrupole moment, measured with respect to the nuclear axis (cf. (Ap. III.10) for the special case of $j = 3/2$).

In the limit of strong coupling, we may replace β and γ by their equilibrium values. From the estimate (II.22) for β we get, for the ground state, $I = K = \Omega$; $\gamma = \pi$, (cf. FEENBERG and HAMMACK, 1951; GALLONE and SALVETTI, 1951, 1951a)

$$Q_0 = -\frac{3}{4\pi} \frac{2I-1}{2(I+1)} \frac{k}{C} ZR_0^2 \qquad \text{(V.8)}$$

for the intrinsic quadrupole moment. This result is just equal to the perturbation value (4) for the total surface moment.

The factor preceding Q_0 in (6) is a projection factor P_Q relating the quadrupole moment of a given rotational state of a symmetric top to its intrinsic moment. For the ground state, $I = K$, its value is (cf. A. BOHR, 1951)

$$P_Q = \frac{I}{I+1} \frac{2I-1}{2I+3}. \qquad \text{(V.9)}$$

In a similar way, the contribution of the particles in strong coupling is reduced by the factor P_Q. The significance of P_Q is apparent for states of $I = 0$ or $1/2$, where the nucleus, although it may possess an intrinsic asymmetry Q_0, exhibits a spherically symmetric charge distribution ($Q = 0$).

In intermediate coupling, it is convenient to write the quadrupole moment as

$$Q_S = P_Q(x)\, Q_0, \qquad \text{(V.10)}$$

where Q_0 is given by (8) for a one-particle configuration with $j = I$. The projection factor $P_Q(x)$ is then unity for $x \ll 1$ and approaches the value (9) for $x \gg 1$.

The behaviour of the quadrupole moment for intermediate coupling may be studied for the case $I = j = 3/2$ by means of the wave function illustrated in Fig. 4. Moreover, from the solution of the coupled system valid for $I = j \gg 1$ (cf. Ap. IV), one obtains

$$P_Q(x) = 1 - 3\frac{2I+1}{(I+1)(2I+3)}\frac{x^2}{\sqrt{x^4+\frac{4}{9}}} \qquad \text{(V.11)}$$

correct to terms of order I^{-1}.

The gradual transition from weak to strong coupling is illustrated in Fig. 10.

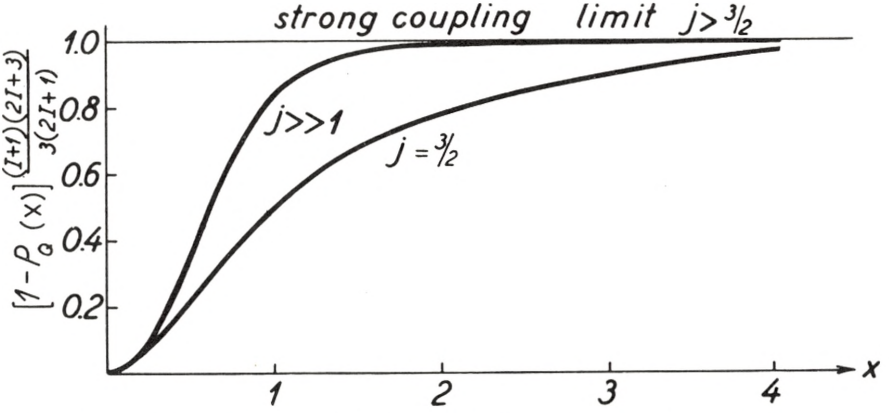

Fig. 10. *Projection factor for quadrupole moments in the coupled system.* The modification in the nuclear coupling scheme, arising from the interaction of the particle with the surface, implies a reduction in the surface quadrupole moment, as compared with that induced by a particle with $m_j = j$. This reduction is expressed by the projection factor $P_Q(x)$ (cf. (10)) which depends on the coupling strength x (cf. (II.14)). For weak coupling ($x \ll 1$), $P_Q \approx 1$ while, in the limit of strong coupling, P_Q approaches the value (9) for $j > 3/2$. In strong coupling, the particle has $\Omega = j$ (cf. Fig. 3) and thus induces the full quadrupole moment with respect to the nuclear coordinate system. The projection factor P_Q then gives the reduction of this intrinsic quadrupole moment Q_0 caused by the deviation of the nuclear axis from the fixed z-axis.

The figure illustrates the gradual development of the projection factor for $j \gg 1$ (cf. (11) and Ap. IV) and for $j = 3/2$ (obtained from Fig. 4). The strong coupling solution for $j = 3/2$ discussed in Ap. III.ii indicates that the curve for $j = 3/2$ may approach a value somewhat in excess of unity, for large x.

c) Discussion of Empirical Data.

The coupling between particle motion and surface deformations provides a mechanism capable of producing nuclear quadrupole moments of the observed order of magnitude (RAINWATER, 1950). In this way, one can account for important trends in the empirical data, in particular the rapid increase of quadrupole moments with A, and the comparable magnitudes of moments of neighbouring odd-proton and odd-neutron nuclei. Also the increase of the moments, as one moves away from closed-shell configurations, which leads to maximum values in the middle of shells, is a direct consequence of the increase in the coupling associated with many-particle configurations (cf. § IIc.ii).*

The empirical quadrupole moments provide valuable evidence on the nuclear deformability and its dependence on shell structure. Thus, it is found that closed-shell nuclei, as expected (cf. Ap. I), possess a much greater stability against surface deformations than is indicated by the hydrodynamic surface tension. For both ${}_8O^{17}$ and ${}_{83}Bi^{209}$, the empirical quadrupole moments are of the order of the single-particle moments and more than ten times smaller than the values estimated from the surface deformation.

The interpretation of these moments as reflecting a sharply decreased deformability is supported by other evidence. Thus, the first excited state of ${}_{82}Pb^{208}$ has an energy about twice the hydrodynamical phonon energy, and the first excited state of ${}_8O^{17}$ has the anomalous $(0+)$ character (cf. § VIc.i). Moreover, the magnetic moment of ${}_8O^{17}$ is very close to the single-particle value; in this respect, ${}_{83}Bi^{209}$ forms an exception, exhibiting a large moment shift of still unexplained origin (cf. p. 81).

The quantitative estimate of quadrupole moments depends sensitively on the assumed surface properties as well as on the details of the particle configuration. However, even a rather crude analysis of the empirical data reveals significant shortcomings of the hydrodynamical model. Thus, for nuclei whose

* PFIRSCH (1952) has discussed the trends of quadrupole moments, but it appears that the states considered do not in general represent nuclear ground states, both because $\Omega \neq I$ and because the chosen configurations do not fill the lowest particle orbitals.

odd structure is that of a single particle, it is found that the hydrodynamical estimate of the quadrupole moment produced by this single particle, with neglect of the deforming influence of the even structure, is already considerably in excess of the observed value.

The comparison* is shown in Table IX. The values of Q_0, listed in column five, are obtained from (8), using the deformabilities of Fig. 1. For a single-particle configuration, the hydrodynamical estimate leads to an intermediate coupling situation (cf. p. 25), and the values of the projection factor $P_Q(x)$, in column seven, are therefore not the full strong coupling values (9), but have been estimated from Fig. 10.** The resultant Q_{hydr} in the next to last column includes the contribution from the particle moment listed in column eight.

The assumption of a single-particle configuration with a constant j in most cases considerably underestimates the deformation; thus, the interaction of neighbouring particle orbitals may increase the coupling strength, and the even structures also in general contribute to the deformation. The resulting approach to the strong coupling scheme, which is also indicated by many other nuclear properties, at the same time implies a decrease in the projection factor.

In spite of the difficulty of a detailed estimate of these effects, it seems clear from the comparison in Table IX that the hydrodynamical values of Q are in general larger than the empirical ones by at least a factor two.

This deficiency of the hydrodynamical model is consistently exhibited by all nuclear properties related to quadrupole moments (cf. § VIc.ii and also p. 75), and gives an important indication as to how the collective properties of the nucleus differ from those of an idealized liquid drop. It seems most likely that

* A comparison of empirical quadrupole moments with those induced by a single particle has been given by VAN WAGENINGEN and DE BOER (1952). These authors find similar Q_0-values to those listed in Table IX, but have used the limiting values (9) for P_Q and thereby obtained appreciably smaller values for Q, than those resulting from the consistent one-particle hydrodynamical approximation employed in Table IX.

** Note added in proof: The projection factors employed in Table IX are in agreement with the recent, more detailed, intermediate coupling calculations by D. C. CHOUDHURY (cf. footnote on p. 24).

TABLE IX. Comparison of quadrupole moments with hydrodynamic estimates.

Nucleus	Configuration		I	Q_0	x	$P_Q(x)$	Q_{sp}	Q_{hydr}	Q_{obs}
	protons	neutrons							
$_5B^{11}$	$(p_{3/2})^{-1}$	—	3/2	+0.07	0.71	0.7	+0.023	+0.06	+0.06
$_8O^{17}$	—	$d_{5/2}$	5/2	−0.20	0.56	0.8	−0.0013	−0.16	−0.005
$_{13}Al^{27}$	$(d_{5/2})^{-1}$	—	5/2	+0.32	0.56	0.8	+0.065	+0.30	+0.16
$_{16}S^{33}$	—	$d_{3/2}$	3/2	−0.31	0.73	0.7	0	−0.22	−0.08
$_{16}S^{35}$	—	$(d_{3/2})^{-1}$	3/2	+0.31	0.73	0.7	0	+0.22	+0.06
$_{17}Cl^{35}$	$d_{3/2}$	$(d_{3/2})^2$	3/2	−0.32	0.73	0.7	−0.055	−0.26	−0.084
$_{17}Cl^{37}$	$d_{3/2}$	—	3/2	−0.32	0.73	0.7	−0.055	−0.26	−0.066
$_{29}Cu^{63}$	$p_{3/2}$	$(p_{3/2}, f_{5/2})^{-4}$	3/2	−0.61	0.76	0.7	−0.08	−0.48	−0.13
$_{29}Cu^{65}$	$p_{3/2}$	$(p_{3/2}, f_{5/2})^{-2}$	3/2	−0.61	0.76	0.7	−0.08	−0.48	−0.12
$_{31}Ga^{69}$	$(p_{3/2})^{-1}$	—	3/2	+0.67	0.77	0.7	+0.08	+0.53	+0.24
$_{31}Ga^{71}$	$(p_{3/2})^{-1}$	—	3/2	+0.67	0.77	0.7	+0.08	+0.53	+0.15
$_{32}Ge^{73}$	$(p_{3/2}, f_{5/2})^4$	$g_{9/2}$	9/2	−1.3	0.45	0.9	0	−1.2	−0.2
$_{49}In^{113}$	$(g_{9/2})^{-1}$	$(d_{5/2}, g_{7/2}, h_{11/2})^{14}$	9/2	+2.4	0.51	0.9	+0.21	+2.4	+1.18
$_{49}In^{115}$	$(g_{9/2})^{-1}$	$(d_{5/2}, g_{7/2}, h_{11/2})^{16}$	9/2	+2.4	0.51	0.9	+0.21	+2.4	+1.20
$_{51}Sb^{121}$	$d_{5/2}$	$(d_{5/2}, g_{7/2}, h_{11/2})^{20}$	5/2	−2.1	0.68	0.7	−0.17	−1.5	−1.0
$_{51}Sb^{123}$	$g_{7/2}$	$(d_{5/2}, g_{7/2}, h_{11/2})^{22}$	7/2	−2.4	0.58	0.8	−0.20	−2.1	−1.2
$_{83}Bi^{209}$	$h_{9/2}$	—	9/2	−6.7	0.68	0.8	−0.32	−5.6	−0.4

The table lists nuclei with measured quadrupole moments, whose odd structure is that of a single particle or hole. The intrinsic quadrupole moment Q_0 in column five is calculated from (V.8). In column six are listed the coupling strengths obtained from (II.14), while in column seven is given an estimate of the projection factor, based upon Fig. 10. The resultant hydrodynamic estimate of Q appears in column nine; in this estimate, the contribution from the particle moment, listed in column eight, has been included. For reference to Q_{obs}, cf. the Addendum.

the empirical data are to be interpreted as indicating that the quadrupole moment associated with a given deformation is overestimated by the hydrodynamical formula (3). Part of the discrepancy may also arise from an underestimate of the mass parameter B (cf. p. 13), in which case the coupling situation for a given deformation would be closer to the strong coupling limit with a resultant smaller projection factor P_Q.

Ratios of quadrupole moments of neighbouring isotopes often do not depend on the specific properties of the collective deformations, and may provide direct evidence on nuclear coupling schemes. Thus, for example, the decrease of Q from $_{17}Cl^{35}$ to

$_{17}Cl^{37}$, the latter with a closed neutron structure, indicates a coupling scheme in $_{17}Cl^{35}$ rather closer to the strong surface coupling than to that produced by particle forces (cf. p. 74).

d) Correlations with Other Nuclear Properties.

The important role of the surface deformation for the structure of nuclear states implies that many nuclear properties follow trends similar to the quadrupole moments and in particular reflect the increasing deformations as one moves away from closed shells. In some cases, there exist simple quantitative correlations.

Intimately connected with the large quadrupole moments are the low-lying nuclear rotational states with their characteristic properties (cf. § VI c.ii). From the lifetimes of these states (§ VII c.iii) or their excitation cross-sections (Ap. VI) one can directly determine the intrinsic quadrupole moment Q_0. The values obtained are just of the magnitude deduced from the spectroscopic Q-values (cf. Table XXVII). The comparison shows that the relationship between Q and Q_0 corresponds to a rather fully developed strong coupling (cf. 9), as is expected for the large deformations in question.

The study of transition probabilities between rotational states thus provides an additional means of determining nuclear quadrupole moments. Since the method also makes possible the determination of deformations in nuclei whose ground states have $I = 0$ or $1/2$, and therefore $Q = 0$, it may add considerably to our knowledge of nuclear deformations.

The excitation energies of the rotational states also depend on the nuclear deformation (§ VI c.ii) and have been observed to exhibit trends parallel to those of the quadrupole moments (Ford, 1953; cf. also Table XXIII).

There is a tendency for large quadrupole moments to be associated with relatively large deviations of the magnetic moments from single-particle values (cf., e. g., Kopfermann, 1951; Miyazawa, 1951 a). The observed correlations can be understood in terms of the magnetic moment shifts arising from the surface coupling (cf. discussion on p. 71).

Certain anomalies in the effective radius of the nuclear charge distribution, derived from spectroscopic isotope shifts, can be related to the observed quadrupole moments (BRIX and KOPFERMANN, 1949). In particular in Eu, the exceptionally large isotope shifts can be attributed to the great difference in the quadrupole moments of the two isotopes (BRIX and KOPFERMANN, 1952). The analysis indicates a relation between Q and Q_0 rather close to that of the strong coupling limit (cf. p. 77).

Addendum to Chapters IV and V.

Details of the Analysis of Nuclear Moments.

In this Addendum, we shall attempt a somewhat detailed analysis of nuclear moments on the basis of the coupled model. The main conclusions of this analysis have been summarized in the preceding chapters (§ IVc and § Vc).

Many of the features of the moments are specific to the configuration in question, and we therefore divide the odd-A nuclei according to spin and parity and consider each group separately. The discussion is confined to nuclei with $A > 8$ (cf. footnote on p. 38).

The tables of empirical moments are based on MACK (1950) and KLINKENBERG (1952) whose compilations we have attempted to bring up to date. The values listed represent what appears to be the most accurate determination, but at the most two significant decimals are quoted. Unless otherwise noted, references to the original experiments can be found in the above compilations.

The magnetic moments include diamagnetic corrections (DICKINSON, 1950) and the quadrupole moments have been corrected for the polarization effect (STERNHEIMER, 1951, 1952). As an aid in the assessment of the reliability of the quoted quadrupole moments, the method of determination is indicated by the letters A, M, and C, referring to atoms, molecules, and crystals, respectively.

i. $(1/2+)$ *nuclei.*

Although states of $I = 1/2$ have no spectroscopically measurable quadrupole moment to reveal directly the deformation of the nucleus, the magnetic moments as well as other nuclear properties (level order, cf. below, and β-decay, cf. § VIIIc) give

Table X. Moments of $(1/2+)$ nuclei).

odd proton ($\mu_{sp} = 2.79$)		odd neutron ($\mu_{sp} = -1.91$)	
nucleus	μ	nucleus	μ
$_{9}F^{19}$	2.63	$_{14}Si^{29}$	−0.56
$_{15}P^{31}$	1.13	$_{48}Cd^{111}$	−0.59
$_{81}Tl^{203}$	1.61	$_{48}Cd^{113}$	−0.62
$_{81}Tl^{205}$	1.63	$_{50}Sn^{115}$	−0.92
		$_{50}Sn^{117}$	−1.00
		$_{50}Sn^{119}$	−1.05
		$_{52}Te^{123}$	−0.74
		$_{52}Te^{125}$	−0.89
		$_{54}Xe^{129}$	−0.78

evidence of the influence of the surface coupling. Direct information on the intrinsic nuclear deformation could be obtained from energies, and especially from lifetimes or excitation cross-sections, for rotational states in these nuclei (cf. § VI c.iii).

The empirical moments of nuclei of this type show peculiar variations, as seen from Table X. Thus, for F^{19}, $\mu \approx \mu_{sp}$, while for P^{31} and Si^{29} in the same shell, very pronounced moment shifts are observed. In this region, the available single-particle orbitals are $d_{5/2}$, $s_{1/2}$ and, a little higher, $d_{3/2}$.

The interaction of these states gives rise to a large surface coupling which makes it appropriate to consider the nuclei in the strong coupling approximation.* The state χ_Ω of the last odd particle with $\Omega_p = 1/2$ then corresponds to the lowest proper value of the matrix (cf. II.26 and Ap. III.1),

$$W' = \begin{pmatrix} 0 & 0 & 0 \\ 0 & \Delta_{3/2} & 0 \\ 0 & 0 & \Delta_{5/2} \end{pmatrix} + k\beta\cos\gamma \sqrt{\frac{5}{4\pi}} \frac{1}{35} \begin{pmatrix} 0 & 7\sqrt{2} & -7\sqrt{3} \\ 7\sqrt{2} & -7 & \sqrt{6} \\ -7\sqrt{3} & \sqrt{6} & -8 \end{pmatrix} \quad \text{(Ad. 1)}$$

where $\Delta_{3/2}$ and $\Delta_{5/2}$ are the energies of the $d_{3/2}$ and $d_{5/2}$ states with respect to the $s_{1/2}$ level. There are additional terms in the nuclear potential energy arising from the surface tension and from the coupling energies of even groups of particles. While these terms are needed for the determination of the equilibrium

* The moment shift arising from the $s_{1/2} - d_{3/2}$ interaction in strong coupling has also been considered by DAVIDSON and FEENBERG (1953).

deformation, they do not otherwise influence the magnetic moment of the nucleus. There are also rotational energy terms (II.30) which may be of significance, especially in light nuclei; they may here be considered as giving additional contributions to the diagonal elements Δ in (1).

The magnetic moment of the state may be written

$$\mu = a_s^2 \mu_s + a_d^2 \mu_d, \tag{Ad. 2}$$

where a_s^2 and a_d^2 are the probabilities of the s and d states, respectively, ($a_d^2 = a_{3/2}^2 + a_{5/2}^2$). The moments μ_s and μ_d are given by (cf. IV.3, II.19, and Ap. III.2; cf. also footnote on p. 44).

$$\left.\begin{aligned} \mu_s = \mu_{sp} &= \begin{Bmatrix} 2.79 \\ -1.91 \end{Bmatrix} \\ \mu_d = a_d^{-2} \Bigg[&\begin{Bmatrix} 1.94 \\ -1.19 \end{Bmatrix} a_{5/2}^2 - \begin{Bmatrix} 2.98 \\ -2.50 \end{Bmatrix} a_{5/2} a_{3/2} + \begin{Bmatrix} 0.41 \\ -0.07 \end{Bmatrix} a_{3/2}^2 \Bigg] \end{aligned}\right\} \tag{Ad. 3}$$

where, in the curly brackets, the upper value refers to a proton, the lower value to a neutron. In Fig. 11, the value of μ_d is plotted as a function of

$$y = \frac{a_{3/2}}{a_{5/2}}. \tag{Ad. 4}$$

The asymmetry with respect to $y = 0$ is due to the interference terms in (3).

In the region just after O^{16}, the value of $\Delta_{5/2}$ is small compared to the surface coupling (cf., e. g., the level inversion of F^{19}, discussed below) and will therefore be neglected in (1). On the other hand, $\Delta_{3/2}$ is large (~ 5 MeV; cf. KOESTER, JACKSON and ADAIR, 1951). If we ignore the influence of the $d_{3/2}$ state, the resultant state χ_Ω is independent of the parameters of the model and corresponds to $a_s^2 \approx 0.5\, a_d^2$ and $y = 0$.

Even a small $d_{3/2}$ admixture may, however, have a rather large effect on μ_d, due to the interference term. The effect depends essentially on the sign of y (cf. Fig. 11), which is determined by the sign of $\cos\gamma$. In the beginning of the combined $d_{5/2} - s_{1/2}$ shell, it is found that the lowest state has $\Omega = 1/2$ and $\gamma = 0$, corresponding to negative y, and one therefore expects $\mu \approx \mu_{sp}$. At the end of the shell, we have $\gamma = \pi$ and

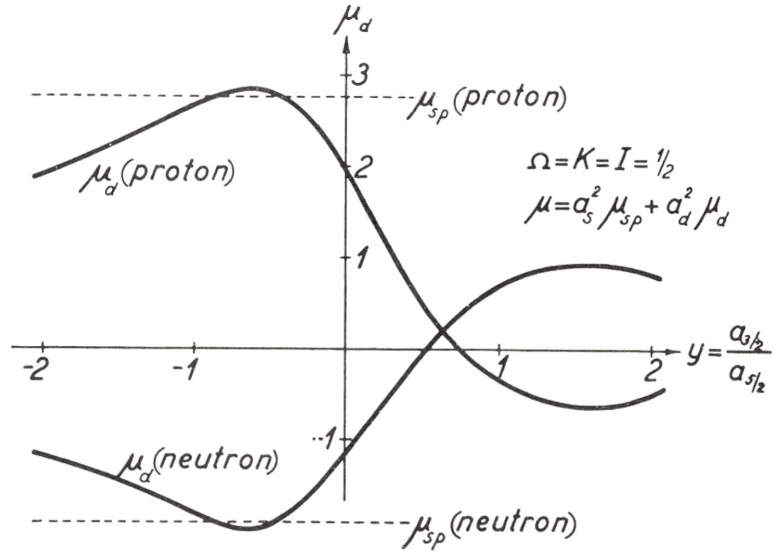

Fig. 11. *Magnetic moments arising from d-state admixture in* $I = \Omega = 1/2$ *states.* In the absence of surface coupling, these states would be pure $s_{1/2}$, but the coupling may introduce large amplitudes of neighbouring particle orbitals, especially d states. In the region after O^{16}, the $s_{1/2}$ and $d_{5/2}$ states are close-lying and one obtains, in strong coupling, $a_s^2 \sim \frac{1}{3}$ and $a_d^2 \sim \frac{2}{3}$. The $s_{1/2}$ state part of the magnetic moment remains equal to the single-particle value, but the d state moment is very sensitive to a small admixture of $d_{3/2}$ state. The figure gives μ_d as a function of the relative amplitude y of the $d_{3/2}$ state, which can be obtained from (1). The strong asymmetry of μ_d with respect to $y = 0$ implies that the moment is especially sensitive to the sign of y, which again depends on the sign of the deformation ($y < 0$ for $\gamma = 0$; $y > 0$ for $\gamma = \pi$).

positive y, and very large moment shifts, of one or two magnetons, may occur.

Thus, the striking difference between the F, and the Si and P moments may be understood in terms of the opposite shapes of the nuclear surface. The moment of F^{19} with a single proton ($y < 0$) can be approximately accounted for by any deformation $\beta \gtrsim 0.1$. In the case of P^{31} and Si^{29}, where the odd configuration is that of a single hole, the μ-values are more sensitive to y, and the empirical moments indicate $y \approx 0.5$. Such a value of y would be obtained, if $\Delta_{3/2} \sim 5$ MeV, for a deformation of $\beta \sim 0.4$ (cf. Table VII). A deformation of this order of magnitude is consistent with the hydrodynamical values for the surface parameters.

A perturbation calculation of the effects of the surface coupling on the magnetic moments gives similar characteristic differences between F^{19} and P^{31}, due to the influence of the $d_{5/2} - d_{3/2}$ interference. However, the magnitude of the observed shifts shows that we are outside the perturbation region and indicates that the strong coupling situation may be approximately realized.

The level shifts arising from the coupling of the $s_{1/2}$ and $d_{5/2}$ levels to the surface may explain the difference in ground state spin between F^{17} ($I = 5/2$) and F^{19} ($I = 1/2$). The comparison of the coupling energy (1) for $\Omega = 1/2$ with that corresponding to $\Omega = 5/2$ shows that the surface coupling favours the spin $I = 1/2$. Thus, the increased deformation in F^{19} as compared with F^{17}, resulting from the addition of the two neutrons, depresses the $I = 1/2$ level with respect to the $I = 5/2$ level.

In the case of Tl^{203} and Tl^{205}, the $s_{1/2}$ and $d_{3/2}$ states are near-lying, while the $d_{5/2}$ state is about an MeV lower. The equilibrium shape is expected to be $\gamma = \pi$ and, if one first ignores the influence of the $d_{5/2}$ state, one finds $a_s^2 = 0.5\, a_d^2$, which corresponds to a magnetic moment $\mu = 1.20$. However, the presence of the $d_{5/2}$ state will tend to increase the moment somewhat (leads to large negative values of y). Similarly, the expected small negative value of $\Delta_{3/2}$ increases a_s^2 and thereby also the moment.

The remaining nuclei, listed in Table X, cannot be studied in as much detail as the above cases due to lack of knowledge of configuration assignments.

ii. $(1/2-)$ *nuclei.*

A striking feature of the empirical moments of this type of nuclei, as compared with all other types, is the close grouping of the values (cf. also Figs. 7 and 8). Apart from the two lightest nuclei, N^{15} and C^{13}, the moments are closely clustered around the values $\mu = -0.12$ for odd proton nuclei, and $\mu = +0.56$ for odd neutron nuclei.

This characteristic feature is a simple consequence of the present model and is largely independent of the coupling. The main interacting states which produce the coupling to the surface are here $p_{3/2}$ and $f_{5/2}$. In perturbation approximation one obtains, from (IV. 7) and Table V, the resulting shift

$$\delta\mu = \begin{Bmatrix} -0.22 \\ +0.18 \end{Bmatrix} \left(\frac{\hbar\omega}{\hbar\omega + |\Delta_{3/2}|}\right)^2 x^2 + \begin{Bmatrix} 0.22 \\ -0.18 \end{Bmatrix} \left(\frac{\hbar\omega}{\hbar\omega + |\Delta_{5/2}|}\right)^2 x^2. \quad \text{(Ad. 5)}$$

Except for N^{15} and C^{13}, one expects $\Delta_{3/2} \sim \Delta_{5/2} \lesssim \hbar\omega$, and so the moment shift practically vanishes.

A similar situation is found when the coupling is strong. The potential energy matrix is then the same as (1), and $\delta\mu$ takes the form

$$\delta\mu = -\begin{Bmatrix} 0.55 \\ -0.45 \end{Bmatrix} a_{3/2}^2 + \begin{Bmatrix} 0.37 \\ -0.30 \end{Bmatrix} a_{5/2}^2. \quad \text{(Ad. 6)}$$

Diagonalizing W' under the assumption $\Delta_{3/2} \sim \Delta_{5/2}$, one finds that, irrespective of Δ, the ground state has $a_{3/2}^2 \sim 0.67\ a_{5/2}^2$, so that $\delta\mu$ practically vanishes.

The absence of a near-lying $f_{5/2}$ state in C^{13} and N^{15} implies a small moment shift outwards from the main group, as is observed. For these nuclei, the large separation of the $p_{1/2}$ level from the combining $p_{3/2}$ level implies a rather weak coupling and from (5) one obtains shifts of the order of 0.1 magneton, assuming $\Delta_{3/2} \sim -5$ MeV and hydrodynamical surface parameters. A similar effect would be obtained in strong coupling (cf. Table VII).

Although the surface coupling thus accounts for the relative values of the observed moments, the position of the main group of empirical values does not quite coincide with the single-particle moment, which might be expected from the above calculations. There thus exists a small residual moment shift, common to all these nuclei, and it is tempting to consider the pos-

TABLE XI. Moments of (1/2 —) nuclei.

odd proton ($\mu_{sp} = -0.26$)		odd neutron ($\mu_{sp} = +0.64$)	
nucleus	μ	nucleus	μ
$_{7}N^{15}$	−0.28	$_{6}C^{13}$	0.70
$_{39}Y^{89}$	−0.14	$_{34}Se^{77}$	0.53 **
$_{45}Rh^{103}$	−0.10 *	$_{70}Yb^{171}$	0.5
$_{47}Ag^{107}$	−0.11	$_{78}Pt^{195}$	0.61
$_{47}Ag^{109}$	−0.13	$_{80}Hg^{199}$	0.50
		$_{82}Pb^{207}$	0.59

* KUHN and WOODGATE (1951).
** DHARMATTI and WEAVER (1952a).

sibility that we may here be observing an interaction effect of the type mentioned on p. 51. This interpretation would require that the individual nucleons embedded in nuclear matter suffer a reduction in the magnitude of their intrinsic magnetic moments of $\delta\mu_s \sim 0.3$ nuclear magnetons.

iii. (3/2 —) *nuclei.*

TABLE XII. Moments of (3/2 —) nuclei.

odd proton ($\mu_{sp} = 3.79$)			odd neutron (μ_{sp}) $= -1.91$		
nucleus	μ	Q	nucleus	μ	Q
$_5B^{11}$	2.69	+0.06 (M) *	$_4Be^9$	−1.18	
$_{29}Cu^{63}$	2.23	−0.13 (C)	$_{24}Cr^{53}$	−0.47 §§§	
$_{29}Cu^{65}$	2.38	−0.12 (C)	$_{28}Ni^{61}$	$\lesssim(\pm)0.2$ §	
$_{31}Ga^{69}$	2.02	+0.24 (A)	$_{76}Os^{189}$	+0.7 §§	+2 (A) §§
$_{31}Ga^{71}$	2.56	+0.15 (A)	$_{80}Hg^{201}$	−0.56	+0.5 (A)
$_{33}As^{75}$	1.44	+0.3 (A) †			
$_{35}Br^{79}$	2.11	+0.34 (A) ††			
$_{35}Br^{81}$	2.27	+0.28 (A) ††			
$_{37}Rb^{87}$	2.75				

* DEHMELT (1952).
† MURAKAWA and SUWA (1952).
†† KING and JACCARINO (1953).
§ KESSLER (1950).
§§ MURAKAWA and SUWA (1952 a).
§§§ ALDER and HALBACH (1953) (added in proof).

In the first $p_{3/2}$ shell, the moments seem to give some indication of deviations from (*jj*) coupling (cf. also INGLIS, 1952 and KURATH, 1952 a). The description of B^{11} as a single $p_{3/2}$ hole, coupled to the surface, does imply a rather large moment shift, but in order to account for the observed moment, a coupling strength of $x \sim 3$ is required (cf. Fig. 5 and (IV.5)). This value of x is several times larger than the hydrodynamical estimate, which may reflect a partial breaking up of the $p_{3/2}$ shells. For Be^9, with a $((p_{3/2})^{-2}; (p_{3/2})^{-1})$ configuration, the observed moment is close to that expected in the absence of surface coupling ($\mu_p = -1.15$; cf. Table III). However, a perturbation estimate as well as the strong coupling treatment (cf. Ap. III.ii) indicate that the surface coupling should produce a reduction in the magnitude of the moment by a few tenths of a magneton (cf. Table VII).

In the higher $p_{3/2}$ shells, a strong interaction is expected between the neighbouring $p_{3/2}$ and $f_{5/2}$ levels. While a pure $j = 3/2$ state has the anomalous strong coupling behaviour, considered in Ap. III.ii, the $p_{3/2} - f_{5/2}$ interaction may lead to a stabilization of the surface shape and the usual strong coupling scheme. For a single $p_{3/2} - f_{5/2}$ particle, the $\Omega = 3/2$ state with

$$W' = \begin{pmatrix} 0 & 0 \\ 0 & \Delta_{5/2} \end{pmatrix} + k\beta \cos\gamma \sqrt{\frac{5}{4\pi}} \frac{1}{35} \begin{pmatrix} 7 & 6 \\ 6 & -2 \end{pmatrix} \qquad \text{(Ad. 7)}$$

is expected to represent the ground state if $\Delta_{5/2} > 0$. For small values of $\Delta_{5/2}$, one finds for this state $a_{3/2} \approx 2\,a_{5/2}$. A similar situation is found for a $p_{3/2} - f_{5/2}$ hole if $\Delta_{5/2} < 0$. The magnetic moment for this state is $\mu_c \approx \left\{ \begin{matrix} 2.15 \\ -0.55 \end{matrix} \right\}$. Thus, a rather fully developed strong coupling may account for the moments of Cr^{53}, $Cu^{63, 65}$, and Rb^{87}, whose odd configurations are those of a single particle or hole.

A contribution to the moment may also arise from a small admixture of $f_{7/2}$, due to interference with the $f_{5/2}$ state. This effect may shift the moment by about 0.1 magneton, inwards for a single-particle configuration (Cu and Cr) and outwards for a hole (Rb), and may thus be partly responsible for the relatively large moment of Rb^{87}. The largeness of this moment may also in part reflect the closed neutron structure which is expected to give rise to a lower deformability and thus to a less developed strong coupling situation.

For the other nuclei in this group, which are essentially many-particle configurations, the analysis is more complex. However, it is expected that, during the simultaneous filling of the $p_{3/2}$ and $f_{5/2}$ levels, $\Omega = 3/2$ ground states will occur in which the last odd particle is predominantly of $f_{5/2}$ character. The large moment shift of As^{75} may indicate such a configuration. It is of interest that the corresponding odd-neutron nucleus, Ni^{61}, seems also to have an especially large moment shift.

The (3/2 —) group of nuclei provides interesting evidence on the correlation between quadrupole moments and magnetic moment shifts. This relationship can especially be studied for

isotopic pairs for which the spectroscopic data are most unambiguously compared. It has been suggested that there is, in such cases, an approximate proportionality between $\delta\mu$ and Q (KOPFERMANN, 1951). The examples of this rule among the (3/2 —) nuclei are listed in Table XIII. The existence of an approximate relationship of this type can be understood from the fact that the major part of $\delta\mu$ is attributed to the approach of the moment to the strong coupling value μ_c and that also Q is relatively insensitive to the coupling strength x. While the deformation in-

TABLE XIII. Correlations between magnetic moments and quadrupole moments for (3/2 —) nuclei.

Element	$\delta\mu_A / \delta\mu_{A+2}$	Q_A / Q_{A+2}
$_{29}Cu^{63,\ 65}$	1.11	1.08 *
$_{31}Ga^{69,\ 71}$	1.44	1.59
$_{35}Br^{79,\ 81}$	1.10	1.20 **

* KRÜGER and MEYER-BERKHOUT (1952).
** DEHMELT and KRÜGER (1951).

creases, the projection factor decreases with x (cf. Fig. 10) and the two effects tend to compensate each other in the relevant coupling region. Thus, for two isotopes, the ratios of the $\delta\mu$'s and the Q's are usually both of order unity and differ from this value in the same direction. From this interpretation it is expected, however, that this particular correlation is not of a general character, and, in fact, counterexamples are anticipated (cf. K, p. 75).

Further evidence for a correlation between $\delta\mu$ and Q may be seen in the general tendency, among the (3/2 —) nuclei in the region $29 \leq Z \leq 37$, for large quadrupole moments to accompany large magnetic moment shifts (cf. MIYAZAWA, 1951 a). Moreover, certain trends in the moments can be understood in terms of the expected deformability of the configurations in question. Thus, the two largest magnetic moments are those of Rb^{87} and Ga^{71}, both with closed neutron shells.

iv. $(3/2+)$ *nuclei.*

TABLE XIV. Moments of $(3/2+)$ nuclei.

odd proton ($\mu_{sp} = 0.12$)			odd neutron ($\mu_{sp} = 1.15$)		
nucleus	μ	Q	nucleus	μ	Q
$_{17}Cl^{35}$	0.82	−0.084 (A)	$_{16}S^{33}$	0.64	−0.08 (M)
$_{17}Cl^{37}$	0.68	−0.066 (A)	$_{16}S^{35}$		+0.06 (M)
$_{19}K^{39}$	0.39		$_{54}Xe^{131}$	0.68 †	−0.12 (A) †
$_{19}K^{41}$	0.22		$_{56}Ba^{135}$	0.83	
$_{77}Ir^{191}$	0.16 *	+1 (A) *	$_{56}Ba^{137}$	0.94	
$_{77}Ir^{193}$	0.17 *	+1 (A) *			
$_{79}Au^{197}$	0.14 **	+0.5 (A) ***			
$_{11}Na^{23}$	2.22		$_{10}Ne^{21}$	< 0	

* MURAKAWA and SUWA (1952 a). *** SIEMENS (1951).
** KELLY (1952). † BOHR, KOCH and RASMUSSEN (1952).

The coupling of a pure $d_{3/2}$ state to the nuclear surface has only little effect on the magnetic moment, due to the rather small value of $(g_j - g_R)$. In intermediate coupling, the moment shift can be obtained from Fig. 5 and (IV.5), and in strong coupling, the approximate treatment in Ap. III.ii indicates a limiting moment shift inwards of only a few tenths of a magneton (cf. Figs. 7 and 8).

While a pure $j = 3/2$ state leads to the anomalous strong coupling scheme with no definite equilibrium shape γ (cf. Ap. III.ii), the interaction of neighbouring orbitals or the presence of an even non-closed structure may lead to a stabilization of the nuclear shape at the positions $\gamma = 0$ or π.

If the shape is such that the ground state has $\Omega = 3/2$ ($\gamma = \pi$ for $(d_{3/2})^{+1}$, or $\gamma = 0$ for $(d_{3/2})^{-1}$), the W' matrix is the same as (7), where $\Delta_{5/2}$ is now negative and represents the spin-orbit splitting. In Fig. 12 is plotted the magnetic moment as a function of $z = a_{5/2}/a_{3/2}$, and one sees the characteristic asymmetry resulting from the interference between the spin-orbit partners. With increasing deformation, the moment moves rapidly away from μ_{sp} for a single-particle configuration ($\gamma = \pi$; $z < 0$) and the opposite way for a hole in the $d_{3/2}$ shell ($\gamma = 0$; $z > 0$).

For the opposite shape ($\gamma = 0$ for $(d_{3/2})^{+1}$, or $\gamma = \pi$ for

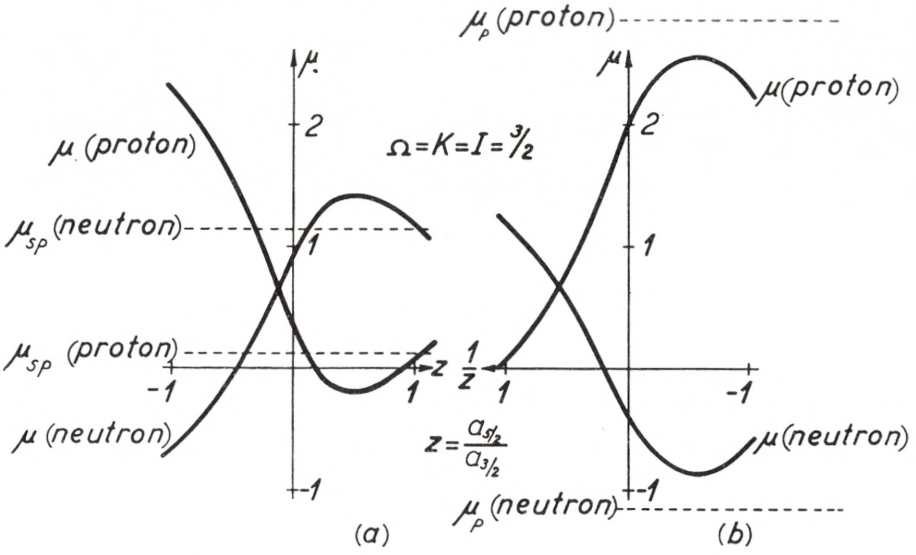

Fig. 12. *Magnetic moments arising from decoupling of spin and orbit in d-states with* $I = \Omega = 3/2$. In states of (3/2+) character, the surface deformation leads to a particle state which is a combination of $d_{3/2}$ and $d_{5/2}$. The figure shows the nuclear magnetic moment for the $I = K = \Omega = 3/2$ state as a function of the ratio of the $d_{5/2}$ and $d_{3/2}$ amplitudes. Fig. 12a gives the moment in the region of predominantly $d_{3/2}$ state and the values μ_{sp} correspond to an uncoupled $d_{3/2}$ nucleon. Fig. 12b gives the moment for a predominantly $d_{5/2}$ state with $\Omega = 3/2$, such as may occur for $(d_{5/2})^3$ configurations. The value of μ_p corresponds to an uncoupled $(d_{5/2})^3{}_{3/2}$ configuration.

$(d_{3/2})^{-1}$), one obtains $K = \Omega = 1/2$, but the ground state still has $I = 3/2$ (cf. II.24). Also the sign of the quadrupole moment is the usual one ($Q < 0$ for $(d_{3/2})^{+1}$ and $Q > 0$ for $(d_{3/2})^{-1}$), since the reversed sign for Q_0 is compensated by a change of sign of the projection factor (V.6). The W' matrix is the same as (1) and the magnetic moment exhibits the same difference between particles and holes as for the $\Omega = 3/2$ state, but the effect is somewhat smaller in magnitude.

The expected trends are found in the empirical magnetic moments which, for the $(d_{3/2})^{+1}$ configurations (S^{33}, $Cl^{35, 37}$, and Xe^{131}), are appreciably shifted inwards with respect to the moments of the $(d_{3/2})^{-1}$ configurations ($K^{39, 41}$, $Ba^{135, 137}$, $Ir^{191, 193}$, and Au^{197}).

In the first $d_{3/2}$ shell, where the level orders are best known, one finds that the coupling to the $d_{5/2}$ and $s_{1/2}$ states favours

the shape $\gamma = \pi$ for the isotopes of S and Cl as well as of K. The presence of two $f_{7/2}$ neutrons in K^{41} further stabilizes this shape. For S^{33} and $Cl^{35, 37}$, the moment values μ_c, listed in Table VII, are obtained from Fig. 12, using $\Delta_{5/2} \sim -5$ MeV, and the observed moments are consistent with a deformation of about $\beta = 0.2$. For $K^{39, 41}$, the μ_c values in Table VII refer to the state ($\gamma = \pi$, $\Omega = 1/2$, $I = 3/2$) and include the influence of the $s_{1/2}$ admixture ($\Delta_{1/2} \sim -5$ MeV).

The influence of a small interaction effect on the nucleon moment, of similar magnitude as that discussed for the (1/2—) nuclei (cf. p. 69), may be indicated by the moment of K^{39}, which is larger by about a tenth of a magneton than the estimated values.

The interpretation of the $K^{39} - K^{41}$ moment differences, as arising from interference with the $d_{5/2}$ level, receives some further support from the measured hyperfine structure anomaly (Ochs, Logan and Kusch, 1950), which gives information on the distribution of the magnetic moment over the nuclear volume (Bohr and Weisskopf, 1950; A. Bohr, 1951a; Eisinger, Bederson and Feld, 1952).

The quadrupole moment ratios in the (3/2+) group provide further interesting information on the coupling scheme. Thus, the decrease of Q from Cl^{35} to Cl^{37} is, as expected, due to the extra deformation caused by the unfilled neutron shell in Cl^{35}, which is also indicated by the observed magnetic moments of these nuclei. The opposite trend would have resulted if the particle forces dominated over the surface coupling, in which case the particle structure in Cl^{35} would have had a quadrupole moment and an effective coupling constant 11/15 times that of Cl^{37} (cf. II.31 and Table III).*

The quadrupole moments of the odd-neutron S isotopes are of the same order of magnitude as those of the neighbouring Cl isotopes, thus confirming the collective nature of these moments. The change of sign of Q from S^{33} to S^{35} is as expected, and the reduction in magnitude can also be understood in terms of the smaller deformability of a shell of 20 than a shell of 16. A determ-

* This conclusion is opposite to that drawn by Flowers (1952c). However, in this case, as well as in others in Table II of this reference, it appears necessary to allow for the difference between adding neutrons at the beginning and end of a shell.

ination of the magnetic moment of S^{35} would be of interest, since its configuration $(d_{3/2})^{-1}$, implies that it should be about a third of a magneton larger than the moment of S^{33}.

As already mentioned, the absolute values of the quadrupole moments of the Cl and S isotopes are considerably smaller than the hydrodynamical estimates (cf. Table IX and the discussion on p. 59). In this connection, it is of interest that the interpretation of the magnetic moments of these nuclei provide independent evidence for appreciable deformations, of the order of those estimated in the hydrodynamical approximation.

Evidence on the quadrupole moments of the K isotopes would be of interest. They are expected to be positive and Q (K^{41}) should be larger than Q (K^{39}) because of the deforming influence of the $f_{7/2}$ neutrons. The larger deformation is also indicated by the magnetic moments which, for these nuclei, decrease with increasing deformation. Such a correlation between Q and $\delta\mu$ is opposite to that usually observed (cf. p. 71).

The two last nuclei in Table XIV, Na^{23} and Ne^{21}, occur during the filling of the $d_{5/2}$ shell and have been classified by the shell model as $(d_{5/2})^3_{3/2}$, The spin $I = j - 1$ indicates that the surface coupling dominates over the particle forces (cf. § III.iii). The strong coupling state is then described by $\Omega = 3/2$ and has a limiting magnetic moment of $\mu_c = \left\{ \begin{matrix} 2.00 \\ -0.42 \end{matrix} \right\}$ for a pure configuration. Small admixtures of the $d_{3/2}$ state will produce shifts from this value, depending on the nuclear shape. For $\gamma = 0$, the moments increase in magnitude, while they decrease for $\gamma = \pi$. From considerations of the level filling in this region, Na^{23} is expected to prefer the $\gamma = 0$ shape (positive Q)*, in accordance with the indication from the observed μ-value (cf. Table VII).

v. $(5/2+)$ *nuclei.*

The magnetic moments of the nuclei in the first $d_{5/2}$ shell may, as already mentioned (cf. Table VI), be interpreted in terms of the coupling of a $d_{5/2}$ state to the nuclear surface. In

* Note added in proof: Recently, P. SAGALYN, working with F. BITTER, has found evidence for a positive quadrupole moment of Na^{23}. (Private communication from Professor BITTER).

TABLE XV. Moments of $(5/2+)$ nuclei.

odd proton ($\mu_{sp} = 4.79$)			odd neutron ($\mu_{sp} = -1.91$)		
nucleus	μ	Q	nucleus	μ	Q
$_{13}Al^{27}$	3.64	+0.16 (A)	$_{8}O^{17}$	−1.89	−0.005 (M)
$_{51}Sb^{121}$	3.36	−1.0 (A)***	$_{12}Mg^{25}$	−0.86	
$_{53}I^{127}$	2.81	−0.6 (A)	$_{40}Zr^{91}$	−1.1 ††	
$_{55}Cs^{131}$	3.48 *		$_{42}Mo^{95}$	−0.91	
$_{59}Pr^{141}$	3.9 **		$_{42}Mo^{97}$	−0.93	
$_{63}Eu^{151}$	3.6	+1.2 (A)	$_{46}Pd^{105}$	−0.6 §	
$_{63}Eu^{153}$	1.6	+2.6 (A)	$_{48}Cd^{111}$ †	−0.7 †	
$_{75}Re^{185}$	3.17	+2.9 (A)			
$_{75}Re^{187}$	3.20	+2.7 (A)			

* BELLAMY and SMITH (1953).
** LEW (1953); BRIX (1953).
*** DEHMELT and KRÜGER (1951 a).
† Refers to excited state ($E = 247$ keV); AEPPLI et al. (1952).
†† SUWA (1952).
§ STEUDEL (1952).

strong coupling, one obtains $\mu_c = \begin{cases} 3.75 \\ -1.04 \end{cases}$, which accounts approximately for the moments of Mg^{25} and Al^{27}.

For O^{17}, the magnetic moment and quadrupole moment are very little affected by the surface coupling, as is expected due to the high stability of the closed-shell core. The Q-value is comparable with the recoil moment (cf. § IVa; see also GESCHWIND et al., 1952), which is about -0.0013. Another measure of the quadrupole moment induced in the core by the odd neutron would be provided by the lifetime of the $(1/2+)$ excited state of O^{17} at 0.8 MeV (cf., e. g., AJZENBERG and LAURITSEN, 1952). The decay is of $E2$ character and, for a pure shell model state, will be determined by the small recoil quadrupole moment. This would lead to a lifetime of $\tau \sim 10^{-7}$ sec., which is longer than for a corresponding single-proton transition by a factor of 10^3 (cf. VII.7). However, the lifetime is very sensitive to impurities in the state.

In the region just beyond nucleon number 50, the $d_{5/2}$ and $g_{7/2}$ levels are near-lying, and nuclei of $(5/2+)$ character are expected to contain components of both orbitals. The ratio of the two orbitals in a state with $\Omega = 5/2$ depends rather sensitively on the spacing $\Delta_{7/2}$ of the $g_{7/2}$ level with respect to the $d_{5/2}$ level.

The spin of Sb^{121} indicates a positive $\Delta_{7/2}$ for this single-proton nucleus. A calculation of the type carried out in the preceding pages then shows that the content of $g_{7/2}$ is quite small ($a_{7/2}^2 \sim 0.1$), corresponding to the rather small deviation of $\mu(Sb^{121})$ from μ_c. While again the moment of Mo^{95} with 3 valence neutrons is consistent with a rather pure $d_{5/2}$, $\Omega = 5/2$ state, the small moment of I^{127} could be interpreted in terms of a negative $\Delta_{7/2}$. Already for small negative $\Delta_{7/2}$ (~ -0.5 MeV), additional moment shifts of the order of a magneton may be obtained.

The remaining $(5/2+)$ nuclei have more complex configurations. An exceptionally large shift is observed for Eu^{153}. It seems possible to account for such large moment shifts in terms of a state with $\Omega = 5/2$, but predominantly of $g_{7/2}$ character. A test of the strong coupling interpretation of this moment would be provided by a measurement of the $M1$ transition probability from the expected $(7/2+)$ rotational state (cf. VI c.iii and VII.20). An analogous situation is found for Yb^{173} (cf. Table XVI).

Further information on the coupling scheme in Eu comes from the anomalously large isotope shift which has been interpreted in terms of the large change in the quadrupole moments of the two isotopes (Brix and Kopfermann, 1949, 1952). Such an effect contributes to the isotope shift an amount δE given by*

$$\frac{\delta E}{\delta E_0} = \frac{15\,A}{8\pi}\frac{\Delta\beta^2}{\Delta A}\left(1 - 0.09\left(\frac{Ze^2}{\hbar c}\right)^2\right) \qquad \text{(Ad. 8)}$$

in units of the normal isotope shift δE_0, corresponding to an increase in the nuclear radius by the amount $\Delta R/R = 1/3\,\Delta A/A$. The change in β^2 is related to that of the intrinsic quadrupole moment (cf. V.7) and, for the contribution to the isotope shift between Eu^{153} and Eu^{151}, one obtains

$$\delta E = 0.056\;\; \Delta Q_0^2\;\; \delta E_0, \qquad \text{(Ad. 9)}$$

where Q_0 is measured in units of 10^{-24} cm^2. Deriving Q_0 from the measured Q by assuming the strong coupling projection factor (V.9), one obtains $\delta E = 2.4\,\delta E_0$, while the omission of the

* This expression is equivalent to formula (4) of Brix and Kopfermann (1949), except for the small relativistic correction which has been calculated by Mr. Jens Bang, to whom we are indebted for informing us of his results.

projection factor gives $\delta E = 0.3\,\delta E_0$. The measured isotope shift of about $2.2\,\delta E_0$ (Brix and Kopfermann, 1952) gives support to the assumption of a rather fully developed strong coupling in these nuclei.

vi. (5/2 —) *nuclei.*

Table XVI. Moments of (5/2 —) nuclei.

odd proton ($\mu_{sp} = 0.86$)		odd neutron ($\mu_{sp} = 1.37$)		
nucleus	μ	nucleus	μ	Q
$_{37}Rb^{85}$	1.35	$_{30}Zn^{67}$	0.88 *	
		$_{70}Yb^{173}$	−0.65	+4.0 (A)
$_{25}Mn^{55}$	3.47			

* Dharmatti and Weaver (1952).

In the first $f_{5/2}$ shell, the main influence of the surface on the magnetic moment is expected from the interference of the $f_{7/2}$ state. The Rb and Zn isotopes, containing a single $f_{5/2}$ hole, should resemble K rather than Cl (cf. p. 73). Thus, the inward moment shift of 0.4 — 0.5 magnetons is somewhat difficult to explain. It may be partly due to the influence of the near-lying $p_{3/2}$ level which, for weak or intermediate couplings, would cause inward moment shifts. Partly it may reveal an interaction effect on the intrinsic nucleon moment, possibly of somewhat larger magnitude than that considered for $p_{1/2}$ and $d_{3/2}$ nuclei.

Some further information on the structure of the Rb^{85} moment may be obtained from the observed hyperfine structure anomaly in the Rb isotopes (Bitter, 1949; Ochs and Kusch, 1952). Previous estimates of the effect (Bohr and Weisskopf, 1950; A. Bohr, 1951 a) are somewhat improved by including an interaction contribution to the nucleon moment (cf. Eisinger, Bederson and Feld, 1952).

The nucleus Mn^{55} occurs during the filling of the $f_{7/2}$ shell and has been classified by the shell model as $(f_{7/2})^{-3}{}_{5/2}$, which would correspond to a magnetic moment of $\mu_p = 4.13$ neglecting the neutron-proton forces. The spin anomaly suggests a rather fully developed strong coupling (cf. § III.iii), for which the magnetic moment is $\mu_c = 3.27$.

vii. (7/2—) *nuclei.*

TABLE XVII. Moments of (7/2—) nuclei.

odd proton ($\mu_{sp} = 5.79$)		odd neutron ($\mu_{sp} = -1.91$)		
nucleus	μ	nucleus	μ	Q
		$_{20}Ca^{43}$	−1.32 §	
$_{21}Sc^{45}$	4.76	$_{22}Ti^{49}$ **	−1.10 **	
$_{23}V^{51}$	5.15	$_{60}Nd^{143}$	−1.0	
$_{27}Co^{57}$	4.6 *	$_{60}Nd^{145}$	−0.6	
$_{27}Co^{59}$	4.65	$_{62}Sm^{147}$	(±) 0.7 †	
		$_{62}Sm^{149}$	(±) 0.6 †	
		$_{68}Er^{167}$		(±) 10 (C) ††

* BAKER et al. (1953).
** JEFFRIES et al. (1952); the mass assignment as well as the spin of the detected Ti isotope are in doubt.
† ELLIOT and STEVENS (1952).
†† BOGLE et al. (1952).
§ JEFFRIES (1953). (Added in proof).

The moments of the nuclei in the first $f_{7/2}$ shell may all be accounted for in terms of the coupling of an $f_{7/2}$ state to the surface. The moments of Sc^{45}, $Co^{57, 59}$, and Ti^{49} are all close to the strong coupling limit $\mu_c = \left\{ \begin{matrix} 4.86 \\ -1.14 \end{matrix} \right\}$, while the larger moment of Ca^{43} and V^{51} may indicate a somewhat weaker coupling, associated with the closed shells in the even structures. This smaller coupling may also be indicated by the fact that the ground state spin equals j rather than $j - 1$ for these $(j)^3$ configurations (cf. § III.iii).

viii. (7/2+) *nuclei.*

Due to the simultaneous filling of the $d_{5/2}$, $g_{7/2}$, and $h_{11/2}$ shells, most of the nuclei in this group possess complex configurations. One may attempt, however, a more detailed discussion of Sb^{123} with its single-proton configuration. In strong coupling, the main influence of the surface on the magnetic moment is expected from the small admixture of $g_{9/2}$ to the predominantly $g_{7/2}$ state. For a pure $g_{7/2}$ state, the strong coupling moment is very close to μ_{sp} (cf. Fig. 7). Since Sb^{123} with a single particle is analogous to Cl rather than to K (cf. p. 73), the interference of the spin orbit partner will increase the moment. The effect

TABLE XVIII. Moments of (7/2 +) nuclei.

odd proton ($\mu_{sp} = 1.72$)			odd neutron ($\mu_{sp} = 1.49$)	
nucleus	μ	Q	nucleus	Q
$_{51}Sb^{123}$	2.55	−1.2 (A)	$_{34}Se^{79}$	+1.2 (M) †
$_{53}I^{129}$	2.62	−0.44 (A)		
$_{55}Cs^{133}$	2.58	<0.3 (A)		
$_{55}Cs^{135}$	2.73			
$_{55}Cs^{137}$	2.84			
$_{57}La^{139}$	2.78			
$_{71}Lu^{175}$	2.9	+6.5 (A)		
$_{73}Ta^{181}$	2.1 *	+6.5 (A) *		

* BROWN and TOMBOULIAN (1952). † HARDY et al. (1952).

depends on the relative magnitude of $k\beta$ and $\Delta_{9/2}$, and assuming values of $\beta \approx 0.2$ and $\Delta_{9/2} \approx -2$ MeV, one obtains $\mu = 2.3$.

The nuclei having neutron configurations in the neighbourhood of the closed shell at 82 are expected to have relatively small deformability and there is evidence for a small quadrupole moment of the stable Cs isotope, Cs^{133}. For these nuclei, the surface should play a lesser role in causing magnetic moment shifts. However, the complex configurations in question make it difficult to decide whether the observed moment shifts can be explained by the particle structure itself or whether some additional effects are operating.

In Se^{79}, one expects a predominantly $(g_{9/2})^5$ neutron configuration. Such a half filled shell will in itself generate no quadrupole moment, although it may produce a large nuclear deformation (cf. § II c.ii and § III.iii). The observed positive sign of Q may be the result of the proton structure which is expected to favour a prolate shape.

ix. (9/2 +) *nuclei.*

The major part of the magnetic moment shifts for these nuclei may be accounted for in terms of the coupling between a $g_{9/2}$ state and the surface, which leads to the strong coupling moment $\mu_c = \left\{ \begin{matrix} 5.93 \\ -1.20 \end{matrix} \right\}$. In some cases, such as In, additional effects must be present, possibly in part due to interaction contributions to the nucleon moment.

TABLE XIX. Moments of (9/2 +) nuclei.

odd proton ($\mu_{sp} = 6.79$)			odd neutron ($\mu_{sp} = -1.91$)		
nucleus	μ	Q	nucleus	μ	Q
$_{41}Nb^{93}$	6.17		$_{32}Ge^{73}$		−0.2 (M)
$_{43}Tc^{99}$	5.68 *		$_{36}Kr^{83}$	−0.97	+0.16 (A)
$_{49}In^{113}$	5.49	+1.18 (A)	$_{38}Sr^{87}$	−1.1	
$_{49}In^{115}$	5.50	+1.20 (A)			

* WALCHLI et al. (1952).

x. (9/2 —) *nuclei.*

TABLE XX. Moments of (9/2 —) nuclei.

odd proton ($\mu_{sp} = 2.62$)		
nucleus	μ	Q
$_{83}Bi^{209}$	4.08	−0.4 (A)

The closed-shell structure of the Pb^{208} core implies a very small deformability, as is confirmed by the observed quadrupole moment of Bi^{209}, which is of the order of the single-particle value (cf. Table IX). However, in contrast to the case of O^{17}, the magnetic moment of Bi^{209} is very strongly shifted from the single-particle value. This moment shift is even larger than would have been expected for a normally deformable nucleus (cf. the case of Sb^{123}, p. 79). Since the observed quadrupole moment supports the expected negligible effect of the surface on the coupling scheme of this nucleus, it is probable that the magnetic moment reveals some as yet unexplained aspect of the particle structure. If the shift is interpreted as an interaction effect, the intrinsic proton moment is reduced to one magneton, a reduction many times larger than that indicated by the magnetic moments of other nuclei (cf. p. 52).

xi. *Odd-odd nuclei.*

For the self-mirrored nuclei ($N = Z$), the symmetry between neutrons and protons implies that the total g-factor will almost always be close to 0.5 and be insensitive to the detailed coupling

TABLE XXI. Moments of odd-odd nuclei.

Nucleus	Configurations		I	μ	Q
	protons	neutrons			
$_5B^{10}$	$(p_{3/2})^{-1}$	$(p_{3/2})^{-1}$	3	1.80	+0.13 (M) §§
$_7N^{14}$	$p_{1/2}$	$p_{1/2}$	1	0.40	+0.02 (M)
$_{11}Na^{22}$	$(d_{5/2})^3$	$(d_{5/2})^3$	3	1.75	
$_{11}Na^{24}$	$(d_{5/2})^3$	$(d_{5/2})^{-1}$	4	1.69 *	
$_{17}Cl^{36}$	$d_{3/2}$	$(d_{3/2})^{-1}$	2		−0.018 (M,A)
$_{19}K^{40}$	$(d_{3/2})^{-1}$	$f_{7/2}$	4	−1.30 **	
$_{19}K^{42}$	$(d_{3/2})^{-1}$	$(f_{7/2})^3$	2	−1.14 *	
$_{23}V^{50}$	$(f_{7/2})^3$	$(f_{7/2})^{-1}$	6 §	3.35 ***	
$_{27}Co^{58}$	$(f_{7/2})^{-1}$	$(p_{3/2}, f_{5/2})^3$	2	3.5 †	
$_{27}Co^{60}$	$(f_{7/2})^{-1}$	$(p_{3/2}, f_{5/2})^5$	5	3.3 † ††	
$_{37}Rb^{86}$	$(p_{3/2}, f_{5/2})^{-1}$	$(g_{9/2})^{-1}$	2	−1.69 *	
$_{55}Cs^{134}$			4	2.96 * †††	
$_{71}Lu^{176}$			$\geqslant 7$	4.2	+8 (A)

* BELLAMY and SMITH (1953).
** EISINGER et al. (1952).
*** WALCHLI et al. (1952 a).
† DANIELS et al. (1952).
†† GORTER at al. (1952).
††† JACCARINO et al. (1952).
§ KIKUTCHI et al. (1952).
§§ DEHMELT (1952).

scheme (cf. TALMI, 1951). For nuclei of this type, it is indeed found that μ_c and μ_p are nearly the same and agree closely with the observed moments.

For B^{10}, the μ_c value listed in Table VII refers to a state with $\Omega_{\text{prot}} = \Omega_{\text{neut}} = 3/2$ $(I = K = \Omega = 3)$ and pure $p_{3/2}$ configurations. In the case of N^{14}, the listed μ_c values refer to the state $\Omega_{\text{prot}} = \Omega_{\text{neut}} = 1/2$ $(I = K = \Omega = 1)$, and take into account the $p_{3/2}$ admixture.

For Na^{22}, the strong surface coupling leads to a state with $\Omega_{\text{prot}} = \Omega_{\text{neut}} = 3/2$ $(I = K = \Omega = 3)$. For pure $d_{5/2}$ orbitals, one obtains $\mu_c = 1.67$. For the expected nuclear shape $(\gamma = 0)$, the interference of the $d_{3/2}$ state tends slightly to increase μ, but, due to the neutron-proton symmetry, the effect is small, amounting to only 0.1 magneton for a deformation of $\beta \sim 0.3$ (cf. Table VII).

The corresponding interference effect is much larger in Na^{24} $(\Omega_{\text{prot}} = 3/2,\ \Omega_{\text{neut}} = 5/2)$, since it does not affect the neutron state. Neglecting the $d_{3/2}$ admixture, the strong coupling moment is $\mu_c = 1.13$, but the observed moment can be accounted for by a deformation of the same magnitude as considered for Na^{22}

(cf. Table VII). The shell model magnetic moment of Na^{24} depends upon the nuclear forces and is not made unique by the assumption of charge symmetry.

For K^{40} ($\Omega_{prot} = 1/2$, $\Omega_{neut} = 7/2$), the strong coupling magnetic moment for a pure configuration is $\mu_c = -1.14$, while the interference of the $d_{3/2}$ orbital and the admixture of $s_{1/2}$ in the proton state decreases the magnitude of the moment (cf. Table VII). The shell model gives $\mu_p = -1.68$. The observed moment thus indicates an intermediate coupling situation, consistent with the proximity to the doubly closed shell at Ca^{40}.

In K^{42}, the extreme strong coupling ($\Omega_{prot} = -1/2$, $\Omega_{neut} = 5/2$) with pure configurations gives $\mu_c = -0.65$. Additional shifts arise from admixtures of $f_{5/2}$ orbital to the neutron state, and $d_{5/2}$ and $s_{1/2}$ orbitals to the proton state. The μ_c values in Table VII are based on $\Delta(f_{5/2}) \sim 5$ MeV, $\Delta(d_{5/2}) \sim -5$ MeV, and $\Delta(s_{1/2}) \sim -5$ MeV.

For V^{50}, the coupling scheme arising from particle forces has been discussed and for forces of zero range a ground state of $I = 6$ has been obtained (Hitchcock, 1952) with $\mu_p = 3.21$*. However, forces of the expected range appear to favour $I = 5$. The effect of the surface coupling is somewhat complicated, since in strong coupling the neutrons and protons favour different surface shapes, with the result that neither $\gamma = 0$ nor π are stable positions.

The two Co isotopes can be accounted for by the strong coupling states ($\gamma = 0$, and $\Omega_{prot} = 7/2$; $\Omega_{neut} = \pm 3/2$), the upper sign referring to Co^{60}, the lower to Co^{58}. However, the great difference in the observed g-factors indicates a difference in the nature of the $|\Omega| = 3/2$ neutron states. Thus, for Co^{58}, the observed moment indicates a predominantly $f_{5/2}$ neutron state which leads to a strong coupling moment of $\mu_c = 3.61$, while, for Co^{60}, a predominantly $p_{3/2}$ neutron state, giving $\mu_c = 3.60$, is indicated. It is of interest that similar effects in the filling of the $p_{3/2}$, $f_{5/2}$ shells seem to occur in the $I = 3/2$ odd-A nuclei in this region (cf. p. 70).

The Rb^{86} nucleus can be described in terms of a single proton and a single neutron (cf. Table II). The observed spin of 2 suggests a $f_{5/2}$ assignment for the proton hole, which leads to the

*) Private communication from Dr. A. Hitchcock.

strong coupling moment $\mu_c = -1.56$. The shell model value for this configuration is $\mu_p = -2.13$.

Additional evidence on the nuclear states in question may be obtained from the observed quadrupole moments.

For the case of B^{10}, although the absolute magnitude of Q is probably rather uncertain, the observed ratio $Q(B^{10})/Q(B^{11}) = 2.08$ (DEHMELT, 1952) is significant. According to the (jj) coupling shell model, this ratio should be unity, whereas the surface coupling gives a ratio of about two.

The evidence for a moderate quadrupole moment for N^{14} indicates appreciable impurities in the listed configuration (cf. also the β-decay of C^{14}).

The Cl^{36} nucleus has the symmetry associated with the fact that the neutron structure is obtained from the proton structure by replacing particles with holes (cf. § IIc.ii). Neglecting inter-configuration effects, the quadrupole moment therefore vanishes, as also for the shell model state. The influence of the coupling to the $d_{5/2}$ and $s_{1/2}$ states favours the shape $\gamma = \pi$, and gives rise to a small negative Q value.

VI. Nuclear Level Structure.

a) General Features of Levels in the Coupled System.

The nuclear level spectrum, resulting from the interplay of particle and collective motion, depends essentially on the strength of the coupling. For weak coupling, there is associated with each particle level a spectrum of excited states with a spacing corresponding to the phonon energy (cf. Fig. 2 for the hydrodynamic estimate of $\hbar\omega$, which yields about 2 MeV for the quadrupole oscillations of a medium heavy nucleus). With increasing coupling, the two level structures become essentially interwoven. For intermediate coupling strength, a rather complicated spectrum may result but, in the limit of strong coupling, the low energy nuclear spectrum acquires a relative simplicity which bears some analogy to molecular spectra.

The strongly coupled nucleus thus exhibits two different types of excitation: The first corresponds to a change of state of the particle motion relative to the deformed surface and is in general associated with a readjustment of the surface. Such particle excitations are analogous to electronic transitions in molecules. The second type of excitation is a collective excitation corresponding to vibration or rotation of the coupled particle-surface system, and is the analogue of vibrational and rotational molecular transitions. While the energies of particle excitations depend on the configuration energies in the deformed nucleus, the vibrational quanta are of the order of the phonon energy. The rotational energies decrease strongly with increasing nuclear deformation and may become much smaller than the phonon energy.

The collective and particle excitations possess very distinct properties. Thus, it is characteristic of the collective excitations that levels of the same family have the same parity and small spin changes between neighbouring states ($\Delta I = 1$ or 2). In

contrast, particle excitations may involve change of parity as well as large spin changes. Further, the character of a given excitation reveals itself in the transition probability. While the particle transitions are in general slowed down by the differences in the surface shape of the combining states, the large electric quadrupole of the oscillating surface may greatly enhance the radiative probability for collective transitions.

With increasing excitation energy, the spacing of both particle and collective states rapidly decreases, and even a small perturbation in the ordered motion is sufficient to destroy any simple coupling scheme. In such a situation, the only remaining constants of the motion are the parity and total angular momentum. Still, provided the interactions are not so strong that they prevent the system from completing even a few periods of the simple particle or surface motion between energy exchanges, some of the gross features of the unperturbed level spectrum are preserved.

In the region of high excitation, additional types of collective motion, such as surface oscillations of higher order and compressive oscillations, may play an important role. Further, the number of excitable particle degrees of freedom increases. Finally, for the very high energies, at which an appreciable fraction of the nucleons is simultaneously excited, the distinction between particle and collective degrees of freedom ceases to have a simple significance.

b) Particle Excitations.

For each particle configuration there exists a lowest level in the coupled system which, as discussed in Chapter III, usually has the same spin and parity as the pure particle state. If the nucleus possesses several neighbouring configurations, there will thus be corresponding states in the low energy spectrum which, as regards spin and parity, may be classified by means of the shell model.

Striking evidence for such particle excitations is afforded by the occurrence of low-lying states with a spin very different from that of the ground state and often with different parity. These states give rise to the long lived isomers, whose interpretation has provided such an important support for the shell model (Gold-

HABER and SUNYAR, 1951; MOSZKOWSKI, 1951). The transition probabilities of these states, however, are found to be smaller than shell model estimates by a considerable factor, indicating that the excitations cannot be described in terms of particles moving in a fixed potential, but involve the surface readjustments characteristic of the particle transitions in the strongly coupled system (BOHR and MOTTELSON, 1952; cf. also § VII d.i).

The β-decays constitute another group of particle transitions in the classification of which the shell model has been a valuable guide (MAYER, MOSZKOWSKI and NORDHEIM, 1951; NORDHEIM, 1951). Again the observed transition probabilities are in general reduced as compared with shell model estimates, indicating the influence of a rather strong surface coupling (§ VIIIc.ii and iv).

The particle transitions also exhibit other features which may be attributed to the influence of the surface coupling. Thus, selection rules appropriate to the motion of particles in a spherical potential are often violated (l- and j-forbiddenness, cf. § VIIIc.iii and § VIIc.ii). The occurrence of such transitions provides evidence for configuration admixtures of a similar type as discussed for the magnetic moments (cf. § IVc).

The relative position of particle levels may depend on the nuclear deformation which can cause level shifts of the order of a few MeV* (cf., e. g., the spin difference of the F-isotopes, p. 67). Also the level order of the particle states within a many-particle configuration depends in an important way on the surface coupling (cf. § III.iii).

In the strong coupling scheme, particle modes of excitation which do not involve change of configuration, but only changes in the Ω_p quantum numbers, in general require a rather large energy. In cases where there are special degeneracies, however, they may occur among the lowest states. Thus, in strong coupling, the ground states of odd-odd nuclei are expected to be close doublets, the members of which have the same parity, but may differ appreciably in spin (cf. § IIc.ii). There seems to be evidence in spectra of odd-odd nuclei for a rather general occurrence

* Such a contribution to the nuclear energy may be interesting in connection with the estimates of the spin-orbit energy and pairing effects obtained from the analysis of binding energies (HARVEY, 1951; SUESS and JENSEN, 1952). Moreover, it may be significant in influencing the trends in the separations of isomeric levels (HILL, 1950; MITCHELL, 1951; GOLDHABER and HILL, 1952).

of such doublets (cf., e. g., GOLDHABER and HILL, 1952). Since the two members of the doublet have approximately the same shape, the γ-transition between them should be somewhat faster than most other particle transitions of similar type (cf. § VII d.i).

While in regions removed from closed shells, the particle excitation spectrum is thus essentially modified by the coupling to the nuclear deformation, the particle-surface coupling is expected to be rather ineffective in the immediate vicinity of major closed shells. These regions should offer relatively favourable conditions for studying the particle level order in a spherical nucleus and the effects of particle forces (cf., e. g., INGLIS, 1952; PRYCE, 1952).

In the light nuclei, the study of excited states by means of nuclear reactions has revealed levels, especially in the neighbourhood of He^4, C^{12}, and O^{16}, which correspond approximately to single-particle excitations in the uncoupled system (cf., e. g., KOESTER, JACKSON and ADAIR, 1951; and also AJZENBERG and LAURITSEN, 1952). These levels are identified by their reduced widths which are comparable to those of single-particle scattering in a fixed potential.

In the region around Pb^{208}, pure particle transitions may also be encountered (PRYCE, 1952; HARVEY, 1953). Lifetimes are here an important guide in interpreting the level scheme (cf. Chapter VII, and especially pp. 117 and 112, for comments on the Pb^{204} and Pb^{207} isomeric transitions).

c) Collective Excitations.

i. *Excitation of closed-shell nuclei.*

The weak coupling situation expected in the immediate vicinity of major closed-shells implies that the collective excitations are essentially of the simple phonon character.

The closed-shell nuclei themselves are of special interest. One here expects among the first excited states a $(2+)$ level, representing an approximately free surface oscillation of the quadrupole type. States of $(2+)$ character have been observed in ${}_8O^{16}$ and ${}_{82}Pb^{208}$ (the 3.8 MeV state in ${}_{20}Ca^{40}$ is also a possible example) and are difficult to interpret as particle excita-

tions (cf. PRYCE, 1952). Lifetime measurements for these states would provide crucial evidence regarding the nature of the excitation, since the phonon decay probability is much larger than that of a particle transition (cf. § VII b.i).

The fact that the first excited state of Pb^{208} ($E = 2.62$ MeV; $I = 2(+)$) is considerably in excess of the phonon energy ($\hbar\omega = 1.3$ MeV), calculated in the hydrodynamic approximation, supports the expectation of a very low deformability for such a doubly closed-shell structure (cf. Ap. I).

The O^{16} nucleus has, as one of the very few exceptions among even-even nuclei, a $(0+)$ first excited state. This state is difficult to account for as a particle excitation, especially because of its parity. One is driven to assume a two-particle excitation from $p_{1/2}$ into $d_{5/2}$ or $s_{1/2}$ orbits, which cannot, however, account for the observed rather large transition probability for pair emission (cf. AJZENBERG and LAURITSEN, 1952). It is possible that we here encounter a compressive oscillation of lowest order*. That such an excitation mode, in this special case, lies lower than the lowest surface excitation is perhaps not surprising, considering the large ratio of surface to volume energy for such a light nucleus and the fact that its closed-shell structure favours excitation modes which do not destroy its spherical symmetry.

ii. *Rotational states in even-even nuclei.*

For the strongly deformed nuclei, encountered in regions away from closed shells, the collective excitations can be characterized as vibrations and rotations**.

Especially characteristic of the strong coupling spectrum are the rotational states which may have energies much smaller than the phonon energy. These low-lying states correspond to rotations about an axis perpendicular to the nuclear symmetry

* This interpretation is rather similar to that of the α-particle model which describes the excitation of the $(0+)$ state as due to a radial oscillation of the whole structure (DENNISON, 1940).

** FORD (1953) has calculated excitation energies for a number of configurations, using the strong coupling representation. For the states considered, involving one or a few particles outside of closed shells, the limiting strong coupling situation is not well developed, and the spectra do not exhibit the regularities discussed in the present paragraph. In such cases, it seems necessary to employ methods appropriate to an intermediate coupling situation (cf. the more detailed calculations of D. C. CHOUDHURY, referred to in footnote on p. 24).

axis (cf. Fig. 3) and are labeled by varying I, for fixed values of Ω, K, n_β, and n_γ. Rotations about the nuclear axis, labeled by varying K, have energies which, in most cases, remain of the order of the phonon energy, and these excitations are considered together with the vibrational states (§ VIc.iv).

A special regularity in the collective spectrum occurs for the even-even nuclei, which have in their ground state $I = K = \Omega = 0$ (cf. § III.ii). The expected cylindrically symmetric deformation ($\gamma = 0$ or π) leads to rotational states with even I and with $K = \Omega = 0$. The odd values of I do not occur, since such states would have odd parity (cf. § IIc.ii for the appropriate symmetry properties of the wave function). From (II.30) we get for the rotational excitation energies

$$E_I = \frac{\hbar^2}{2\Im} I(I+1) \quad \underset{\text{even parity}}{I = 0, 2, 4 \cdots} \tag{VI.1}$$

where the moment of inertia $\Im$ is given by (cf. II.25)

$$\Im = 3 B \beta^2 \tag{VI.2}$$

in terms of the nuclear equilibrium deformation β and the mass parameter B (cf. II.5).

The spectrum (1) is the same as that for the rotation of a rigid body, but the rotational motion arises in essentially different ways in the two cases. The collective motion in the nucleus is of irrotational character (cf. p. 11), and the angular momentum is carried only by the surface waves. The effective moment of inertia associated with this motion depends on the square of the amplitude of the waves (cf. (2)), in a similar manner as the momentum in a sound wave is proportional to the square of the amplitude of oscillation.

Deviations from the limiting strong coupling scheme imply corrections to the spectrum (1). Some of these have the same I-dependence as (1) and give rise to corrections to the moment of inertia (2). Others involve higher powers of I and produce a distortion of the spectrum. Thus, the rotation-vibration interaction (cf., e. g., Herzberg 1950; Nielsen, 1951), which implies that β increases somewhat with I due to centrifugal distortions, gives to first order the energy shift

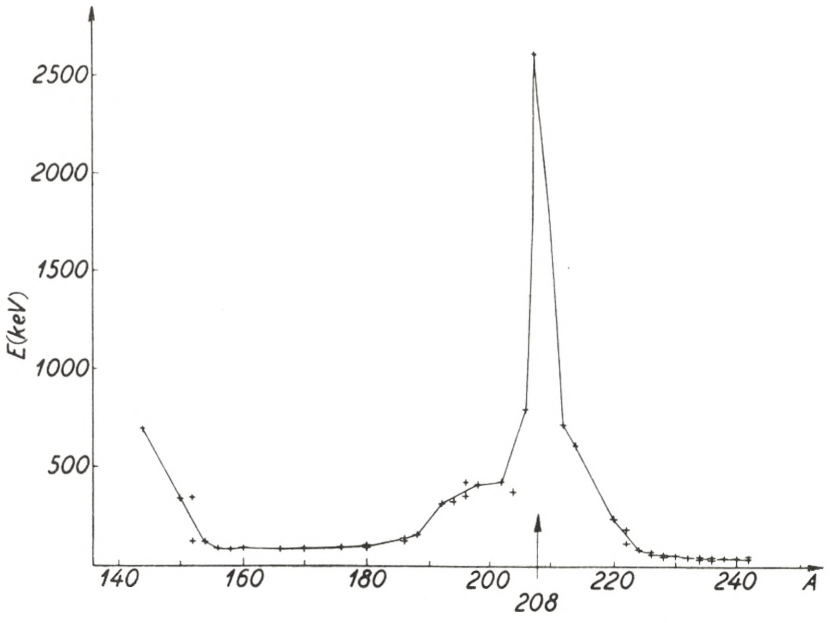

Fig. 13. *First excited states in even-even nuclei with* $A > 140$. The energy of the first excited state is plotted as a function of A. The data is taken from HOLLANDER, PERLMAN and SEABORG (1952) and from SCHARFF-GOLDHABER (1953). The evidence is consistent with a (2+) assignment for all the levels. Similar curves have been given by STÄHELIN and PREISWERK (1951), ROSENBLUM and VALADARES (1952), ASARO and PERLMAN (1952), and SCHARFF-GOLDHABER (1952, 1953).

$$(\Delta E_I)_1 = -2\frac{E_I}{C\beta^2}E_I = -\frac{3}{2}\left(\frac{1}{\hbar\omega_\beta}\right)^2\left(\frac{\hbar^2}{\Im}\right)^3 I^2(I+1)^2, \quad \text{(VI. 3a)}$$

where $\hbar\omega_\beta$ is the excitation energy of the β-vibration (cf. § VIc.iv). Another term of the same order of magnitude as (3a) arises from the influence of the γ-vibrations which imply a departure from the rotational spectrum of a symmetric top. The effect can be found as a second order perturbation produced by the operator U_3 (cf. A. 96), and one obtains

$$(\Delta E_I)_2 = -\frac{1}{2}\left(\frac{1}{\hbar\omega_\gamma}\right)^2\left(\frac{\hbar^2}{\Im}\right)^3 I^2(I+1)^2, \quad \text{(VI. 3b)}$$

where $\hbar\omega_\gamma$ is the energy of the γ-vibration.

Rotational states in regions of large deformations have recently been identified by their very striking properties: regu-

TABLE XXII. Energies of (2+) and (4+) states in even-even nuclei with $A > 140$.

Nucleus	E_2	E_4	$E_4:E_2$	Ref.
$_{62}Sm^{150}$	337	777	2.3	*
$_{72}Hf^{176}$	89	289	3.2	** †††
$_{72}Hf^{180}$	93	307	3.3	**
$_{82}Pb^{208}$	2614	3200	1.2	*
$_{88}Ra^{226}$	67	217	3.2	***
$_{90}Th^{228}$	58	187	3.2	†
$_{90}Th^{230}$	50	167	3.3	††
$_{94}Pu^{238}$	43	146	3.4	††

* SCHARFF-GOLDHABER (1953).
** GOLDHABER and HILL (1952).
*** BOUISSIÈRES et al. (1953), (added in proof).
† BLACK (1924).
†† HOLLANDER, PERLMAN and SEABORG (1952).
††† ARNOLD and SUGIHARA (1953), (added in proof).

The table lists the energies (in keV) of the (2+) and of the tentatively assigned (4+) states. While these assignments are consistent with the available empirical evidence, they are in many cases in need of further examination. For rotational states, the ratio $E_4:E_2$ is expected to approach the value 10:3 for large deformations (cf. 1).

larities of spins and parities, characteristic energy trends, simplicity of the excitation spectrum, and very large $E2$ transition probabilities (BOHR and MOTTELSON, 1952, 1953, 1953a; FORD, 1953; ASARO and PERLMAN, 1953).

Systematic studies of the first excited states of even-even nuclei (GOLDHABER and SUNYAR, 1951; HORIE, UMEZAWA, YAMAGUCHI and YOSHIDA, 1951; STÄHELIN and PREISWERK, 1951; PREISWERK and STÄHELIN, 1952; ASARO and PERLMAN, 1952; ROSENBLUM and VALADARES, 1952; WAPSTRA, 1952, 1953; SCHARFF-GOLDHABER, 1952, 1953*), have revealed that, with very few exceptions, the first excited state is of (2+) character**, and that the excitation energy exhibits definite trends with respect to

* We are indebted to Dr. G. SCHARFF-GOLDHABER for making available to us these results in advance of publication.

** It has been suggested that the excited states of even-even nuclei can be interpreted as a recoupling of the particles outside of closed shells (cf., e. g., HORIE et al., 1951; FLOWERS, 1952b). While this description may, for many configurations, explain the (2+) nature of the first excited levels, it has not provided an explanation of the many other striking features of the levels discussed in the present paragraph.

the shell structure, reaching maxima around the closed-shell configurations and minima as much as fifty times smaller in the middle of shells.

This trend is especially conspicuous in the region of the heavier nuclei where the shell structure is dominated by the doubly closed shells at Pb^{208} (cf. Fig. 13). Similar regularities are also observed for the lighter elements, but the trends are somewhat more complicated due to the fact that neutrons and protons form closed shells for different A-values (cf especially SCHARFF-GOLDHABER, 1953).

While the excitations of closed-shell nuclei may represent simple phonon states (cf. § VI c.i), a decreasing energy, as we move away from closed shells, results from the coupling with the particle structure, which leads to increasing nuclear deformations. The rapid decrease for the first few particles added to closed configurations, which develops into a rather flat minimum, can be understood from the fact that the particle states with large deformative power are the first to be filled, while in the middle of shells the last added particles are less coupled to the deformed nucleus.

The small excitation energies encountered in the regions $155 < A < 185$ and $A > 225$ imply that, in these cases, the coupling is very strong and that the rotational energies should be rather accurately represented by the simple formula (1), corrections of magnitude (3a and b) being small.

A direct measure of the validity of the strong coupling approximation is afforded by the location of the expected higher members of the rotational family. The available evidence on energies of the (4+) state, in the region covered by Fig. 13, is listed in Table XXII. It is seen that the energy ratio $E_4 : E_2$ shows the expected trend, approaching the strong coupling value 10:3 (cf. 1) in the regions of large deformation.*

* Note added in proof: ASARO and PERLMAN (1953), from a study of the α-spectra of the heavy elements, have recently obtained evidence for the systematic occurrence of a rotational spectrum in even-even nuclei in the region well beyond Pb^{208}. With the approach to Pb^{208}, deviations from the energy spectrum (1) are observed, which can be interpreted as distortions of the type (3a and b), corresponding to a vibrational energy of about one MeV, which is of the same magnitude as indicated by the hydrodynamical estimate (cf. Fig. 2). We are indebted to these authors for having informed us of their results in advance of publication.

TABLE XXIII Deformations deduced from properties of rotational states.

Nucleus	E (keV)	F	β_E	β_Q
$_{66}Dy^{160}$	85	140	0.65	0.28
$_{68}Er^{166}$	80	180	0.65	0.31
$_{70}Yb^{170}$	84	140	0.62	0.27
$_{72}Hf^{176}$	89	120	0.58	0.24
$_{76}Os^{186}$	137	55	0.45	0.15
$_{80}Hg^{198}$	411	6	0.25	0.05
$_{84}Po^{212}$	719	5	0.18	0.04
$_{84}Po^{214}$	606	7	0.19	0.05

The table lists the first excited states of even-even nuclei, classified as collective excitations on the basis of measured lifetimes (cf. Table XXVII). The factor F in the third column gives the enhancement of the transition probability over that expected for a particle transition (cf. Table XXVII). From a rotational interpretation of the states, the deformation β_E may be calculated from the excitation energy by means of (VI.1 and 2), and is listed in column four. The last column gives the deformation β_Q estimated from the intrinsic deformation Q_0 by means of (V.7). The value of Q_0 is obtained from the observed transition probability (cf. Table XXVII).

The large excitation energies, as well as the relatively small F-factors, for the last three cases in the table indicate an intermediate coupling situation, in which the rotational description is less appropriate.

The spin of 4 for the second rotational excitation and the $E_4:E_2$ ratios confirm the expected axial symmetry of the nuclear deformation (cf. p. 28). For a nucleus with an asymmetric equilibrium shape, the rotational spectrum would exhibit a sequence of I-values and energy ratios different from (1).

It is a characteristic of the rotational spectrum that the excitation of a high member is followed by a cascade of $E2$ gamma transitions with energy values in the ratio $\cdots$ 15:11:7:3, and with no cross-overs. There is indeed evidence (BOHR and MOTTELSON, 1953a) for such cascades involving states up to $I = 8$ with energies closely given by (1).*

The observed very short γ-ray lifetimes of low-lying excited states in even-even nuclei clearly indicate the collective nature of the excitation (GOLDHABER and SUNYAR, 1951). The ratio of

* Note added in proof: The recent measurement (ARNOLD and SUGIHARA, 1953) of the γ-spectrum following the β-decay of Lu^{176} considerably improves the agreement with the rotational spectrum in Hf^{176}.

the observed transition probabilities to those expected for particle transitions increases as one moves away from closed-shell configurations and reaches values of more than a hundred in regions far removed from closed shells (cf. Table XXIII).

The $E2$ transition probability of a rotational state is directly related to the intrinsic nuclear quadrupole moment Q_0 (cf. § Vb and § VIIc.ii), and the values derived from the observed lifetimes are just of the magnitude deduced from spectroscopic data for neighbouring odd-A isotopes (cf. Table XXVII on p. 116).

Another measure of the deformation is provided by the excitation energies which yield, by (1), the nuclear moment of inertia. Assuming the hydrodynamic value (II.6a) for B, the deformation β_E can be obtained from (2). This estimate of the deformation is compared, in Table XXIII, with the deformation β_Q estimated from the $E2$ transition probability, assuming the hydrodynamic relation (V.7) for Q_0.

It is seen that, although β_E and β_Q show parallel trends, β_E exceeds β_Q by about a factor of two in the region of the fully developed strong coupling. This effect is quite similar to the overestimate of the static quadrupole moments by the hydrodynamic model (cf. p. 59), and lends support to the view that the simple model of the collective deformations underlying (V. 7) is inadequate. As in the case of the static Q, it is also possible that some part of the discrepancy arises from an underestimate of B.

A general correlation has been found (Ford, 1953) between the energies of the first excited states of even-even nuclei, interpreted as rotational states, and the magnitude of the quadrupole moments of odd-A nuclei. The quantitative comparison shows the same feature encountered above, that, although the two estimates of the deformation exhibit similar trends, the β-values derived from quadrupole moments are several times smaller than those derived from excitation energies.

For the smaller deformations encountered in the regions of closed shells, perturbation terms of the magnitude (3a and b) may essentially modify the spectrum and also particle forces may have an important influence. The expected intermediate coupling situation is clearly revealed by the deviations of the $E_4 : E_2$ ratio (cf. Table XXII) from the strong coupling value of 10:3, with the approach to closed-shell configurations.

iii. *Rotational states in odd-A nuclei.*

The rotational spectrum in odd-A nuclei depends on the angular momentum I_0 of the ground state. If $I_0 = \Omega = K \geqslant 3/2$, we get a series of states with energies

$$E_I = \frac{\hbar^2}{2\Im}[I(I+1) - I_0(I_0+1)] \quad \underset{\text{same parity as ground state}}{I = I_0, I_0+1, I_0+2, \cdots} \qquad \text{(VI.4)}$$

If the system does not strongly prefer the symmetric shape ($\gamma = 0$ or π), as for a single particle with $j = 3/2$, a more complicated rotational spectrum may arise (cf. Ap. III.ii).

In the case $\Omega = K = 1/2$, there is the additional contribution to the rotational energy (cf. II.30)

$$\Delta E_I = (-)^{I-j+1} \frac{\hbar^2}{2\Im}(j+1/2)(I+1/2), \qquad \text{(VI.5)}$$

where j refers to the odd particle with $\Omega_p = 1/2$. In this case, the ground state spin is in general no longer 1/2, and a less regular sequence of rotational states appears.

Since the odd-A rotational states depend more specifically on the properties of the ground state, they do not exhibit the same simple trends as those in even-even nuclei. Moreover, since consecutive levels have $\Delta I = 1$, except in some cases with $\Omega = 1/2$, they may decay by $M1$ radiation, for which the transition probability is not enhanced.

A specially suited method for identifying and studying the rotational states in odd-A nuclei may be provided by the Coulomb excitation which directly measures the $E2$ transition probability (cf. Ap. VI). The collective excitations therefore manifest themselves by their especially large cross-sections.*

Measurements of the γ-decay probabilities of the rotational states are also of interest, since the $M1$ transition probability can be directly compared with the static magnetic moment of the ground state (cf. VII.20). The strong enhancement of the $E2$ radiation implies that appreciable $E2$ admixtures may be expected in many cases, although for a single-particle γ-transition

* Note added in proof: Recently, rotational states in odd-A nuclei have been identified by the method of Coulomp excitation (Huus and Zupančič, 1953; cf. also note on p. 166).

with $\Delta I = 1$ (no), the $E2$ radiation is extremely weak in comparison with $M1$. Moreover, it is expected that cross-over transitions ($\Delta I = 2$) may in some cases compete with the cascade.

iv. *Vibrational excitations.*

The vibrational states are characterized by the quantum numbers n_β and n_γ, and in the limit of strong coupling the excitation energies approach the phonon energy (cf. A. 108 and 113). A comparable energy is associated with changes in the quantum number K. Due to the symmetry of the surface, the n_γ- and K-excitations only occur in definite combinations, since n_γ must have the same parity as $1/2\ (K - \Omega)$ (cf. A. 92).

The vibrational states have strongly enhanced $E2$ decay probabilities, characteristic of collective excitations, and could be especially studied by the method of Coulomb excitation (cf. Ap. VI). In an even-even nucleus, an $E2$ transition from the ground state can lead to the vibrational states ($n_\beta = 1$; $n_\gamma = 0$; $I = 2$; $K = \Omega = 0$) and ($n_\beta = 0$; $n_\gamma = 1$; $I = K = 2$; $\Omega = 0$). In an odd-A nucleus, several rotational states can be reached for each type of vibrational excitation, and in addition there are two vibrational excitations with $n_\gamma = 1$, having $\Delta K = \pm 2$.

d) Higher Excitation. The Compound Nucleus.

The more highly excited states, produced in nuclear reaction processes, though characterized by a somewhat greater complexity than the low energy spectrum, can provide further insight into the dynamics of the nuclear system. Since the present discussion is concerned principally with the phenomena occurring in the low energy region, we shall attempt only a rather brief description of the properties of the coupled system for higher excitations.

In the present paragraph, we consider the general features of the level structure in this region, and summarize some of the consequences for nuclear reactions*, **. A more detailed formu-

* We are indebted to Professor N. Bohr for illuminating discussions on the influence of single-particle motion on the compound nucleus formation.

** Cf. also Hill and Wheeler (1953), who have pointed out many important consequences of the strong interaction between the nucleonic and surface motion for various nuclear processes, and especially the fission reaction.

lation of nuclear reaction theory, incorporating individual-particle as well as collective features, is attempted in Appendix V.

With increasing nuclear excitation, the level spacing rapidly decreases and any simple coupling scheme will be destroyed by even relatively small perturbations, which result in a sharing of properties between neighbouring levels of the same spin and parity. A simplified picture of the level structure may be obtained by characterizing the rate of exchange of energy in the system by an energy interval W within which the sharing of properties among levels is more or less complete. This energy is related to the mean free path λ_a of single-particle motion by

$$W = \frac{\hbar v}{\lambda_a}, \tag{VI.6}$$

where v is the particle velocity*. The coupling thus tends to obscure finer features in the level structure, associated with simple types of motion with frequencies smaller than $W/\hbar$.

The significance of single-particle motion depends on the relative magnitude of W and the single-particle level spacing Δ given by

$$\Delta = \pi K R_0 \frac{\hbar^2}{M R_0^2}, \tag{VI.7}$$

where K is the nucleon wave-number in the average potential. For W larger than Δ ($\sim 110\, A^{-1/3}$ MeV), the interactions destroy the effects of undisturbed single-particle motion, and the properties of the individual configurations are uniformly distributed over the whole energy spectrum. Such a situation corresponds to the strong interaction theory of nuclear reactions, according to which the incident particle shares its energy with many degrees of

* The energy exchange between surface and nucleonic motion has been discussed by HILL and WHEELER (1953) from a somewhat different point of view. These authors attempt a rather detailed description of the nuclear state in the region of high excitation by assuming the nucleus to occupy, at any given moment, a strong coupling state with a definite division of the energy between nucleonic, vibrational and rotational motion. The surface motion is treated in the semi-classical approximation appropriate to large quantum numbers. Exchanges of energy between nucleonic and vibrational motion occur with a frequency (the slippage or damping frequency) closely related to the quantity $W/\hbar$. It is found that the validity of this description requires W to be small compared with the energies of vibration and rotation. The estimate given in the present paragraph indicates that, in general, W is of the order of the vibrational energies, in accordance with tentative estimates by HILL and WHEELER.

freedom of the compound system in a time short compared to that required for a traversal of the nucleus (N. BOHR, 1936; cf. also FESHBACH and WEISSKOPF, 1949).

The existence of nuclear shell structure suggests a value of W small compared to Δ. If the main interaction is due to the particle-surface coupling, one obtains, for energies of the incident particle small compared with the nuclear potential, estimates of W which are on the average about 2–3 MeV, but depend on A and on the nuclear deformation (cf. Ap. Vc). For such values of W, the existence of relatively undisturbed single-particle motion is expected to manifest itself in the properties of the nuclear spectrum.

Thus, in a nuclear reaction, the first stage will be the action of the average nuclear field on the incident particle. The coupling between the particle and the internal degrees of freedom of the target nucleus may, in subsequent stages, lead to energy exchanges which may eventually result in the complex types of motion characteristic of the compound system.

Recent measurements of total neutron cross-sections (BARSCHALL, 1952; MILLER, ADAIR, BOCKELMAN and DARDEN, 1952; NERESON and DARDEN, 1953; WALT et al., 1953) confirm the expectation that the limit of strong interaction is not quite reached, and that single-particle effects are still discernible in the scattering process (WEISSKOPF, 1952). The measured cross-sections represent averages over levels and the data below 3 MeV have been accounted for in terms of single-particle scattering in a complex potential (FESHBACH, PORTER, and WEISSKOPF, 1953)*. The imaginary part of the potential represents the absorption into the compound nucleus and is closely related to the quantity W. The empirical data indicate an absorption which corresponds to $W \sim 2$ MeV. It thus appears that the properties of the higher excitation region may be understood in terms of the same couplings which operate at lower energies (cf. Ap. Vc).

A coupling energy W small compared with Δ has important implications for the whole course of nuclear reaction processes. Thus, the scattering widths of the individual states of the compound system depend on the distance from the nearest

* We are indebted to these authors for making available their results in advance of publication. Cf. also p. 158 ff. below for further discussion of this analysis, and of the conditions under which nuclear cross-sections can be described in terms of the scattering in a complex potential.

virtual level for single-particle potential scattering. The reduced width of the single-particle level is mainly distributed over the compound states within a distance W. Outside of this region, the compound states are much narrower, and appear as a fine structure on a background of potential scattering (cf. Ap. Vb)*.

Moreover, for $W < \Delta$, direct couplings between entrance and exit channels may lead to nuclear reactions which do not pass through the compound stage (direct ejection of particles or direct excitation of rotational or vibrational modes). The coupling energy W would also reveal itself in the relative probability of the various modes of decay of the compound state, which often depend on the amplitude of a few simple types of motion (cf. Ap. Vc).

* A formulation of the nuclear dispersion theory, incorporating single-particle features as well as the compound nucleus formation, has also recently been considered by FESHBACH, PORTER, and WEISSKOPF. We are indebted to these authors for a private communication of results of their investigation.

VII. Electromagnetic Transitions.

An essential part of the present knowledge of the low energy nuclear spectrum has been obtained from the study of γ-transitions. The determination of multipole orders is a valuable tool in assigning spins and parities to the nuclear states, and the measurement of transition probabilities yields further important information on the nature of the excitations involved.

The general implications of the empirical evidence for the nuclear level structure have already been considered in Chapter VI. In the present chapter, we give the calculation of electromagnetic transition probabilities in the coupled system and the more detailed analysis of the available empirical data.

a) Transition Operators.

The transition probability for radiation of a photon of multipole order λ and of frequency ω is given by (WEISSKOPF, 1951; MOSZKOWSKI, 1951, 1953; STECH, 1952; BLATT and WEISSKOPF, 1952, p. 595)

$$T(\lambda) = \frac{8\pi(\lambda+1)}{\lambda[(2\lambda+1)!!]^2}\frac{1}{\hbar}\left(\frac{\omega}{c}\right)^{2\lambda+1} B(\lambda) \qquad \text{(VII.1)}^*$$

where the reduced transition probability $B(\lambda)$ can be written as

$$B(\lambda) = \sum_{\mu, M_f} |<i|\mathfrak{M}(\lambda,\mu)|f>|^2 \qquad \text{(VII.2)}$$

in terms of the matrix elements of the multipole operator $\mathfrak{M}(\lambda,\mu)$ of order λ,μ between an initial state i and a final state f, with magnetic quantum number M_f.

* $(2\lambda+1)!! \equiv 1\cdot 3\cdot 5\ldots(2\lambda+1)$.

The electric and magnetic multipole operators are given by*

$$\mathfrak{M}_e(\lambda, \mu) = \sum_{p=1}^{A} e_p r_p^\lambda Y_{\lambda\mu}(\vartheta_p, \varphi_p) \tag{VII.3}$$

and

$$\mathfrak{M}_m(\lambda, \mu) = \frac{e\hbar}{2Mc} \sum_{p=1}^{A} \left(g_s \vec{s} + \frac{2}{\lambda+1} g_l \vec{l} \right)_p \cdot \vec{\nabla}_p \left(r_p^\lambda Y_{\lambda\mu}(\vartheta_p, \varphi_p) \right), \tag{VII.4}$$

respectively, where e_p, $(g_l)_p$, and $(g_s)_p$ refer to the charge, orbital and spin g-factors of the particle p.

In the unified description of the nuclear dynamics, the state of the nucleus is described in terms of collective and particle degrees of freedom. The former represent the bulk of the nucleons, which are strongly bound, while the latter represent the most loosely bound particles, which may be individually excited (cf. § IIa.iii). In the coordinates appropriate to this description, the multipole operators (3) and (4) take the form

$$\mathfrak{M}_e(\lambda, \mu) = \sum_p \left(e_p - \frac{Ze}{A^\lambda} \right) r_p^\lambda Y_{\lambda\mu}(\vartheta_p, \varphi_p) + \frac{3}{4\pi} ZeR_0^\lambda \alpha^*_{\lambda\mu} \tag{VII.5}$$

and

$$\left.\begin{aligned} \mathfrak{M}_m(\lambda, \mu) = {} & \frac{e\hbar}{2Mc} \sum_p \left(g_s \vec{s} + \frac{2}{\lambda+1} g_l \vec{l} \right)_p \cdot \vec{\nabla}_p \left(r_p^\lambda Y_{\lambda\mu}(\vartheta_p, \varphi_p) \right) \\ & + \frac{e\hbar}{Mc} \frac{1}{\lambda+1} g_R \int \vec{R}(r) \cdot \vec{\nabla} \left(r_\lambda Y_{\lambda\mu}(\vartheta, \varphi) \right) d\tau, \end{aligned}\right\} \tag{VII.6}$$

where the sums over p include the particle degrees of freedom, while the last terms refer to the multipole moments generated by the collective motion of the nucleons.

The particle part of the electric moment (5) includes the effect of the recoil of the nuclear core, which is of special importance for dipole transitions; for $\lambda \geqslant 2$, the recoil term also contains many-particle operators, which have been omitted in (5).

The coefficient of $\alpha^*_{\lambda\mu}$ in (5) is obtained from (II.2), which is based upon a hydrodynamical description of the collective motion. Inadequacies of this approximation of the kind indicated by the nuclear quadrupole moments (cf. § Vc) would imply a

* In (3), we neglect the contribution of the intrinsic magnetic moment of the particle, which is of the same order as that of the magnetic multipole of one higher order.

somewhat smaller value of the coefficient. The density of angular momentum in the collective motion is denoted by $\vec{R}(\vec{r})$ and may be expressed as a quadratic form in the α-coordinates.

The reduced transition probability $B(\lambda)$, which is related by (1) to the lifetime for γ-emission, can also be determined from the cross-section for Coulomb excitation by impact of heavy ions (TER-MARTIROSYAN (1952); cf. also Appendix VI; e. g. (Ap. VI.17)).

The two methods for determining B complement each other in the sense that the lifetime measurements are most easily performed when B is small, while large excitation cross-sections are obtained when B is large. Moreover, the relative intensity of the different multipole components in the field of the impinging particle is very different from that of the radiation field produced by a source of nuclear dimensions.

b) Transitions in the Weakly Coupled System.

i. *Particle transitions.*

In the case of a single particle moving in a spherical potential, a transition between states of angular momenta j_i and j_f is electric of order $\lambda = |j_i - j_f|$, if the spins and orbits are parallel in the initial as well as the final states, or if they are antiparallel in both cases. The value of B is given by (STECH, 1952; BLATT and WEISSKOPF, 1952; MOSZKOWSKI, 1953)

$$B_e(\lambda) = \frac{1}{4\pi}\left(e_p - \frac{Ze}{A^\lambda}\right)^2 |<i|r^\lambda|f>|^2 c(j_>, j_<) \frac{2j_f+1}{2j_<+1}, \qquad \text{(VII.7)}$$

where $<i|r^\lambda|f>$ is the radial matrix element, and where the $c(j_>, j_<)$ are numerical coefficients of order unity, which can be expressed in terms of Racah coefficients*. Values of $c(j_>, j_<)$ are listed in Table XXIV. The arguments $j_>$ and $j_<$ denote the larger and smaller, respectively, of j_i and j_f.

If $j_>$ has parallel spin and orbit, while $j_<$ has antiparallel spin and orbit, the transition is magnetic, of order $\lambda = |j_i - j_f|$, and (cf. the references of (7))

* STECH (1952) uses a corresponding quantity $\overline{|F(j_A, j_B)|^2}$ equal to $(j_< + 1/2)^{-1}\, c(j_>, j_<)$. MOSZKOWSKI (1953) uses the quantity $S(I_i, L, I_f)$ which, for $|I_i - I_f| = \lambda$, equals $(2j_f + 1)(2j_< + 1)^{-1}\, c(j_>, j_<)$.

TABLE XXIV. Coefficients $c(j_>, j_<)$ in transition probabilities.

$j_<$ \ $j_>$	3/2	5/2	7/2	9/2	11/2	13/2
1/2	1	1	1	1	1	1
3/2	1	$\frac{6}{5}$	$\frac{9}{7}$	$\frac{4}{3}$	$\frac{15}{11}$	$\frac{18}{13}$
5/2		1	$\frac{9}{7}$	$\frac{10}{7}$	$\frac{50}{33}$	$\frac{225}{143}$
7/2			1	$\frac{4}{3}$	$\frac{50}{33}$	$\frac{700}{429}$
9/2				1	$\frac{15}{11}$	$\frac{225}{143}$
11/2					1	$\frac{18}{13}$
13/2						1

The transition probability for a single particle transition $j_i \to j_f$ of multipole order $\lambda = |j_i - j_f|$ involves the coefficients $c(j_>, j_<)$ tabulated above. (Cf. equations (VII.7 and 8) and footnote on p. 103). The larger and smaller of j_i, j_f are denoted by $j_>$ and $j_<$, respectively.

$$B_m(\lambda) = \frac{\lambda^2}{4\pi}\left(\frac{e\hbar}{2Mc}\right)^2\left(g_s - \frac{2}{\lambda+1}g_l\right)^2 |\langle i|r^{\lambda-1}|f\rangle|^2 c(j_>, j_<)\frac{2j_f+1}{2j_<+1}. \quad \text{(VII.8)}$$

Finally, if $j_>$ has antiparallel while $j_<$ has parallel spin and orbit, the transition is forbidden in order $\lambda = |j_i - j_f|$. For a pure configuration, the transition would be electric of order $\lambda = |j_i - j_f| + 1$, but small admixtures of other configurations may suffice to produce a predominantly magnetic transition of order $\lambda = |j_i - j_f|$.

For many-particle configurations, similar expressions may be obtained, provided the coupling scheme is known (cf., e. g., MOSZKOWSKI, 1953). Thus, for two equivalent protons, the transition $(j^2)_{J=2} \to (j^2)_{J=0}$ is of electric quadrupole type with a reduced transition probability

$$B_e(2) = \frac{1}{16\pi}e^2|\langle i|r^2|f\rangle|^2\frac{(2j-1)(2j+3)}{j(j+1)}. \quad \text{(VII.9)}$$

In the estimates of transition probabilities in § VII d, we use the simple estimate

$$< i | r^{\lambda} | f > = \frac{3}{3+\lambda} R_0^{\lambda} \qquad \text{(VII.10)}$$

which would be obtained for a radial wave-function constant within the nuclear volume and vanishing outside. More detailed calculations have been made (MOSZKOWSKI, 1953) which yield similar results.

ii. *Phonon transitions.*

The radiation emitted by the freely oscillating nuclear surface is of electric multipole type of the same order λ as the surface deformation. For the decay of a one-phonon state to a no-phonon state, one finds from (5) and (A. 38) (cf. FLÜGGE, 1941; LOWEN, 1941; FIERZ, 1943; BERTHELOT, 1944; JEKELI, 1952)*

$$B_e(\lambda) = \left(\frac{3}{4\pi} Z e R_0^{\lambda}\right)^2 \frac{\hbar \omega_{\lambda}}{2 C_{\lambda}} \qquad \text{(VII.11)}$$

for the reduced transition probability in terms of the frequency ω_{λ} and deformability C_{λ} of the λ^{th} surface mode (cf. Figs. 1 and 2). The cooperative nature of such a transition, as expressed in the appearance of the factor Z^2 in (11), in general leads to a much faster decay than for a corresponding particle transition.

iii. *Surface moments induced by particle transitions.*

In weak coupling, a transition between two different particle states induces a moment in the surface which may be calculated in the perturbation approximation. Although the admixture of collective excitation is small, its influence may be important in the case of electric multipole transitions, due to the larger charge involved in the surface motion. The induced surface moment is proportional to the mass moment of the particle transition, and the operator (5) becomes (cf. II. 5 and 9)

$$\left.\begin{aligned} \mathfrak{M}_e(\lambda, \mu) &= R_0^{\lambda} \sum_p Y_{\lambda\mu}(\vartheta_p, \varphi_p) \\ &\left\{ e_p \left(\frac{r_p}{R_0}\right)^{\lambda} + \frac{3}{4\pi} Z e \, \frac{k}{C_{\lambda}} \, \frac{(\hbar\omega_{\lambda})^2}{(\hbar\omega_{\lambda})^2 - (E_i - E_f)^2} \right\} \end{aligned}\right\} \qquad \text{(VII.12)}$$

* The results of the quoted authors differ somewhat from each other in numerical coefficients. Also the matrix element quoted by BLATT and WEISSKOPF (1952, p. 628) appears to lead to a transition probability too small by a factor four.

for a transition between particle states with energies E_i and E_f. It is of significance that the particle part of $\mathfrak{M}_e$ depends on the charge of the particles, while the surface part involves only the coupling constant k, which is the same for neutrons and protons. The hydrodynamic estimate of the second term in (12) (cf. Figs. 1 and 2) indicates that it is somewhat larger than the first term (by about a factor of four for a medium heavy nucleus).

c) Transitions in the Strongly Coupled System.

i. *Particle transitions.*

In the strong coupling representation (II.15), it is convenient to expand the multipole operators along the nuclear axis

$$\mathfrak{M}(\lambda, \mu) = \sum_{\nu} \mathfrak{M}'(\lambda, \nu)\, \mathfrak{D}^{\lambda}_{\mu\nu}(\theta_i), \qquad \text{(VII.13)}$$

where $\mathfrak{M}'(\lambda, \nu)$ is expressed in the nuclear coordinate system, and where the $\mathfrak{D}$-functions are the same as used in (II. 15).

For a particle transition between states with $I_i = K_i = \Omega_i$ and $I_f = K_f = \Omega_f$ one obtains, for $\lambda = |I_i - I_f|$,

$$B(\lambda) = \left| \int \chi^*_{\Omega_i} \mathfrak{M}'(\lambda, \pm\lambda)\, \chi_{\Omega_f} \right|^2 \left| \int \varphi_i^*(\beta, \gamma)\, \varphi_f(\beta, \gamma) \right|^2 \frac{2I_f + 1}{2I_> + 1}. \qquad \text{(VII.14)}$$

In special cases, the symmetrization of the wave function (II.15) may introduce additional terms.

In the strong coupling scheme, where the particles move independently with respect to the nuclear axis, the particle transitions are always one-particle transitions. Thus, the first factor in (14) is simply related to the transition probability for a single uncoupled particle, provided the particle wave functions χ have a definite j, and provided the collective part of the multipole moments (5 and 6) can be neglected. For a transition from $j_i = \Omega_i = I_i$ to $j_f = \Omega_f = I_f$, one then obtains

$$B(\lambda) = B_{\mathrm{sp}}(\lambda) \left| \int \varphi_i^* \varphi_f \right|^2 \frac{2I_< + 1}{2I_> + 1}, \qquad \text{(VII.15)}$$

where $B_{\mathrm{sp}}(\lambda)$ is given by (7) or (8). However, in some cases, important differences between (14) and (15) may arise from the

modification of the particle wave function caused by the non-spherical character of the potential, and from the collective contributions to the multipole operators.

Thus, the tendency of the surface coupling to admix certain neighbouring orbitals in the particle state may, in particular, cause transitions to occur, even when B_{sp} vanishes due to shell model selection rules (l-forbiddenness; j-forbiddenness).

An important contribution to electric transitions with $\lambda > 2$ may arise from the coupling to the surface mode of order λ. Since the coupling to these higher order modes may be considered as weak, the effect can be included by using the form (12) for the multipole operator. This contribution to the transition may be particularly significant in leading to comparable lifetimes for electric multipole transitions of odd-neutron and odd-proton nuclei.

The last factors in (15) imply reductions in the transition probability of the type known in molecular spectroscopy (Franck-Condon principle; (cf., e. g., HERZBERG, 1950, p. 199)). The factor involving the vibrational wave functions gives the reduction arising from the partial orthogonality of two states with differing magnitude or shape of deformation. This effect depends on the difference of the two equilibrium deformations as compared with the zero point amplitude. The dependence is exponential, and great reductions may result when the coupling is strong. If the two states have different shapes (strong coupling solutions centered on different values of γ), it is necessary to consider the full symmetry of the wave function (A.118), since it may be easier for the surface to oscillate from oblate to prolate form along different intrinsic nuclear axes (cf. HILL and WHEELER, 1953, fig. 28). The last factor in (15) involving the spins is a projection factor associated with the fact that only the projection of the particle multipole along the nuclear axis is effective.

The reduction in transition probability due to the surface coupling is illustrated in Fig. 14 for an $M1$ transition of $p_{3/2} \rightarrow p_{1/2}$ type. From the $I = j = 3/2$ wave function given in Fig. 4 (p. 25), the transition probability to an uncoupled $p_{1/2}$ state may be simply obtained. The "unfavoured factor", F, representing the ratio of B and B_{sp}, is plotted as a function of x. As an example of the effect due to differences in shape, we have also plotted

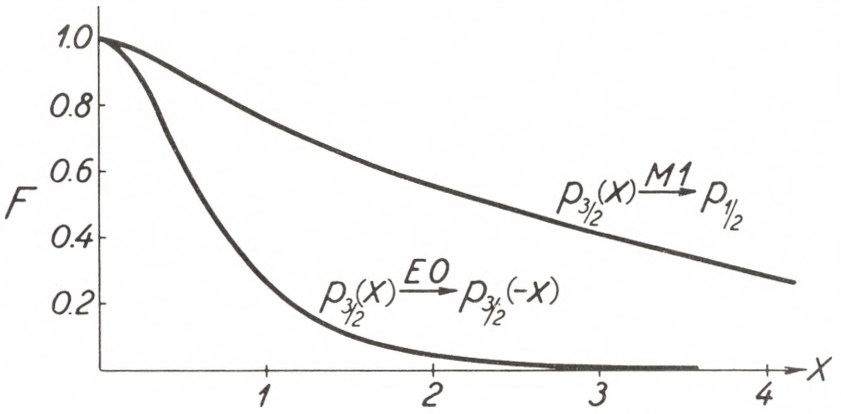

Fig. 14. *Unfavoured factors in intermediate coupling.* The coupling between particle and surface motion implies that particle transitions are in general slowed down by the partial orthogonality of the surface states of the combining levels. The ratio of the resulting transition probability to that for an uncoupled particle is referred to as the unfavoured factor, F. The figure illustrates the behaviour of F as a function of the dimensionless coupling constant x (II.14).

The upper curve corresponds to a $p_{3/2} \rightarrow p_{1/2}$ $M1$ transition; the $p_{3/2}$-state appropriate to a given x is obtained from Fig. 4, while the pure $p_{1/2}$-state has no coupling to the surface. The lower curve gives the square of the overlap integral between two $p_{3/2}$-states with equal magnitude, but opposite sign of the coupling parameter. This quantity would correspond to the F-factor for a hypothetical $E0$ transition.

the square of the overlap integral (F-factor for a hypothetical $E0$ transition) for two $p_{3/2}$ states with opposite sign, but same magnitude of the coupling constant.

One may also employ the strong coupling solutions (A. § V.3) to calculate the F-factors for large couplings. For a transition $j \rightarrow j$ between states with coupling strengths x and x', one finds that F contains the factor

$$F \sim \exp\left\{ -\frac{1}{2}\left(\frac{2j-1}{2j+2}\right)^2 j\,(x-x')^2 \right\} \qquad \text{(VII.16)}$$

which exhibits the exponential decrease of F with increasing coupling.

ii. *Collective transitions.*

In collective transitions of the strongly coupled system, the last term in (5) may give rise to strongly enhanced $E2$ transition probabilities.

Of special interest are the rotational excitations, which, in even-even nuclei, form a spectrum with $I = 0, 2, 4, \cdots$ (cf. VI.1). The γ-decay proceeds in cascades of $E2$ radiation, and for the transition $I + 2 \rightarrow I$, the reduced transition probability, which may be obtained by using (V. 5), is given by

$$B_e(2) = \frac{15}{32\pi} e^2 Q_0^2 \frac{(I+1)(I+2)}{(2I+3)(2I+5)}, \qquad \text{(VII.17)}$$

where Q_0 is the intrinsic quadrupole moment (V.7). The expression (17) exceeds the one-phonon decay probability (11) by a factor of the order of the average number of phonons present in the strong coupling state.

In odd-A nuclei, the rotational levels form a sequence with $I = K, K + 1, K + 2, \cdots$ (cf. VI.4), except for the case of $K = \Omega = 1/2$. For a transition $I + 1 \rightarrow I$, one obtains

$$B_e(2) = \frac{15}{16\pi} e^2 Q_0^2 \frac{K^2 (I+1-K)(I+1+K)}{I(I+1)(2I+3)(I+2)}, \qquad \text{(VII.18)}$$

while for the cross-over transitions $I + 2 \rightarrow I$

$$B_e(2) = \frac{15}{32\pi} e^2 Q_0^2 \frac{(I+1-K)(I+1+K)(I+2-K)(I+2+K)}{(I+1)(2I+3)(I+2)(2I+5)}. \qquad \text{(VII.19)}$$

For the $I + 1 \rightarrow I$ transitions, $M1$ radiation is also present, with a reduced transition probability given by

$$B_m(1) = \frac{3}{4\pi} \left(\frac{e\hbar}{2Mc}\right)^2 (g_\Omega - g_R)^2 \frac{\Omega^2 (I+1-K)(I+1+K)}{(I+1)(2I+3)}, \qquad \text{(VII.20)}$$

in terms of the g-factors of the particle and collective motion, g_Ω and g_R, respectively (cf. IV.4 and 10). While, for a similar sequence of particle excitations, the decay would proceed by a cascade of almost pure $M1$ radiation, the considerable enhancement of the $E2$ radiation produced by the collective deformation

may, in some cases, give rise to an appreciable admixture of $E2$ radiation, and also to cross-overs of the type (19).

For odd-A nuclei with $K = \Omega = 1/2$, the rotational spectrum is more complicated (cf. § VI c.iii). The electric radiation is still given by (18) and (19), but the matrix element for $M1$ transitions cannot be related so simply to the magnetic moment of the ground state as in (20).

Transitions involving a change of vibrational quantum numbers (cf. § VI c.iv) are of pure $E2$ type in the limit of strong coupling. The decay of a higher vibrational state may in general proceed to several rotational levels of the lower vibrational state. The transition probabilities can be obtained from (5), using the vibrational wave functions (A. 109 and 114). The matrix elements are of the same order of magnitude as for a single phonon decay (11) and thus are larger than for a particle transition, although smaller than for a rotational transition.

d) Discussion of Empirical Data.

The classification of the isomeric transitions, as well as the empirical decay energies, lifetimes, and the conversion coefficients used in this paragraph are, except where otherwise noted, taken from the articles by GOLDHABER and SUNYAR (1951) and GOLDHABER and HILL (1952).

In a field of such rapid development, it may be expected that improved experiments will modify some of the data considered here. Without evaluating the individual experiments, we have tried to confine ourselves to those classes of transitions which, at the present time, seem to provide the most reliable and significant information.

i. *$M4$ transitions; unfavoured factors.*

The strong spin-orbit coupling shell model predicts low-lying isomeric states of long lifetime in the regions before the closed shells at 50, 82, and 126. In these regions, particle levels of high spin ($g_{9/2}$, $h_{11/2}$, and $i_{13/2}$, respectively) are being filled simultaneously with levels of low spin and opposite parity ($p_{1/2}$, $d_{3/2}$, and $f_{5/2}$) and isomeric states decaying by $M4$ radiation are

TABLE XXV. $M4$ transitions in odd-A nuclei.

Nucleus	E (keV)	$-\log T$ ($\sec^{-1}$)	F	Nucleus	E (keV)	$-\log T$ ($\sec^{-1}$)	F
	$g_{9/2} \leftrightarrow p_{1/2}$				$h_{11/2} \leftrightarrow d_{3/2}$		
$_{30}Zn^{69}$	439	4.88	.060	$_{50}Sn^{117}$	159	7.95	.120
$_{36}Kr^{85}$	305	5.18	.101	$_{50}Sn^{119}$	65	11.13	.234
$_{38}Sr^{87}$	390	4.27	.089	$_{52}Te^{121}$	82	10.67	.082
$_{39}Y^{87}$	384	4.97	.055	$_{52}Te^{123}$	88	10.35	.086
$_{39}Y^{89}$	913	1.31	.098	$_{52}Te^{125}$	110	9.43	.094
$_{39}Y^{91}$	555	3.68	.037	$_{52}Te^{127}$	88	10.36	.080
$_{40}Zr^{89}$	588	2.61	.092	$_{52}Te^{129}$	106	9.34	.156
$_{41}Nb^{91}$	104	8.90	.73	$_{52}Te^{131}$	183	7.00	.236
$_{41}Nb^{95}$	216	6.39	.061	$_{54}Xe^{129}$	196	7.39	.056
$_{41}Nb^{97}$	747	1.94	.024	$_{54}Xe^{131}$	163	7.91	.086
$_{43}Tc^{95}$	39	~ 13.22	~ .046	$_{54}Xe^{133}$	232	6.42	.105
$_{43}Tc^{97}$	96	9 67	.046	$_{54}Xe^{135}$	520	3.22	.116
$_{43}Tc^{99}$	142	8.03	.057	$_{56}Ba^{133}$	275	6.05	.054
$_{49}In^{113}$	390	4.14	.038	$_{56}Ba^{135}$	269	5.77	.121
$_{49}In^{115}$	335	4.67	.044	$_{56}Ba^{137}$	661	2.40	.085
					$i_{13/2} \leftrightarrow f_{5/2}$		
				$_{78}Pt^{195}$	129	8.64	.049
				$_{78}Pt^{197}$	337	4.86	.053
				$_{80}Hg^{197}$	165	7.67	.048
				$_{80}Hg^{199}$	368	4.50	.054
				$_{82}Pb^{207}$	1063	0.113*	.084

The F-factor gives the ratio of the observed transition probability to that of a single-particle transition between the states indicated at the head of the column (cf. (8) and (10)).

* HOPKINS (1952).

expected. These expectations have been strikingly confirmed (GOLDHABER and SUNYAR, 1951; MOSZKOWSKI, 1951).

The lifetimes of these isomeric transitions yield further evidence on the properties of the combining states. The known $M4$ transition probabilities are listed in Table XXV. The last column gives the ratio F (the unfavoured factor) of the observed transition probability to that calculated for the appropriate single-particle transition (cf. (8) and (10), and (II.7))†. The F-factors are sensitive to the assumed value of the nuclear radius.

† The F-factors are analogous to the quantities $|M|^2$ listed by GOLDHABER and SUNYAR (1951), but are obtained by comparison with a somewhat more detailed theoretical estimate. In the notation of MOSZKOWSKI (1953), F equals the ratio of $|M|^2$ and M^2_{ML}, for magnetic transitions of order L.

Thus, a decrease of 10 % in the value (II.7) leads to an increase by about a factor two in the F-values of Table XXV.

Despite this uncertainty, it is evident that the transitions are consistently slower than expected for an uncoupled particle by a significant factor. This reduction provides evidence that the particle transitions are associated with an appreciable readjustment of the collective field. The observed unfavoured factors correspond to a nuclear coupling scheme resulting from an intermediate to strong particle-surface coupling (cf. § VII c.i).

From such an interpretation of the transitions, one can also correlate some of the observed trends of the unfavoured factor with the expected surface deformations. Thus, one notices that, for the nuclei possessing closed shells, and especially for those possessing double closed shells ± 1 particle, the F-factors are among the largest*. Moreover, for a series of isotopes of the same element, the F-values decrease as we move away from a closed-shell nucleus (cf. Bohr and Mottelson, 1952; Moszkowski, 1953). These trends can be understood in terms of the increased deformation, produced by the added particles and reflected in many nuclear properties (cf., e. g., § III.iii; § V c; § VI c.ii).

In the estimate of the F-factor, the transitions are compared with one-particle transitions, although many of the nuclei in question have several particles outside of closed shells. In the strong coupling approximation, where the particles are coupled separately to the nuclear axis, the transitions do indeed only involve changes in the quantum numbers of a single particle, and the F-factor can be directly related to the change in the vibrational state (cf. 15). If, however, the interparticle forces influence the coupling scheme in the nucleus (cf. Fig. 6), there will be an additional effect contributing to the F-factor (cf. Moszkowski. 1953). Still, it seems excluded that this latter effect gives the main part of F, since in Table XXV there are several nuclei with single-particle configurations, and also for these the transition probabilities are considerably reduced as compared with shell model estimates.

Reduction in the transition probability, associated with the

* In view of the marked stability of $_{82}Pb^{208}$, it may be significant that the F-factor for $_{82}Pb^{207}$ is as small as 0.08.

partial orthogonality of the vibrational states of different particle configurations, is expected as a very general feature of nuclear particle transitions. This is indeed observed and, besides the $M4$ isomeric transitions, especially the allowed unfavoured and the pure GT forbidden β-transitions provide evidence for the effect (cf. § VIIIc.ii and iv).

A consequence of this interpretation of the unfavoured factor is its absence in certain special cases where the combining states have similar surface shapes. Thus, the mirror β-transitions which, due to the symmetry in the particle configurations, have almost identical deformations are known to be conspicuously faster than other allowed β-transitions (cf. § VIIIc.i).

Another class of unretarded particle transitions is expected for the γ-transitions between the two members of the ground state doublet in an odd-odd nucleus, where the deformations are expected to be rather similar (cf. § VIb). There is some evidence that the low energy $M1$ transitions in odd-odd nuclei are faster than in odd-A nuclei (GRAHAM and BELL, 1953). Some of the long lived $M3$ isomers in odd-odd nuclei (cf. GOLDHABER and HILL, 1952) may also be of this type, but uncertainties in the spin assignments as well as in the conversion coefficients prevent as yet a quantitative analysis of the lifetimes.

It would also be of interest to compare β- or γ-transitions to different members of a rotational family, since the vibrational integral in F does not affect the branching ratio.

ii. *$E3$ transitions; j-forbiddenness.*

In the region before the closed shell at 50, another important group of long lived isomers has been found. These have been identified as $E3$ transitions of the $(7/2+) \leftrightarrow (1/2-)$ type and occur for the nucleon numbers 43, 45, and 47. The $(7/2+)$ states have been classified on the basis of the shell model as $(g_{9/2})^{3,5,7}_{7/2}$ (GOLDHABER and SUNYAR, 1951; MOSZKOWSKI, 1951). For pure configurations of this type, the transitions would be forbidden to order $E3$ (j-forbiddenness). For odd-neutron nuclei, there is an additional forbiddenness for these transitions which require an electric multipole moment. Both these types of forbiddenness are removed by the surface coupling which is expected to be rather large in these nuclei, as evidenced by the energy

TABLE XXVI. $E3$ transitions of $(7/2+) \leftrightarrow (1/2-)$ type.

Nucleus	E (keV)	$-\log T$ ($\sec^{-1}$)	F
$_{34}Se^{77}$	160	1.68	.013
$_{34}Se^{79}$	80	3.89	.0025
$_{34}Se^{81}$	98	4.64	.0004
$_{36}Kr^{79}$	127	2.47	.0026
$_{36}Kr^{81}$	187	1.45	.0017
$_{36}Kr^{83}$	32.2	~ 7.39	$\sim .0004$
$_{45}Rh^{103}$	40	~ 6.95	$\sim .0007$
$_{45}Rh^{105}$	130	2.55	.0010
$_{47}Ag^{107}$	93.9	3.03	.013
$_{47}Ag^{109}$	87	3.04	.021
$_{74}W^{183}$	80	~ 3.02	$\sim .014$

The shell model assigns a $(g_{9/2})^{3, 5, 7}$ configuration to the $(7/2+)$ state. The anomalous spin $I = j - 1$ may be explained as a result of the surface coupling (cf. § III.iii). For a pure $g_{9/2}$ configuration, the transition would be forbidden to order $E3$ (j-forbiddenness). The transition is assumed to occur due to the admixture of a small amount of the $g_{7/2}$ orbital. The coupling to deformations of order three, which induces an $E3$ moment in the surface, may also be important for these transitions, especially in the odd-neutron nuclei. The F-factor gives the ratio of the observed transition probability to that of a $g_{7/2} \leftrightarrow p_{1/2}$ single-proton transition (cf. (7) and (10)).

depression of the $(7/2+)$ level (cf. § III.iii). The surface coupling will admix particle states of $g_{7/2}$ type and, furthermore, the coupling to the $\lambda = 3$ surface mode produces an $E3$ moment also in odd-neutron states (cf. (12)).

In Table XXVI are listed the known $E3$ transitions of $(7/2+) \leftrightarrow (1/2-)$ type. The F-factors listed in the last column of the table are derived by comparison with the transition of a single proton between $p_{1/2}$ and $g_{7/2}$ states ((7) and (10)). The comparable magnitude of the observed F-factors for odd-neutron and odd-proton nuclei is an indication that the second term in (12) is at least comparable to the first term, as suggested by the hydrodynamic estimate. There may be a tendency for the odd-neutron F-values to be somewhat smaller than those of odd-proton nuclei; this could be understood from the effect of the first term in (12) together with the A-dependence of the last term.

The appearance of smaller F-factors in this group as compared with the $M4$ transitions, as well as the somewhat larger

spread in values, may reflect the fact that the transition depends entirely on the admixture of the $g_{7/2}$ state, which again depends on the degree of deformation of the nucleus.

Examples of $E3$ transitions between other configurations have also been identified, some with very small F-factors (cf. GOLDHABER and SUNYAR, 1951). While the detailed classification of these transitions is difficult at the present time, such highly unfavoured transitions may be expected in regions of strong coupling, due to selection rules associated with the Ω_p and K quantum numbers.

iii. *$E2$ transitions; collective excitations.*

Collective excitations give rise in general to $E2$ or $M1$ radiation (cf. § VIc), and are expected to reveal themselves especially by their strongly enhanced $E2$ transition probabilities, resulting from the large electric quadrupole of the oscillating surface.

In the strongly coupled system, the low-lying collective excitations can be characterized as rotational levels. The spectrum is particularly simple in even-even nuclei where a series of states with even I decaying by pure $E2$ radiation is obtained (cf. § VIc.ii).

The first excited $(2+)$ states in even-even nuclei with measured lifetimes are listed in Table XXVII. The F-factors in column four provide a comparison of the observed transition probability with that expected for a proton transition $(j^2)_2 \rightarrow (j^2)_0$ for large j (cf. (9)).

The very large F-factors for the nuclei in regions away from closed shells confirm the interpretation of the states as rotational levels of the strongly coupled system. From the measured lifetimes one can deduce, by means of (17), the intrinsic quadrupole moments Q_0 which are listed in column five. These may be compared with the Q_0-values derived from the spectroscopically measured quadrupole moments of neighbouring isotopes, listed in column six. In the derivation of Q_0 from Q, the full strong coupling projection factor (V.9) has been assumed. The two determinations of Q_0 yield similar values. The spectroscopic values are somewhat larger than those deduced from transition probabilities, but the difference may not be significant, considering

TABLE XXVII. $E2$ transitions in even-even nuclei.

Nucleus	E (keV)	log T (sec^{-1})	F	$\|Q_0\|$ (10^{-24} cm^2) (transition)	$\|Q_0\|$ (10^{-24} cm^2) (spectroscopic)
$_{66}Dy^{160}$	85	7.91	140	9	
$_{68}Er^{166}$	80	7.91	180	10	~ 20 ($_{68}Er^{167}$)
$_{70}Yb^{170}$	84	7.94	140	9	11 ($_{70}Yb^{173}$)
$_{72}Hf^{176}$	89	8.01	120	9	14 ($_{71}Lu^{175}$)
$_{76}Os^{186}$	137	8.64	55	6	8 ($_{75}Re^{185}$)
$_{80}Hg^{198}$	411	10.1 *	6	2	2 ($_{80}Hg^{201}$)
$_{82}Pb^{204}$	374	6.34	2×10^{-3}		
$_{84}Po^{212}$	719	11.2 **	5	2	
$_{84}Po^{214}$	606	11.1 **	7	2	

* MALMFORS (1952); corrected for the statistical factor in the resonance formula (cf., e. g., STORRUSTE, 1951).

** Deduced from the branching ratio of α- and γ-decay (cf. BETHE, 1937, p. 229). The lifetime for the long range α-groups is calculated from that of the ground state by the semi-empirical formula of WAPSTRA (1953) with the inclusion of the appropriate statistical factor. The empirical energies and lifetimes are taken from the compilation of WAY et al. (1950) and HOLLANDER, PERLMAN and SEABORG (1953). The branching ratios are obtained from these references and from ELLIS and ASTON (1930) and RYTZ (1951).

The table lists the $E2$ transitions in even-even nuclei with measured lifetimes. All the transitions go from a first excited state of $(2+)$ character to the ground state $(0+)$. The F-factor in column four is the ratio of the observed transition probability to the value calculated for a proton transition $(j^2)_2 \rightarrow (j^2)_0$ for large j (cf. (9)). The intrinsic quadrupole moments Q_0 in column five are deduced from (17), assuming the levels to be of rotational character. For comparison, the last column lists the intrinsic quadrupole moment derived from available spectroscopic data on neighbouring odd nuclei (cf. Addendum to Chapters IV and V). The projection factor (V. 9) has been assumed in calculating Q_0 from Q.

the experimental uncertainties involved in both types of measurements.

The table exhibits the intimate correlations between excitation energies, reduced transition probabilities, and quadrupole moments, and also shows the expected variations of these quantities with the number of particles outside of closed shells.*

With the approach to the closed-shell configuration of Pb^{208}, the rotational description of the states becomes less appropriate, and in the immediate neighbourhood of Pb^{208} a

* Note added in proof: Recently, HUUS and ZUPANČIČ (1953) have produced the $(2+)$ first excited states in the even $_{74}W$ isotopes by means of Coulomb excitation. From the measured excitation cross section they have deduced a deformation $|Q_0| \approx 7\times10^{-24}$ cm^2 in good agreement with the trends exhibited in Table XXVII (cf. also footnote on p. 166).

TABLE XXVIII. $E2$ transitions in odd-A nuclei.

Nucleus	E (keV)	$\log T$ ($\sec^{-1}$)	states		F	$\lvert Q_0 \rvert$ (10^{-24} cm^2) (transition)
			i	f		
$_{48}Cd^{111}$	243	6.91	5/2+	1/2+	0.12	
$_{73}Ta^{181}$	481	7.74	3/2+	7/2+	0.005	
$_{80}Hg^{197}$	134	7.47	5/2—	1/2—	4.0	2
$_{80}Hg^{199}$	159	7.94	5/2—	1/2—	5.0	2

The F-factors have been calculated by comparison with a single-proton transition between states with the listed spins and parities. The Q_0-values for the Hg isotopes are obtained from (19).

weak coupling situation is expected. In this region, the collective excitations represent simple surface oscillations (cf. § VIc.i).

In the weakly coupled system, also particle excitations may be encountered among the first excited states (cf. § VIb). An example may be provided by the Pb^{204} activity with its relatively long lifetime. The fact that, for this transition, F is small compared to unity may indicate a rather pure neutron excitation, corresponding to the closed-shell structure of the protons.

The observed $E2$ transitions in odd-A nuclei are listed in Table XXVIII. The two first have the small F-factors characteristic of particle excitations. For the Hg transitions, the F-factors are larger than unity and indicate collective excitations. A first excited level of I_0+2 in these nuclei can be obtained for a rotational family with $\Omega = 1/2$ (cf. § VIc.iii); this interpretation could also account for the relatively low excitation energies as compared with that in Hg^{198}. The Q_0-values derived from (19) are just of the same magnitude as obtained for Hg^{198}, and derived from the spectroscopic data of Hg^{201} (cf. Table XXVII). The intermediate F-factors of the Hg transitions, as well as the rather large excitation energies, indicate that the strong coupling scheme is not very fully developed, and deviations from the simple rotational character of the states may be of importance.*

* Note added in proof: An example of a strongly enhanced $E2$ transition ($F \sim 100$) in an odd-A nucleus ($_{73}Ta^{181}$) has recently been found by the Coulomb excitation process (HUUS and ZUPANČIČ 1953; cf. footnote on p. 166 below).

VIII. Beta Transitions.

The analysis of β-transitions has the dual purpose of determining the intrinsic properties of the nucleon-lepton coupling, and providing information on the nuclear structure. The recent progress in experimental techniques as well as the understanding of nuclear states have led to an improved evaluation of the coupling constants in β-decay. This, in turn, now makes possible more detailed tests of nuclear wave functions.

The type of information provided by the analysis of β-transitions is in many respects similar to that derived from electromagnetic particle transitions (cf. § VIb). In particular, the classification of transitions in degrees of forbiddenness provides evidence on the spins and parities of nuclear states, while a closer study of β-decay transition probabilities gives more detailed information on the nuclear coupling scheme. In the present chapter, we consider the calculation of transition probabilities in the coupled system, and the more detailed analysis of the empirical data.*

a) Transition Operators.

The comparative half lives of allowed transitions may be written in the form

$$f_0 t = B_g \left[(1 - x) D_F(0) + x D_{GT}(0)\right]^{-1}, \qquad \text{(VIII.1)}$$

where t is the half life and f_0 the integrated Fermi function for an allowed transition (cf., e. g., KONOPINSKI, 1943), while

$$B_g = \frac{2\pi^3 \hbar^7 \ln 2}{g^2 m_e{}^5 c^4}. \qquad \text{(VIII.2)}$$

* We are indebted to Dr. O. KOFOED-HANSEN and M. Sc. A. WINTHER for valuable discussions on theoretical and experimental aspects of β-transitions.

The partial coupling constants for Fermi and Gamow-Teller interactions are $g(1-x)^{1/2}$ and $gx^{1/2}$, respectively*.

The reduced transition probabilities are given by**

$$D_F(0) = \sum_{M_f} |<i| T_\pm |f>|^2 \qquad \text{(VIII.3)}$$

and

$$D_{GT}(0) = 4 \sum_{M_f} |<i| \sum_p \vec{s}_p \tau_\pm^{(p)} |f>|^2, \qquad \text{(VIII.4)}$$

where $T_\pm = \sum \tau_\pm^{(p)}$ are components of the total isotopic spin. The operators s and τ are normalized in such a way that their proper values are $1/2$ and $-1/2$.

For the forbidden β-decays, the transition operator may consist of several terms giving rise to different spectral shapes. The analysis of such mixed transitions is of special interest for the study of the β-decay coupling, but the influence of nuclear structure is as yet more difficult to evaluate.

The forbidden transitions, which have a parity change of $(-)^{\Delta I+1}$ (with $\Delta I \neq 0$) are, however, more simple to interpret. These transitions are of pure Gamow-Teller type and exhibit a spectrum of unique shape. They are intimately related to the magnetic multipole transitions of order $\lambda = \Delta I$. The comparative half life is given by

$$f_n t = B_g [x D_{GT}(n)]^{-1}, \qquad \text{(VIII.5)}$$

where f_n is the integrated Fermi function appropriate to the considered type of transition of forbiddenness $n = \Delta I - 1$ (cf. KONOPINSKI and UHLENBECK, 1941; GREULING, 1942). The normalization employed here is such that

$$f_n = \frac{1}{[(n+1)!]^2} \int_1^{W_0} \sum_{\nu=0}^{n} (B_{n\nu} K^{2(n-\nu)} L_\nu) F_0(W, Z) p W (W_0 - W)^2 dW, \qquad \text{(VIII.6)}$$

where the symbols are defined by DAVIDSON (1951).

The reduced transition probability $D_{GT}(n)$ may be written in the form

* The influence of the so-called cross-terms (FIERZ, 1937) has been neglected. Estimates of the possible magnitude of such terms have recently been given by MAHMOUD and KONOPINSKI (1952) and by WINTHER and KOFOED-HANSEN (1953).

** The quantities $D_F(0)$ and $D_{GT}(0)$ are often denoted by $|\int 1|^2$ and $|\int \vec{\sigma}|^2$, respectively (cf., e. g., KONOPINSKI, 1943).

$$D_{GT}(n) = \sum_{\mu, M_f} |<i| \mathfrak{O}_{GT}(n, \mu) |f>|^2, \qquad \text{(VIII.7)}$$

where the transition operator is given by*, **

$$\left.\begin{aligned} \mathfrak{O}_{GT}(n, \mu) = &\left[\frac{4\pi 2^{n+3}}{(2n+3)!}\right]^{1/2} \frac{[(n+1)!]^2}{n+1} \left(\frac{mc}{\hbar}\right)^n \\ &\sum_p \vec{s}_p \cdot \vec{\nabla}_p \left[r_p^{n+1} Y_{n+1,\mu}(\vartheta_p, \varphi_p)\right] \tau_\pm^{(p)}, \end{aligned}\right\} \qquad \text{(VIII.8)}$$

which exhibits the analogy to the magnetic multipole transitions with $\lambda = n + 1$ (cf. (VII.2 and 4)). For $n = 0$, (8) reduces to

$$\mathfrak{O}_{GT}(0, \mu) = 2 \sum_p s_\mu^{(p)} \tau_\pm^{(p)}, \qquad \text{(VIII.9)}$$

where s_μ are the spherical vector components of $\vec{s}$. Equation (7) is then equivalent to (4).

b) Evaluation of Transition Probabilities.

i. *Transitions in an undeformed nucleus.*

The matrix element for allowed Fermi transitions can be simply expressed in terms of the total isotopic spin quantum numbers of the combining states if charge independence of the forces in the nucleus is assumed (cf. WIGNER and FEENBERG, 1941). From (3) one obtains the selection rule $\Delta T = 0$ and the value

$$D_F(0) = (T \mp T_z)(T \pm T_z + 1) \qquad (T_z \to T_z \pm 1) \qquad \text{(VIII.10)}$$

for the reduced transition probability.

The Gamow-Teller transition probability is more dependent on the nuclear coupling scheme. For transitions of a single particle, (4) gives

* In the notation of GREULING (1942), we have

$$D_{GT}(n) = |Q_{n+1}(\vec{\sigma}, \vec{r})|^2$$

while KONOPINSKI and UHLENBECK (1941), for $n = 1$, use the quantity B_{ij}, where

$$D_{GT}(1) = \Sigma |B_{ij}|^2.$$

** BLATT and WEISSKOPF (1952) write the transition operator in terms of

$$r^n \mathcal{Y}^\mu_{n+1,n} = 2\left[(n+1)(2n+3)\right]^{-1/2} \vec{s} \cdot \vec{\nabla}(r^{n+1} Y_{n+1,-\mu}).$$

$$D_{GT}(0) = \left\{ \begin{array}{ll} \dfrac{j+1}{j} & j = l+1/2 \\ \dfrac{j}{j+1} & j = l-1/2 \end{array} \right\} \Delta j = 0 \quad \text{(VIII.11)}$$

and

$$D_{GT}(0) = \frac{4\,l}{2\,l+1} \frac{2j_f+1}{2j_<+1} \qquad \Delta j = 1\,. \qquad \text{(VIII.12)}$$

The last formula assumes $j_> = l + 1/2$ and $j_< = l - 1/2$ ($\Delta l = 0$). For $\Delta j = 1$ and no parity change, one may also have $\Delta l = 2$, in which case the transition is second forbidden, according to the single-particle model (l-forbiddenness; cf. NORDHEIM, 1951).

For two-particle configurations, and a few three- and four-particle configurations, the matrix elements are unique for transitions between states of given J and T (cf., e. g., Table III). In more complicated configurations, the value of $D_{GT}(0)$ will depend on the particular coupling scheme.

For the forbidden transitions of pure GT type, the transition probability for a single-particle transition may be obtained from (7) and (8) by using the result (VII.8).

ii. *Transitions in the strongly coupled system.*

The value (10) for the Fermi transition probability follows directly from the assumption of a constant total isotopic spin for the nuclear states, and is not affected by the surface coupling.

The transition probabilities for Gamow-Teller transitions in the strongly coupled system can be evaluated by the same methods as used for the electromagnetic particle transitions (§ VII c.i).

The transition operators are conveniently expanded along the nuclear axis, giving (cf. VII.13)

$$\mathfrak{O}_{GT}(n,\mu) = \sum_{\nu} \mathfrak{O}'_{GT}(n,\nu)\, \mathfrak{D}^{n+1}_{\mu\nu}(\theta_i) \qquad \text{(VIII.13)}$$

in terms of the operators $\mathfrak{O}'$ expressed in the nuclear coordinate system.

For transitions with $\Delta I = n+1$ between strong coupling states with $\Omega_i = K_i = I_i$ and $\Omega_f = K_f = I_f$, one obtains

$$D_{GT}(n) = \left|\int \chi^*_{\Omega_i} \mathfrak{O}'_{GT}(n, \pm(n+1))\, \chi_{\Omega_f}\right|^2 \left|\int \varphi_i^* \varphi_f\right|^2 \frac{2I_f+1}{2I_>+1}. \quad \text{(VIII.14)}$$

If $j_i = (\Omega_p)_i = I_i$ and $j_f = (\Omega_p)_f = I_f$, for the transforming particle, the expression (14) can be written

$$D_{GT}(n) = \{D_{GT}(n)\}_{sp} \left|\int \varphi_i^* \varphi_f\right|^2 \frac{2I_<+1}{2I_>+1} \quad \text{(VIII.15)}$$

in terms of the transition probability for a single uncoupled particle (cf. § VIIIb.i). The significance of the last factors in (15) in retarding the transition has been discussed in connection with the analogous formula (VII.15).

In the discussion of the empirical data, this retardation is expressed as the unfavoured factor F, representing the ratio of D and D_{sp}. It is convenient to generalize the definition of F to include cases where $j_p \neq \Omega_p$ for the states of the transforming particle, and for which the coupling scheme has no simple analogue in the shell model. Thus, in general, for ground state transitions with $\Delta I = n + 1$,

$$F = D_{GT}(n) \left|\int \chi^*_{\Omega_i} \mathfrak{O}'_{GT}(n, \pm(n+1))\, \chi_{\Omega_f}\right|^{-2} \frac{2I_<+1}{2I_f+1}, \quad \text{(VIII.16)}$$

The above discussion includes the allowed transitions ($n = 0$) with $\Delta I = 1$. For allowed transitions with $\Delta I = 0$, one obtains directly from (4)

$$D_{GT}(0) = 4 \left|\int \chi^*_{\Omega_i} s_3 \tau_\pm \chi_{\Omega_f}\right|^2 \left|\int \varphi_i^* \varphi_f\right|^2 \frac{I}{I+1}, \quad \text{(VIII.17)}$$

where s_3 is the component of $\vec{s}$ along the nuclear axis. In this case, the F-factor is

$$F = D_{GT}(0) \frac{1}{4} \left|\int \chi^*_{\Omega_i} s_3 \tau_\pm \chi_{\Omega_f}\right|^{-2} \frac{I}{I+1}. \quad \text{(VIII.18)}$$

Additional symmetry terms may appear in (17) in the special case of $K = \Omega = 1/2$.

For the mirror transitions, the symmetry of the combining states implies an intimate relation between D_{GT} and the expect-

ation value of s_z for the states involved. For a one-particle configuration, one obtains directly from (4)

$$D_{GT}(0) = 4\frac{I+1}{I} < s_z >^2_{M=I}. \qquad \text{(VIII.19)}$$

In the strongly coupled system where the particles are coupled separately to the nuclear axis, (19) holds quite generally for mirror transitions, with s_z referring to the last odd particle. The quantity $< s_z >$ also occurs in the static magnetic moment and may be evaluated by the methods of § IVb.*

c) Discussion of Empirical Data.

Recent studies of the *ft*-values of simple nuclei have led to an improved determination of the coupling constants of β-decay (Bouchez and Nataf, 1952; Kofoed-Hansen and Winther, 1952; Trigg, 1952; Blatt, 1953). We here use the values

$$\left.\begin{aligned} B_g &= 2.6 \times 10^3 \,\text{sec} \\ x &= 0.5 \end{aligned}\right\} \qquad \text{(VIII.20)}$$

which seem to be consistent with available empirical data (cf., e. g., Winther and Kofoed-Hansen, 1953).

i. *Mirror transitions.*

The absence of an unfavoured factor arising from different surface shapes of the combining states makes possible a rather detailed analysis of the *ft*-values of mirror decays, from which information about the nuclear coupling scheme may be obtained.

Since the nuclear magnetic moment, due to the large intrinsic nucleon *g*-factor, primarily depends on $< s_z >$ (cf. IV.3), which also determines the *GT* transition probability (cf. 19), one expects rather strong correlations between magnetic moments and *ft*-values of mirror transitions. Indeed, it is found that, when the magnetic moment deviates from the shell model values, there are corresponding deviations in the mirror *ft*-values and that

* The strong coupling matrix elements for mirror transitions have been given by Davidson and Feenberg (1953) for j a constant.

TABLE XXIX. *ft*-values of mirror transitions.

Product nucleus	I	E_{max} (Me V)	$t_{1/2}$	$(ft)_{exp}$	$(ft)_p$	$(ft)_c$
$_5B^{11}$	3/2	0.958	20.39^m	3840(70)	1950	3060
$_6C^{13}$	1/2	1.200	10.1^m	4560(100)	3900	3900
$_7N^{15}$	1/2	1.683	2.1^m	3800(200)	3900	3900
$_8O^{17}$	5/2	1.745	65^s	2320(100)	2160	2160
$_9F^{19}$	1/2	2.234	19.5^s	1970(100)	1300	1800
$_{10}Ne^{21}$	3/2	2.50	22.8^s	3700(200)	—	3600
$_{11}Na^{23}$	3/2	3.073	12.0^s	4780(150)	—	3600
$_{12}Mg^{25}$	5/2	—	7.3^s	—	—	3030
$_{13}Al^{27}$	5/2	3.48	5.0^s	3350(600)	2160	3030
$_{14}Si^{29}$	1/2	3.60	4.6^s	3510(700)	1300	4350
$_{15}P^{31}$	1/2	4.06	3.1^s	4020(600)	1300	4400
$_{16}S^{33}$	3/2	4.43	2.0^s	3800(650)	3250	4850
$_{17}Cl^{35}$	3/2	4.4	1.90^s	3420(800)	3930	4850
$_{18}A^{37}$	(3/2)	4.57	1.2^s	2520(600)	3930	3750
$_{19}K^{39}$	3/2	5.13	1.06^s	3740(500)	3250	3750
$_{20}Ca^{41}$	(7/2)	4.9	0.87^s	2430(800)	2280	(2920)

The empirical data are taken from WINTHER and KOFOED-HANSEN (1953). Their estimated uncertainties for the experimental *ft*-values in column five are listed in parentheses. The second to last column gives the shell model *ft*-values, wherever they are independent of specific assumptions about nuclear forces. In the last column are listed *ft*-values for the coupled system, obtained from the wave functions discussed in the text.

the observed correlation can be understood from simple assumptions about the nuclear states (TRIGG, 1952; WINTHER, 1952; WINTHER and KOFOED-HANSEN, 1953). The existence of such a correlation strongly supports the interpretation of the observed moment shifts as reflecting a modified nuclear coupling scheme (cf. p. 52).

The calculation of mirror *ft*-values in the coupled system follows the same lines as employed in the Addendum to Chapters IV and V. Some of the details of this analysis are given below and the results are summarized in Table XXIX. In cases where the *ft*-value depends sensitively on the nuclear deformation, the coupling situation indicated by the magnetic moment has been used. For comparison, *ft*-values calculated from shell model wave functions are listed wherever the states are unique.

Calculation of mirror *ft*-values.

$A = 11$.

The magnetic moment of B^{11} indicates a rather strong surface coupling (cf. p. 48), which is further supported by the *ft*-value. The listed $(ft)_c$-value is obtained by determining the coupling situation from the magnetic moment, assuming a pure $p_{3/2}$ state ($\mu = (g_j - g_R) < j_z > + g_R I$). However, as discussed on p. 69, it seems unlikely that such a configuration can account for the whole observed moment shift. The deviation from (*jj*) coupling indicated by the magnetic moment seems also reflected in the observed *ft*-value.

$A = 13$ and 15.

The $p_{1/2}$-nuclei are influenced by the surface only through the coupling to the $p_{3/2}$ state (cf. p. 68). However, this coupling has no effect on the *ft*-value. The discrepancy between $(ft)_p$ and $(ft)_{exp}$ for $A = 13$ may again indicate a deviation from (*jj*) coupling.

$A = 17$.

Due to the stability of the O^{16} core (cf. p. 76), one expects only very little influence of the surface coupling on the *ft*-value. This is consistent with the empirical data.

$A = 19$, 29, and 31.

The magnetic moments of these $(1/2+)$ nuclei have been accounted for in terms of strong coupling states with $\Omega = 1/2$, containing $s_{1/2}$, $d_{5/2}$, and $d_{3/2}$ orbitals (cf. p. 63 ff.). The magnetic moment depends sensitively on the interference between the $d_{3/2}$ and $d_{5/2}$ orbitals, and the *ft*-value is expected to show a similar effect. Fig. 15, which is the analogue of Fig. 11, shows the characteristic asymmetry of *ft* with respect to the sign of the deformation, which accounts for the conspicuous difference between the *ft*-values for $A = 19$ and those for $A = 29$ and 31. The $(ft)_c$-values in Table XXIX have been obtained from *y*-values consistent with the observed magnetic moments. It is of interest that for F^{19} the $(ft)_c$-value differs appreciably from $(ft)_p$, although $\mu \approx \mu_{sp}$. The empirical data seem to support this expectation.

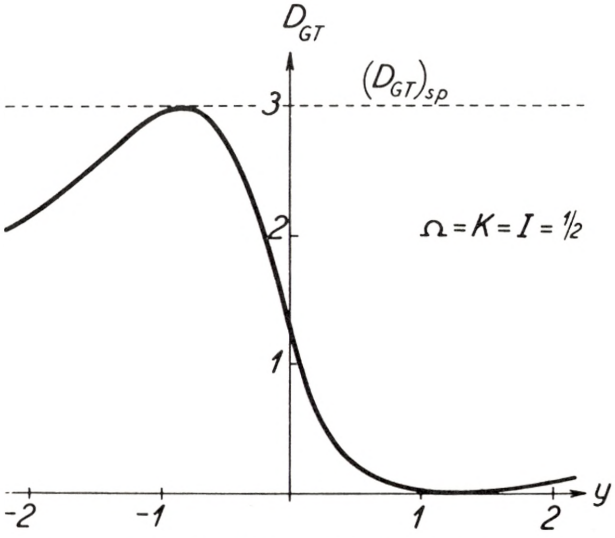

Fig. 15. *Beta decay transition probabilities arising from d-state admixture in* $I = \Omega = 1/2$ *states.* The figure gives the reduced GT-transition probability for mirror transitions between states of the type discussed in Ad. i (cf. especially caption to Fig. 11). The states are characterized by the amplitudes $a_s^2 \sim 1/3$ and $a_d^2 \sim 2/3$. The ratio of $d_{3/2}$ to $d_{5/2}$ is denoted by y. The strong asymmetry of D_{GT} with respect to the sign of y arises from the $d_{3/2}$—$d_{5/2}$ interference, and is similar to the behaviour of the magnetic moment.

$A = 21$ and 23.

In the strong coupling approximation, these nuclei are represented as $\Omega = 3/2$ states containing $d_{5/2}$ orbitals with a small admixture of $d_{3/2}$ (cf. p. 75). The $(ft)_c$-value is very sensitive to this admixture and the values given in Table XXIX correspond to a $d_{3/2}$ amplitude of $a_{3/2} = -0.2 \cdot a_{5/2}$, which is in accordance with μ (Na^{23}). In the absence of the $d_{3/2}$ interference, one would have $(ft)_c = 4300$.

$A = 25$ and 27.

The $(ft)_c$-values are calculated for strong coupling states with $j = \Omega = 5/2$ which account approximately for the magnetic moments of Mg^{25} and Al^{27} (cf. p. 76).

$A = 33$, 35, 37, and 39.

In the strong coupling approximation, these nuclei are described as $\Omega = 3/2$ states, predominantly of $d_{3/2}$ type, with a

small admixture of $d_{5/2}$. One expects the $(ft)_c$-values, just like the magnetic moments (cf. p. 72), to depend rather sensitively on the sign of the interference term, which again depends on whether the configuration is that of a single odd particle or hole. In the former case, corresponding to $A = 33$ and 35, the $(ft)_c$-values in Table XXIX are calculated for the value $a_{5/2} = -0.15\, a_{3/2}$ suggested by the magnetic moments. In the latter case ($A = 37$ and 39), the opposite sign for $a_{5/2}$ applies.

$A = 41$.

The $(ft)_c$-value listed in parenthesis corresponds to the strong coupling limit ($j = \Omega = 7/2$), but the stability of the Ca^{40} core may imply a weak coupling for Ca^{41}.

ii. *Allowed unfavoured transitions.*

The shell model has been a valuable guide in the classification of β-transitions in degrees of forbiddenness, especially through its ability to predict the parities of the combining states (MAYER, MOSZKOWSKI and NORDHEIM, 1951; NORDHEIM, 1951). At the same time, the quantitative analysis of the ft-values indicates an important influence of the dynamical aspects of the collective field. This is strikingly illustrated by the difference between the ft-values of mirror transitions and other allowed transitions. While the symmetry of the mirror states implies almost identical surface shapes, other types of transitions are in general expected to be appreciably retarded, due to surface readjustments accompanying the particle transitions.

Table XXX lists the ground state transitions in odd-A nuclei, excepting the mirror transitions, which have been classified as allowed (MAYER, MOSZKOWSKI and NORDHEIM, 1951). The F-factor in the last column provides a measure of the retardation of the observed transitions as compared with a single-particle transition between the states listed in columns four and five (cf. (16) and (18)).

It is seen that the transitions are slowed down by a factor of the order of 10—100, which is of the same order of magnitude as the reductions for $M4$ transitions (cf. Table XXV).

The allowed transitions in even-A nuclei show a behaviour

TABLE XXX. Allowed unfavoured β-transitions in odd-A nuclei.

Nucleus	E_0 (MeV)	$\log f_0 t$	particle states		F
			i	f	
$_{10}Ne^{23}$	−4.1	4.9	$d_{5/2}$	$d_{5/2}^{3/2}$	.16
$_{11}Na^{25}$	−3.7	5.2	$d_{5/2}^{3/2}$	$d_{5/2}$	.056
$_{16}S^{35}$	−0.17	5.0	$d_{3/2}$	$d_{3/2}$	.083
$_{20}Ca^{45}$	−0.22	5.6	$f_{7/2}$	$f_{7/2}$	.010
$_{21}Sc^{49}$	−1.8	5.5	$f_{7/2}$	$f_{7/2}$	.013
$_{27}Co^{61}$	−1.3	5.2	$f_{7/2}$	$f_{5/2}$	.019
$_{30}Zn^{63}$	+2.36	5.4	$p_{3/2}$	$p_{3/2}$	.012
$_{30}Zn^{69}$	−1.0	4.6	$p_{1/2}$	$p_{3/2}$	.050
$_{31}Ga^{73}$	−1.4	5.9	$p_{3/2}$	$p_{1/2}$	.0050
$_{32}Ge^{75}$	−1.1	5.0	$p_{1/2}$	$p_{3/2}$	.020
$_{33}Aa^{71}$	+0.6	5.1	$p_{3/2}$	$p_{1/2}$	.030
$_{33}As^{77}$	−0.7	5.7	$p_{3/2}$	$p_{1/2}$	.077
$_{34}Se^{73}$	+1.29	5.3	$p_{1/2}$	$p_{3/2}$	.0098
$_{34}Se^{81}$	−1.5	4.8	$p_{1/2}$	$p_{3/2}$	.031
$_{35}Br^{75}$	+1.6	5.6	$p_{3/2}$	$p_{1/2}$	.010
$_{35}Br^{77}$	+0.36	5.0	$p_{3/2}$	$p_{1/2}$	.038
$_{35}Br^{83}$	−1.05	5.3	$p_{3/2}$	$p_{1/2}$	.020
$_{35}Br^{85}$	−2.5	5.1	$p_{3/2}$	$p_{1/2}$	.030
$_{45}Rh^{105}$	−0.57	5.5	$g_{9/2}$	$g_{7/2}$	.0091
$_{50}Sn^{121}$	−0.38	5.0	$d_{3/2}$	$d_{5/2}$	.022
$_{52}Te^{127}$	−0.76	5.6	$d_{3/2}$	$d_{5/2}$	.0056
$_{60}Nd^{141}$	+0.7	5.2	$d_{3/2}$	$d_{5/2}$	.014

The empirical E_0 and $\log f_0 t$ values as well as the spin and parity of the combining states are taken from MAYER, MOSZKOWSKI and NORDHEIM (1951). The F-factors are calculated by comparison with the single-particle transitions listed in columns four and five (cf. (16) and (18)). The superscript gives the value of Ω_p in cases where it differs from j_p.

similar to that of odd-A nuclei (cf. NORDHEIM, 1951). An interesting anomaly is the decay of $_6C^{14}$ whose long lifetime may indicate an accidental cancellation in the matrix element. Additional information on the states involved in this transition could be obtained from a measurement of the γ-decay lifetime of the 2.31 MeV state in $_7N^{14}$. This state is believed to be the $T = 1$ state which is isobaric with the C^{14} ground state (cf., e. g., AJZENBERG and LAURITSEN, 1952); it decays by $M1$ radiation, and the transition matrix element is very similar to that involved in the β-decay of C^{14}.

TABLE XXXI. *l*-forbidden β-transitions in odd-A nuclei.

Nucleus	E_0 (MeV)	$\log f_0 t$	particle states		F
			i	f	
$_8O^{19}$	−4.5	5.5	$d^{3/2}_{5/2}$	$d^{1/2}_{5/2}$	.026
$_{14}Si^{31}$	−1.8	5.9	$d^{3/2}_{3/2}$	$d^{1/2}_{3/2}$	.028
$_{15}P^{33}$	−0.26	5.1	$d^{1/2}_{3/2}$	$d^{3/2}_{3/2}$	.082
$_{28}Ni^{63}$	−0.05	6.8	$f^{5/2}_{5/2}$	$f^{3/2}_{5/2}$	.0040
$_{28}Ni^{65}$	−2.10	6.6	$f^{5/2}_{5/2}$	$f^{3/2}_{5/2}$	.0067
$_{29}Cu^{61}$	+1.22	4.9	$f^{3/2}_{5/2}$	$f^{5/2}_{5/2}$	.22
$_{29}Cu^{67}$	−0.65	5.5	$f^{3/2}_{5/2}$	$f^{5/2}_{5/2}$	.053
$_{30}Zn^{65}$	+0.32	7.0	$f^{5/2}_{5/2}$	$f^{3/2}_{5/2}$	.0026
$_{32}Ge^{69}$	+1.0	6.0	$f^{5/2}_{5/2}$	$f^{3/2}_{5/2}$	.026
$_{46}Pd^{109}$	−1.0	6.2	$g^{5/2}_{7/2}$	$g^{7/2}_{9/2}$	.0018

The empirical E_0 and $\log f_0 t$ values as well as the spin and parity of the combining states are taken from MAYER, MOSZKOWSKI and NORDHEIM (1952). These transitions, which are forbidden for pure shell model configurations, occur in the coupled system due to admixtures of the states listed in columns four and five. The strong coupling notation is used and the superscript denotes the component Ω_p of angular momentum along the nuclear axis. The F-factors are obtained by comparison with a pure particle transition of the listed type (cf. (16)).

There are also other cases where it would be of interest to combine lifetime evidence on allowed GT β-transitions with that of $M1$ transitions between the corresponding isobaric states (e. g., He^6 (β-)Li^6 compared to the γ-decay of the 3.58 MeV level in Li^6. Another example is the Be^7(K)Li^{7*} (478 keV), which may be compared with the γ-decay of the excited Li^7-state.)

iii. *l-forbidden transitions.*

The special type of odd-A transitions with $\Delta I = 1$ and no parity change, which according to the shell model have $\Delta l = 2$, are listed in Table XXXI. They are classified as *l*-forbidden

transitions (MAYER, MOSZKOWSKI and NORDHEIM, 1951). Their ft-values are comparable with, although somewhat larger than those of the allowed unfavoured transitions in Table XXX, and they have spectra of allowed type.

The configuration admixtures which are a general consequence of the surface coupling can destroy the l-forbiddenness in a similar manner as for the j-forbiddenness encountered in the $E3$ transitions (§ VII d.ii). The fourth and fifth columns of Table XXXI list the l, j, and Ω values of the single-particle orbitals, which are assumed to contribute the principal part of the transition matrix element. Assuming pure states of these types, one calculates the F-factors of the last column in the same way as for the transitions in Table XXX (cf. (16)).

The appearance in Table XXXI of somewhat smaller and more erratic F-factors than in Table XXX may reflect the sensitivity of the transitions to small amplitudes of admixed states (cf. the analogous situation for the j-forbidden $E3$ transitions (Table XXVI) as compared with the $M4$ transitions (Table XXV)).

The unfavoured factors of Table XXXI are somewhat larger than those of Table XXVI, which may be associated with the greater ease with which the surface destroys the l-forbiddenness than the j-forbiddenness because of the greater energy separation between the spin-orbit partners than between neighbouring orbitals in the same shell.

iv. *Pure GT forbidden transitions.*

The forbidden transitions which are identified by their spectral shape as being of the pure GT type are listed in Table XXXII. The unfavoured factor F in the last column provides a comparison of the observed transition probability with that of a single-particle transition between the states listed in columns four and five (cf. (16)). It is seen that the F-factors, as expected, are comparable to those of the allowed unfavoured β-transitions (Table XXX) and the $M4$ isomeric transitions (Table XXV).

The two largest F-factors in Table XXXII are those of B^{10} and K^{40}. In the former case, the observed F-factor can be accounted for in terms of the projection factor alone, with no contribution from the vibrational wave functions (cf. 14 and 16). The occurrence of similar surface shapes in the two combining

TABLE XXXII. Forbidden β-transitions of pure GT type.

Nucleus	E_0 (MeV)	log $f_n t$	particle states		F
			i	f	
	odd A		$\Delta I = 2$	yes ($n = 1$)	
$_{18}A^{41}$	−2.55	8.8	$f_{7/2}$	$d_{3/2}$	.03
$_{38}Sr^{89}$	−1.46	8.3	$d_{5/2}$	$p_{1/2}$	.09
$_{38}Sr^{91}$	−3.2	8.4	$d_{5/2}$	$p_{1/2}$	.07
$_{39}Y^{91}$	−1.56	8.5	$p_{1/2}$	$d_{5/2}$	.016
$_{55}Cs^{137}$	−0.53	8.7	$g_{7/2}$	$h_{11/2}$	.011
	even A		$\Delta I = 2$	yes ($n = 1$)	
$_{17}Cl^{38}$	−4.81	8.1	$f_{7/2}^{7/2}$	$d_{3/2}^{3/2}$	.16
$_{19}K^{42}$	−3.58	8.5	$f_{7/2}^{5/2}$	$d_{3/2}^{1/2}$	.16
$_{37}Rb^{86}$	−1.82	8.5	$g_{9/2}^{9/2}$	$f_{5/2}^{5/2}$	.04
$_{38}Sr^{90}$	−0.54	8.2	$d_{5/2}^{5/2}$	$p_{1/2}^{1/2}$	.09
$_{39}Y^{90}$	−2.20	8.1	$d_{5/2}^{5/2}$	$p_{1/2}^{1/2}$	.14
$_{81}Tl^{204}$	−0.765	8.9	$p_{3/2}^{3/2}$	$s_{1/2}^{-1/2}$	.010
	even A		$\Delta I = 3$	no ($n = 2$)	
$_{5}B^{10}$	−0.56	11.3	$p_{3/2}^{-3/2}$	$p_{3/2}^{3/2}$	.23
	even A		$\Delta I = 4$	yes ($n = 3$)	
$_{19}K^{40}$	−1.36	15.1	$f_{7/2}^{7/2}$	$d_{3/2}^{-1/2}$	.24

The table lists the forbidden transitions classified by their measured spectra as of pure GT type (WU, 1950; LIDOFSKY et al., 1952; FELDMAN and WU, 1952). The log $f_n t$ values are obtained by using the formulae and curves of DAVIDSON (1951). The F-factors are obtained by comparison with a pure particle transition between the states listed in columns four and five (cf. (16)).

states is expected, since in strong coupling the occupied particle states have the same deforming power (cf. the similar situation expected for γ-transitions between the members of the ground state doublet in odd-odd nuclei (p. 113)).

In K^{40}, the F-factor as well as the magnetic moment (cf. p. 83) indicate an intermediate coupling situation. In such cases of weak or intermediate surface coupling, it is of interest to compare the observed transition probabilities with those expected for a coupling scheme arising from the influence of particle forces (cf. § IIc.iii). The unfavoured factor F_p obtained in this way is in general somewhat larger than F, in the case of many-particle configurations. Thus, for K^{40}, one finds $F_p = 0.7$.

IX. Summary.

A unified description of the nuclear structure is attempted, which takes into account individual-particle aspects as well as collective features associated with oscillations of the system as a whole (§ I). The most important of the collective types of motion, for the low energy nuclear properties, are oscillations in the nuclear shape, which resemble surface oscillations. The collective motion is associated with variations of the average nuclear field, and is therefore strongly coupled to the particle motion (§ IIa).

The particle-surface coupling implies an interweaving of the two types of motion, which depends on the particle configuration as well as on the deformability of the surface. In the immediate vicinity of major closed shells, the high stability of the spherical nuclear shape makes the coupling relatively ineffective. In such a weak coupling situation, the nucleus can be described in terms of approximately free surface oscillations and the motion of individual nucleons in a spherical potential (§ IIb.i).

With the addition of particles, the coupling becomes more effective, and the nucleus acquires a deformed equilibrium shape. For sufficiently large deformations, a simple limiting coupling scheme is realized, which bears many analogies with that of linear molecules. In the strong coupling situation, the nucleus performs small vibrations about an axially symmetric equilibrium shape. The particles moving in the deformed field are decoupled from each other and precess rapidly about the nuclear axis, following adiabatically the slow rotation of the nuclear shape (§ IIb.ii and § IIc.ii; cf. Figs. 3 and 6).

An analysis of the observed nuclear properties of the low energy region reveals many of the characteristic features of the coupled system.

For nuclei with major closed-shell configurations, or with a single extra particle, the expected weak coupling situation is especially confirmed by the high excitation energies (cf., e. g., Fig. 13) and the small quadrupole moments (§ Vc). Also magnetic moments indicate that particle motion in a closed-shell core is little influenced by the coupling (cf. O^{17}, p. 76), although the anomalous moment of Bi^{209} implies as yet unexplained features of the particle structure (cf. p. 81).

Already for configurations with a few particles, the empirical data give evidence of a major effect of the particle-surface coupling, and in regions further removed from closed shells, a rather fully developed strong coupling situation is found.

In particular, the nuclear excitation spectrum clearly indicates a structure of nuclear states governed by the strongly coupled particle and collective motions. A striking feature is the occurrence of collective excitations of rotational character, which reveal themselves by their energy trends, the regularity of their spectrum, and their short lifetimes (§ VIc.ii). The accuracy of the strong coupling description of these states in regions of large deformations is exhibited by the energy ratios within a rotational family (cf., e. g., Table XXII and also notes on pp. 93 and 166).

The particle modes of excitation can be studied especially in the long lived isomers and the β-activities. For these states, the spins and parities, which account for the order of the transitions, have confirmed the configuration assignments given by the shell model. However, the observed transition probabilities, which are appreciably smaller than would correspond to particles moving in a fixed potential, provide evidence for the readjustments of the collective field, which are a characteristic of the particle transitions in the coupled system (§§ VIb, VIId.i, VIIIc.ii and iv).

The modification of the nuclear coupling scheme arising from a strong particle-surface interaction also manifests itself in the static properties of nuclear ground states. Thus, for many-particle configurations, the ground state spin may differ from that which would result from a coupling due to particle forces (cf. Fig. 6). Especially, the occurrence of $I = j - 1$ in $(j)^3$ configurations gives evidence for a surface coupling dominating over the particle forces (§ III.iii).

The magnetic moments provide a measure of the sharing of

angular momentum between particles and surface, and support the strong coupling interpretation of nuclear states in regions removed from major closed shells (§ IVc; cf. especially Table VI). The moments are also sensitive to modifications of the particle state resulting from the non-spherical character of the potential, and thus provide rather detailed tests of nuclear wave-functions (Addendum to Chapters IV and V; cf. also Table VII). The comparison between magnetic moments and the *ft*-values of mirror β-decays further supports the interpretation of the nuclear states (§ VIIIc.i).

While many of the nuclear properties considered depend primarily on the coupling scheme, information on the collective motion of a more detailed character may be obtained from the analysis of quadrupole moments and of the energies and life-times of rotational states. It is found that the observed quadrupole moments, as well as the related $E2$ matrix elements for rotational transitions, are systematically smaller than would correspond to surface deformations of the simple hydrodynamical type (§ Vc, § VIc.ii). In this deviation, one has an interesting indication of the inadequacy of the liquid drop idealization of the nuclear collective properties, which may be associated with the non-uniformity of the nuclear density distribution (§ IIa).

The present discussion has been restricted principally to low energy phenomena, but the basic features of such a unified description retain their validity also for the higher excitations encountered in nuclear reaction processes (§ VIa). The increased level density implies a certain complexity in the nuclear states, but the fundamental nature of the individual-particle and ordered collective motions is still expected to manifest itself (§ VId; cf. also Ap. Va and b).

Thus, the recent measurements of total neutron cross-sections have revealed a structure associated with potential scattering of a single particle, as well as aspects arising from the coupling to the internal degrees of freedom of the target nucleus, which may lead to the complicated motion of the compound nucleus. It appears that the observed coupling can be understood in terms of an interaction between the incident particle and the nuclear surface oscillations of the same magnitude as implied by the low energy phenomena (Ap. Vc).

Appendix I.

Shell Structure and Deformability.

The nuclear deformability depends on the extent to which the particle structure can adjust to a deformation of the field. Thus, important deviations from the simplified surface tension description may arise for configurations with anomalously large level spacings (closed-shell nuclei) or if the deformation changes too rapidly for the particle structure to follow adiabatically (cf. GALLONE and SALVETTI, 1953; HILL and WHEELER, 1953).

For deformations preserving axial symmetry, the nucleonic states may be characterized by the quantum numbers Ω_p, denoting the components of angular momentum of the individual nucleons along the symmetry axis. For a given set of Ω_p, the deformability coefficients C_λ are proportional to the number of nucleons A, and are thus much larger than estimates based on the surface tension, which are of order $A^{2/3}$ (apart from the influence of electrostatic forces).

As the nucleus is deformed, however, states with different sets of Ω_p will cross and if, instead of following a state of constant Ω_p, one follows the state of lowest energy for any given deformation, the resultant energy dependence will on the average be of the surface tension type. (Illustrations of this effect are given in the above references).

Deviations from axial symmetry, as well as the effect of particle forces, afford a mechanism for keeping the particle structure in the state of lowest energy, provided the region of crossings is passed sufficiently slowly. If this adiabatic condition is violated, exchange of energy takes place between nucleonic and collective motion (HILL and WHEELER, 1953). One then encounters the features of the coupled system characteristic of an intermediate coupling strength (§§ IIa.iii, IIb.i and iii).

In the strong coupling situation where the nucleus performs small oscillations around a deformed equilibrium shape (§ II b.ii), this equilibrium shape may in general be estimated on the basis of a surface tension type of deformability. A finer analysis of the deformation properties in the appropriate region may be required for the detailed treatment of the vibrations around equilibrium.

The surface tension type of deformability is a statistical feature which depends on a regular level spacing. In the neighbourhood of major shell closings, the discontinuity in the level distribution implies a special stability of the spherical form corresponding to a C_λ coefficient of order A for small deformations, until the first few crossings have occurred (cf. GALLONE and SALVETTI, 1953). This results in an anomalously large phonon energy and very small quadrupole moments for such nuclei. For larger deformations, the deformability approaches the normal value with a resulting decrease in the phonon energy. The potential energy function corresponding to these features is somewhat more complicated than given by (II.5).

Appendix II.

Matrix Elements in the Perturbation Representation.

The matrix elements of H_{int} can be obtained from the matrix of $Y_\mu\ (\vartheta, \varphi)$ given by

$$<jm\,|\,Y_\mu\,|\,j'm'> = <j\,|\,h\,|\,j'><j'\,2\,m'\,\mu\,|\,j'\,2jm>, \quad \text{(Ap. II.1)}$$

where the last factor on the right hand side is the coefficient of the vector addition of the angular momenta j' and 2 to give a total j (cf. CONDON and SHORTLEY, 1935, p. 77, Table 4[3]).

The sub-matrix $<j\,|\,h\,|\,j'>$ can be expressed in terms of Racah coefficients and, for particle states of the same parity, is given by

$$<j\,|\,h\,|\,j'> = -\sqrt{\frac{5}{64\,\pi}} \begin{cases} -\sqrt{\dfrac{3\,(2j-1)\,(2j-3)}{2j\,(j-1)}} & j = j'+2 \\ +\dfrac{1}{j}\sqrt{\dfrac{3j\,(2j-1)}{(j-1)\,(j+1)}} & j = j'+1 \\ +\sqrt{\dfrac{(2j-1)\,(2j+3)}{j\,(j+1)}} & j = j' \\ -\dfrac{1}{j}\sqrt{\dfrac{3j\,(2j+3)}{(j+1)\,(j+2)}} & j = j'-1 \\ -\sqrt{\dfrac{3\,(2j+3)\,(2j+5)}{2\,(j+1)\,(j+2)}} & j = j'-2 \end{cases} \quad \text{(Ap. II.2)}$$

From (1) and the matrix elements of α_μ, which can be obtained from (A.38), one derives from (II.9) the expression (II.12) for the first order matrix elements of H_{int}.

To first order in H_{int}, the wave function (II.11) is determined by the coefficients

$$<j'; 12; IM|> = k\sqrt{\frac{\hbar\omega}{2C}}\,\frac{<j|h|j'>}{\hbar\omega + \Delta_{jj'}}, \qquad \text{(Ap. II.3)}$$

where $\Delta_{jj'}$ is the separation between the particle levels j' and j.

In terms of these coefficients, the expectation value of R_z is given by

$$<R_z> = \frac{M}{2I(I+1)}\sum_{j'}(I(I+1) - j'(j'+1) + 6)\left|<j'; 12; IM|>\right|^2 \qquad \text{(Ap. II.4)}$$

which is equivalent to (II.13) if only the diagonal term ($j' = j$) is of importance.

For a more detailed analysis of the nuclear coupling scheme, such as is needed for the evaluation of the magnetic moment, the non-diagonal matrix elements of s_z given by

$$\left.\begin{aligned} &<j = l-\tfrac{1}{2}; 12; IM|\,s_z\,|j' = l+\tfrac{1}{2}; 12; IM> \\ &= \frac{M}{2I(I+1)(2l+1)}\sqrt{\left(I+l-\frac{3}{2}\right)\left(I+l+\frac{7}{2}\right)\left(l-I+\frac{5}{2}\right)\left(I-l+\frac{5}{2}\right)}\end{aligned}\right\} \qquad \text{(Ap. II.5)}$$

are also of interest.

Appendix III.

Features of the Strong Coupling Solution.

i. *Matrix elements.*

The matrix elements of the coupling term (II.26) in the strong coupling approximation may be obtained from

$$
\begin{aligned}
&\langle j\Omega \,|\, Y_0 \,|\, j'\Omega\rangle = \\
&-\sqrt{\frac{5}{64\pi}}\left\{\begin{array}{ll}
-\frac{3}{2}\frac{1}{j(j-1)}\sqrt{(j-\Omega)(j-\Omega-1)(j+\Omega)(j+\Omega-1)} & j=j'+2 \\
\frac{3\Omega}{j(j-1)(j+1)}\sqrt{(j-\Omega)(j+\Omega)} & j=j'+1 \\
\frac{1}{j(j+1)}(3\Omega^2-j(j+1)) & j=j' \\
\frac{3\Omega}{j(j+1)(j+2)}\sqrt{(j-\Omega+1)(j+\Omega+1)} & j=j'-1 \\
-\frac{3}{2}\frac{1}{(j+1)(j+2)}\sqrt{(j-\Omega+1)(j-\Omega+2)(j+\Omega+1)(j+\Omega+2)} & =j'-2
\end{array}\right\} \qquad \text{(Ap. III.1)}
\end{aligned}
$$

which is derived from (Ap. II.1 and 2).

The expectation value $< j_z >$ is given by (II.19), while for the evaluation of $< s_z >$ one also needs the non-diagonal element

$$\left.\begin{aligned} &< j = l - \tfrac{1}{2},\ \Omega;\ IKM \,|\, s_z \,|\, j' = l + \tfrac{1}{2},\ \Omega;\ IKM > \\ &= -\frac{MK}{I(I+1)} \frac{\sqrt{\left(l+\frac{1}{2}\right)^2 - \Omega^2}}{2l+1} \left\{ 1 + (-)^{I-1/2+l} (I + 1/2)\, \delta_{\Omega,1/2}\, \delta_{K,1/2} \right\}. \end{aligned}\right\} \text{(Ap. III.2)}$$

ii. *Strong coupling for a single $j = 3/2$ particle.*

In the special case of a $j = 3/2$ particle coupled to the surface, there exists no regular strong coupling solution since, according to (II.21), the configurations ($\gamma = \pi$; $\Omega = 3/2$) and ($\gamma = 0$; $\Omega = 1/2$) are degenerate. Indeed, the proper values of H_{int} (cf. A.80) are independent of γ. In strong coupling, we may restrict ourselves to the lower of these proper values, and the wave function for the state with $I = 3/2$ may be written

$$\left.\begin{aligned} &= \left\{ |3/2;\ 3/2\ 3/2\, M > \sin\gamma/2 + |-1/2;\ 3/2\ 3/2\, M > \cos\gamma/2 \right\} \varphi_1(\beta, \gamma) \\ &+ \left\{ |1/2;\ 3/2\ 1/2\, M > \cos\gamma/2 + |-3/2;\ 3/2\ 1/2\, M > \sin\gamma/2 \right\} \varphi_2(\beta, \gamma) \end{aligned}\right\} \text{(Ap. III.3)}$$

in terms of the symmetrized basis vectors $|\ \Omega;\ IKM >$ (cf. II.15). The vibrational functions φ_1 and φ_2 represent small oscillations around a definite equilibrium β; however, the independence of the coupling energy of γ implies essential oscillations in γ, and the vibrational energies characterized by n_γ become of the order of rotational energies.

In order to determine the nuclear coupling scheme, one must solve the vibrational equation, which can be written as a matrix in the space of φ_1 and φ_2. From (II.23, 24, and 25) and (A.96 and 121-4) one obtains for the Hamiltonian of the system

$$
\left.
\begin{aligned}
H = H_0(\beta) + \frac{\hbar^2}{2B\beta^2}\frac{1}{\sin 3\gamma}\frac{\partial}{\partial\gamma}\sin 3\gamma\,\frac{\partial}{\partial\gamma} + \frac{\hbar^2}{2B\beta^2}\frac{1}{\sin^2\gamma}
\begin{pmatrix} \cos^2\frac{\gamma}{2} & 0 \\ 0 & \sin^2\frac{\gamma}{2} \end{pmatrix} \\
+ \frac{\hbar^2}{16B\beta^2}\frac{1}{\sin^2\left(\gamma-\frac{2\pi}{3}\right)}
\begin{pmatrix} 3+2\cos^2\frac{\gamma}{2}+\sqrt{3}\sin\gamma & -3\sin\gamma-2\sqrt{3}\cos^2\frac{\gamma}{2}+\sqrt{3} \\ -3\sin\gamma-2\sqrt{3}\cos^2\frac{\gamma}{2}+\sqrt{3} & 5-2\cos^2\frac{\gamma}{2}-\sqrt{3}\sin\gamma \end{pmatrix} \\
+ \frac{\hbar^2}{16B\beta^2}\frac{1}{\sin^2\left(\gamma+\frac{2\pi}{3}\right)}
\begin{pmatrix} 3+2\cos^2\frac{\gamma}{2}-\sqrt{3}\sin\gamma & -3\sin\gamma+2\sqrt{3}\cos^2\frac{\gamma}{2}-\sqrt{3} \\ -3\sin\gamma+2\sqrt{3}\cos^2\frac{\gamma}{2}+\sqrt{3} & 5-2\cos^2\frac{\gamma}{2}+\sqrt{3}\sin\gamma \end{pmatrix}
\end{aligned}
\right\} \quad \text{(Ap. III.4)}
$$

where $H_0(\beta)$ represents small vibrations in β around the equilibrium value (II.22). For sufficiently strong coupling, the vibrations in β and γ are approximately independent.

From (4) it is seen that there is a preference for the shapes $\gamma = 0$ and $\gamma = \pi$, and that there is a symmetry with respect to these two positions. An estimate of the γ-oscillations may be ob-

tained by expanding H around $\gamma = 0$ and π, and by taking into account that for $\gamma = 0$ the value of φ_1 is rather small compared to φ_2, while the opposite holds for $\gamma = \pi$. Neglecting the overlap of the vibrations centered on $\gamma = 0$ and $\gamma = \pi$, one obtains two degenerate solutions, which have the same nuclear moments.

From the wave function (3), one can determine the coupling scheme and the quadrupole moment by means of the operators

$$j_z = \frac{3}{5}\begin{pmatrix} 2\sin^2\frac{\gamma}{2} - \frac{1}{2} & \sin\gamma \\ \sin\gamma & 2\cos^2\frac{\gamma}{2} - \frac{1}{2} \end{pmatrix} \qquad \text{(Ap. III.5)}$$

and

$$Q = Q_0 \cdot \frac{1}{5}\begin{pmatrix} -\cos\gamma & \sin\gamma \\ \sin\gamma & \cos\gamma \end{pmatrix}, \qquad \text{(Ap. III.6)}$$

where Q_0 is the intrinsic quadrupole moment given by (cf. V.7)

$$Q_0 = -\frac{3}{\sqrt{5\pi}} ZR_0^2 < \beta > . \qquad \text{(Ap. III.7)}$$

From the approximate wave function, one obtains

$$< j_z > \approx 0.8 \qquad \text{(Ap. III.8)}$$

leading to (cf. IV.5)

$$\mu_c(p_{3/2}) \approx \begin{Bmatrix} 2.3 \\ -0.7 \end{Bmatrix} \quad \text{and} \quad \mu_c(d_{3/2}) \approx \begin{Bmatrix} 0.4 \\ 0.9 \end{Bmatrix}. \qquad \text{(Ap. III.9)}$$

The quadrupole moment is found to be

$$< Q > \approx 0.16\, Q_0 . \qquad \text{(Ap. III.10)}$$

Thus, the γ-oscillations somewhat reduce the values of $< j_z >$ and $< Q >$ as compared with the state $\Omega = 3/2$, $\gamma = \pi$.

The energy spectrum of the system is rather complex, since low-lying states can be obtained by excitations of the γ-vibrations without change of I, as well as by rotational excitations. A comparison between the equations for states with different I shows, however, that the ground state is an $I = 3/2$ state of the type considered above.

Appendix IV.

Solution of the Coupled Equations for Large j.

In the case of large j, a solution of the coupled system can be obtained for arbitrary strength of the coupling by starting from the corresponding classical equations and considering the quantum effects in first order.

If we assume the magnitude of the particle angular momentum to be a constant of the motion, there exists a simple classical solution for which $\vec{j}$ remains constant in a direction which may be chosen as the z-axis. The surface acquires a static deformation of the α_0 type given by

$$\bar{\alpha}_0 = -\frac{1}{2}\sqrt{\frac{5}{4\pi}}\frac{k}{C}. \qquad \text{(Ap. IV.1)}$$

The quantum effects give rise to an indeterminacy in the direction of $\vec{j}$ and of the axis of deformation. For $j \gg 1$, the angle between j and the z-axis is relatively small for the states $M = I \approx j$. To first order, we may then treat j_z as a constant, equal to j aside from corrections of order unity, and consider only the motion of the perpendicular components

$$j_{\pm} = j_x \pm i j_y. \qquad \text{(Ap. IV.2)}$$

The small inclination of the axis of deformation, with respect to the z-axis, to first order implies excitations of the α_1 and α_{-1} surface modes. In this approximation, the α_0 and $\alpha_{\pm 2}$ modes are not affected and perform independent zero-point oscillations around their equilibrium values $\bar{\alpha}_0$ and 0, respectively.

The nuclear coupling scheme is thus determined by the coupled oscillations of the α_1 and α_{-1} surface modes and the perpendicular j-components. This dynamical system possesses

three degrees of freedom, since j_+ and j_- play the role of canonical conjugates.

The equations of motion may be obtained from the Hamiltonian (II.8), where H_S is given by (II.5) and H_p may be taken as a constant. A convenient form of H_{int} for j a constant is given by (A.76). To leading order in j, one finds

$$\left.\begin{aligned} &\ddot{\alpha}_1 + \omega^2 \alpha_1 - x\omega^2 \sqrt{\frac{3\hbar\omega}{2C}} \frac{1}{\sqrt{j}} j_- = 0 \\ &i\frac{\hbar}{\sqrt{j}} \dot{j}_- + x\sqrt{\hbar\omega C}\left(3x\sqrt{\frac{\hbar\omega}{C}} \frac{1}{\sqrt{j}} j_- - \sqrt{6}\,\alpha_1\right) = 0 . \end{aligned}\right\} \quad \text{(Ap. IV.3)}$$

The dimensionless coupling constant x is given by (II.14).

This system of linear equations can be solved in terms of three independent harmonic oscillators with proper coordinates q_s. We thus write

$$\left.\begin{aligned} \alpha_1 &= \sum_{s=1}^{3} q_s e^{i\omega_s t} \\ j_- &= \sqrt{j}\,\frac{1}{x\omega^2}\sqrt{\frac{2C}{3\hbar\omega}} \sum_s (\omega^2 - \omega_s^2)\, q_s e^{i\omega_s t} . \end{aligned}\right\} \quad \text{(Ap. IV.4)}$$

The proper frequencies are found to be

$$\left.\begin{aligned} \omega_1 &= 0 \\ \left.\begin{matrix}\omega_2 \\ \omega_3\end{matrix}\right\} &= \left(\frac{3}{2}x^2 \pm \frac{1}{2}\sqrt{9x^4 + 4}\right)\omega . \end{aligned}\right\} \quad \text{(Ap. IV.5)}$$

For the uncoupled system ($x = 0$), the frequencies become 0, $\pm\,\omega$ of which the first is associated with the degeneracy of the j_z-levels, while the two latter belong to the surface oscillators. In the limit of strong coupling, the degeneracy with respect to I_z provides the zero frequency, while the rapid precession of $\vec{j}$ around the nuclear axis has the frequency

$$\omega_2 \approx 3x^2\omega , \quad \text{(Ap. IV.6)}$$

and the slow rotational motion of the system takes place with the frequency

$$\omega_3 \approx -\frac{\omega}{3x^2} . \quad \text{(Ap. IV.7)}$$

Both these limiting frequencies agree with those obtained from the strong coupling solution by considering energy level spacings associated with the quantum numbers Ω and I (cf. II.21 and 24). The three remaining degrees of freedom of the system whose frequencies remain to this order equal to ω correspond in strong coupling to the level spacings of the quantum numbers n_β, n_γ, and K.

The commutation relations of the q_s variables may be obtained from those of the α_μ and $\vec{j}$ components. One finds

$$\left.\begin{aligned} [q_1, q_1^*] &= -(\omega_2+\omega_3)\,\frac{\hbar}{C} \\ [q_2, q_2^*] &= -\frac{\omega_3^2}{\omega_2-\omega_3}\,\frac{\hbar}{C} \\ [q_3, q_3^*] &= +\frac{\omega_2^2}{\omega_2-\omega_3}\,\frac{\hbar}{C}. \end{aligned}\right\} \quad \text{(Ap. IV.8)}$$

In these coordinates, the angular momentum transferred to the surface is given by

$$< R_z > = -\frac{B}{\hbar}\sum_s \omega_s < q_s^* q_s + q_s q_s^* > \qquad \text{(Ap. IV.9)}$$

and for the ground state one obtains

$$< R_z > = \frac{I}{I+1}\,\frac{x^2}{\sqrt{x^4+\frac{4}{9}}}. \qquad \text{(Ap. IV.10)}$$

The factor $\dfrac{I}{I+1}$ which has been added equals unity to leading order, and makes the equation, in the limit of strong coupling, exact for all values of I (cf. II.20).

The transfer of angular momentum implied by (10) gives rise to a small static decrease in the magnitude of $\bar{\alpha}_0$ since the latter is proportional to $< 3 j_z^2 - j(j+1) >$ (cf. A.78). From this effect follows the projection factor (V.11).

Appendix V.

Individual-particle and Collective Features of Nuclear Reactions

The recognition of relatively undisturbed single-particle motion as an important aspect of the nuclear dynamics implies a picture of nuclear reactions, in which the incident particle interacts in the first stage with the average nuclear field. In subsequent stages, the coupling between the particle and the internal degrees of freedom of the target nucleus may lead to the formation of a compound nucleus, in which the excitation energy is shared among a large number of degrees of freedom (cf. § VI d).

In Section a) of this Appendix, a description of the reaction process is formulated, based on the assumption that the formation of the compound nucleus is initiated by the interaction of the incident particle with the surface oscillations of the target nucleus.

The formalism is applied in Section b) to the dispersion of neutrons, and the scattering cross-sections are considered for various strengths of the coupling to the compound nucleus. A sum rule for the scattering widths of the resonance levels is discussed.

The parameters of the formalism, which enter into the description of the coupling process, are considered in Section c). Recent empirical evidence, obtained from total neutron cross-sections averaged over many levels, permits an estimate of the coupling strength which may be compared with the particle-surface interaction observed in the low energy nuclear properties.

a) General Formalism.

In order to avoid inessential complexities of the mathematical formalism, we first consider the elastic scattering of an *s*-neutron on a nucleus of spin zero, and neglect the effect of inelastic pro-

cesses. The extension to a more general treatment is indicated below.

The wave function may be expanded in the form

$$\Psi = \frac{1}{r}\varphi(r)\frac{1}{\sqrt{4\pi}}\Phi_0(x) + \sum_i c_i \Psi_i(\vec{r}, x), \qquad \text{(Ap.V. 1)}$$

where Φ_0 is the ground state of the target nucleus, described by the coordinates (x) which may represent individual particles as well as collective degrees of freedom. The radial wave function of the scattered neutron is denoted by $\varphi(r)$. The Ψ_i constitute a complete orthonormal basis in the space orthogonal to Φ_0.

In the mixed representation (1), the state vector is specified by the function $\varphi(r)$ and the coefficients c_i. Assuming the coupling between the incident particle and the internal motion of the target nucleus to take place at a sharp surface ($r = R_0$), one obtains the coupled differential and algebraic equations

$$-\frac{\hbar^2}{2M}\frac{d^2}{dr^2}\varphi + V(r)\varphi = (E - E_0)\varphi \qquad r \neq R_0 \qquad \text{(Ap.V. 2)}$$

$$-\sqrt{\frac{1}{2}R_0}\,\varphi(R_0)\frac{\hbar^2}{MR_0^2}R_0\frac{\varphi'}{\varphi}\Big|_{R_0^-}^{R_0^+} + \sum_i c_i H_{0i} = 0 \qquad \text{(Ap.V. 3)}$$

$$\sqrt{\frac{1}{2}R_0}\,\varphi(R_0)H_{i0} + \sum_j c_j(H_{ij} - E\delta_{ij}) = 0, \qquad \text{(Ap.V. 4)}$$

where $(E - E_0)$ is the kinetic energy of the incident neutron (in the center of mass system) and $V(r)$ the potential to which the neutron is subjected inside the nucleus. For simplicity, we take $V(r)$ to be constant for $r < R_0$ and to rise abruptly to zero at the surface.

The matrix elements are given by

$$H_{0i} = \frac{1}{\sqrt{2\pi}}R_0^{-3/2}\int \vec{dr}\,dx\,\Phi_0^* H_{\text{int}}(\vec{r}, x)\,\Psi_i \qquad \text{(Ap.V. 5)}$$

and

$$H_{ij} = \int \vec{dr}\,dx\,\Psi_i^* H \Psi_j, \qquad \text{(Ap.V. 6)}$$

where $H_{\text{int}}(\vec{r}, x)$ is the coupling between the incident particle and the surface (cf. II.9 and 10) and H is the total Hamiltonian of the system. The most convenient choice of the basis Ψ_i de-

pends on the structure of the coupling process by which the compound nucleus is formed (cf. Ap. Vc). In some simple situations, one may take the Ψ_i to represent stationary states in the absence of the coupling to the entrance channel, i. e.

$$H_{ij} = E_i \delta_{ij}. \qquad \text{(Ap.V. 7)}$$

The equation (3) contains the discontinuity of the logarithmic derivative of φ at the surface, which may be written, by means of (2),

$$\left.\begin{aligned} R_0 \frac{\varphi'}{\varphi}\Big|_{R_0^-}^{R_0^+} &= kR_0 \cot(kR_0 + \delta) - KR_0 \cot KR_0 \\ &\equiv f(E) - f_{\mathrm{sp}}(E), \end{aligned}\right\} \qquad \text{(Ap.V. 8)}$$

where k and K are the outside and inside neutron wave numbers, and δ is the scattering phase.

The scattering cross-section is given in terms of f by (cf., e. g., Blatt and Weisskopf, 1952, Chapter VIII)

$$\sigma_{\mathrm{sc}} = \frac{\pi}{k^2}\left| 1 - \frac{f + ikR_0}{f - ikR_0} e^{-2ikR_0} \right|^2. \qquad \text{(Ap. V.9)}$$

The quantity f_{sp} in (8) is the f-function which corresponds to single-particle scattering in the fixed nuclear potential.

The equations (3) and (4) determine $\varphi(R_0)$ and the c_i; the compatibility condition provides the linear equation for f

$$\begin{vmatrix} \frac{\hbar^2}{MR_0^2}(f_{\mathrm{sp}} - f) & H_{0i} \\ H_{i0} & H_{ij} - E\delta_{ij} \end{vmatrix} = 0. \qquad \text{(Ap.V. 10)}$$

The special basis (7) gives

$$f = f_{\mathrm{sp}} + \frac{MR_0^2}{\hbar^2} \sum_i \frac{|H_{0i}|^2}{E - E_i}. \qquad \text{(Ap.V. 11)}$$

The treatment of partial waves of higher angular momentum and the effect of Coulomb forces leads to the same equation (10) for the function f, which then determines the cross-section by formulae which are generalizations of (9).

If inelastic processes are possible, one chooses an appropriate number of the Ψ_i to represent the open channels (t) other than the entrance channel. The function f is again determined by an equation of the form (10) where, however, for the open channels*

$$H_{tt} - E \to \frac{\hbar^2}{MR_0^2}[(f_{sp})_t - (\Delta_t + is_t)]. \qquad \text{(Ap. V. 12)}$$

The $(f_{sp})_t$ is the single-particle f-function appropriate to scattering in the channel, t, and Δ_t the level shift associated with long range forces. The imaginary term s_t is related to the channel width (cf. BLATT and WEISSKOPF, 1952, p. 332). Similarly, one may include radiative processes by adding a complex term to the nuclear Hamiltonian.

The effect of inelastic processes leads to complex values of f from which the elastic cross-section and the total reaction cross-section may be determined. The distribution of reaction products among the open channels is determined by the values of $\varphi_t(R_0)$.

The formulation given above, some consequences of which are considered in the following, has assumed the coupling between the incident particle and the internal structure of the target nucleus to be located at a sharp surface. The influence of a finite surface thickness as well as of other types of coupling, such as to collective volume oscillations and to particle excitations through direct particle forces, can be treated in a similar way by obtaining from the coupled equations a linear expression for f. The form of this expression may, however, in these cases be somewhat more complicated than (10).

b) Scattering Cross-sections.

In order to illustrate some of the characteristic features of nuclear reaction cross-sections, which are contained in the formalism outlined in Ap.Va, we consider in this paragraph the dispersion of neutrons in the region of sharp resonances ($kR_0 \ll 1$), and restrict ourselves to s-wave scattering.

* If the residual nucleus possesses a spin, there may be an additional constant term in (12), arising from H_{int} and representing the energy shift of the single-particle resonances in the channel t, resulting from the non-spherical nature of the potential.

i. *Weak coupling; one-level resonance.*

The coupling between the entrance channel and the compound nucleus may be termed weak if the second term in (11) is small compared to the first, except in the immediate neighbourhood of the energies E_i, i. e. for

$$\frac{MR_0^2}{\hbar^2}\frac{|H_{0i}|^2}{|f_{sp}|} \ll D, \qquad \text{(Ap.V. 14)}$$

where D is the level distance in the spectrum of E_i.

When the condition (14) is fulfilled, the impinging particle interacts mainly with the average potential of the target nucleus for most incident energies. This potential scattering depends on the distance from the nearest single-particle level and may take on all values from 0 to $4\pi\lambda\!\!\!^{-2}$. If $K R_0 \gg 1$, the potential scattering for most energies is close to that of an impenetrable sphere ($f = \infty$), but characteristic differences from this limit are expected, and experimental evidence on cross-sections far away from resonances may give information on the motion in the average potential*.

In the immediate neighbourhood of an energy E_i, the cross-section varies rapidly. If the potential scattering is small compared to $4\pi\lambda\!\!\!^{-2}$ ($f_{sp} \gg kR$; cf. (9)), one obtains a resonance of the usual type

$$\sigma = \frac{\pi}{k^2}\frac{\Gamma^2}{(E-E_r)^2+\frac{1}{4}\Gamma^2}, \qquad \text{(Ap.V. 15)}$$

where the resonance energy E_r is given by

$$f(E_r) = 0, \qquad \text{(Ap.V. 16)}$$

leading to

$$E_r = E_i - \frac{MR_0^2}{\hbar^2}\frac{|H_{0i}|^2}{f_{sp}} \qquad \text{(Ap.V. 17)}$$

which, in view of (14), is much closer to E_i than the neighbouring levels. The scattering width Γ and the reduced width γ are given by

* The term "potential scattering" is sometimes used to denote the scattering from an impenetrable sphere (cf., e. g., BLATT and WEISSKOPF, 1952). The recognition of the significance of single-particle nuclear motion for the course of nuclear reactions would seem, however, to make it more natural to reserve the term for the scattering in the actual nuclear potential. We here follow this latter terminology.

$$\Gamma = 2\,kR_0\gamma = -\frac{2\,kR_0}{f'(E_r)} \qquad \text{(Ap.V. 18)}$$

which, according to (11) and (17), gives

$$\Gamma = 2\,kR_0\frac{MR_0^2}{\hbar^2}\frac{|H_{0i}|^2}{f_{\mathrm{sp}}^2} \qquad \text{(Ap.V. 19)}$$

This value for the width is small compared to D by (14) and the assumption $f_{\mathrm{sp}} \gg kR_0$.

The potential scattering becomes comparable with the resonance maximum in the neighbourhood of the resonance energies E_n for single-particle scattering, given by

$$f_{\mathrm{sp}}(E_n) = 0\,. \qquad \text{(Ap.V. 20)}$$

The energy regions in which $\sigma_{\mathrm{pot}} \sim 4\pi\lambda^2$ are given by

$$|E - E_n| \lesssim \Gamma_{\mathrm{sp}}\,, \qquad \text{(Ap.V. 21)}$$

where

$$\Gamma_{\mathrm{sp}} = 2\,kR_0\gamma_{\mathrm{sp}} = 2\,kR_0\frac{\hbar^2}{MR_0^2} \qquad \text{(Ap.V. 22)}$$

represents the single-particle scattering width. In the regions (21), the form of the compound resonances is essentially modified by the potential scattering and, for $|E - E_n| \ll \Gamma_{\mathrm{sp}}$, the influence of the compound state appears as a narrow dip in the cross-section.

A simple interpretation of (14) may be obtained by using the approximation

$$f_{\mathrm{sp}}\frac{\hbar^2}{MR_0^2} \approx E_n - E \qquad \text{(Ap.V. 24)}$$

valid for $|E - E_n| \ll \Delta$, where Δ is the single-particle level distance (cf. (VI.7)). By means of (24) the condition (14) may be written

$$\frac{|H_{0i}|^2}{|E - E_n|\,D} \ll 1 \qquad \text{(Ap.V. 25)}$$

which is just the condition that the coupling H_{0i} to the entrance channel does not appreciably modify the compound states. Therefore, the states Ψ_i act individually and influence the scattering only in small energy intervals around the E_i-values.

In the region $|E-E_n| < \Gamma_{sp}$, the condition for weak coupling is modified, corresponding to the fact that the single-particle levels are only defined to within an energy Γ_{sp}. The analysis of (11) shows that in this region the less stringent condition

$$\frac{|H_{0i}|^2}{\Gamma_{sp} D} \ll 1 \qquad \text{(Ap.V. 26)}$$

is sufficient to ensure that the Ψ_i states act individually. The fact that (26) implies a scattering which, to first approximation, is of potential character, may be understood by observing that $2\pi(\hbar D)^{-1}|H_{0i}|^2$ represents the probability per unit time for coupling of the incident particle to the compound states. If this probability is small compared to $\hbar^{-1}\Gamma_{sp}$, which is the probability per unit time for escape from the single-particle state, the coupling is of only minor importance.

For $|E-E_n| \sim \Delta$, several single-particle levels are simultaneously effective, and the condition (14) can be interpreted in the same way as (25) by considering the total perturbation caused by all the single-particle levels.

ii. *Strong coupling; many-level resonances.*

When the conditions (14) or (26) are not fulfilled, the coupling between the states Ψ_i and the entrance channel leads to quasi-stationary states of the compound nucleus, essentially different from the Ψ_i. The coupling strongly mixes the states Ψ_i over an energy region given by the left hand side of (14).

Some of the properties of the scattering in the strong coupling region can be illustrated by assuming that, over the region of strong mixing, the Ψ_i can be approximated by a spectrum of uniform spacing D with a constant coupling matrix element $|H_{0i}| = H_c$. In this case, (11) can be written

$$f = f_{sp} + \frac{MR_0^2}{\hbar^2}\frac{\pi H_c^2}{D}\cot\frac{\pi}{D}(E-E_i). \qquad \text{(Ap.V. 27)}$$

It is seen that the resonances E_r of the compound nucleus ($f(E_r)=0$), which are close to E_i for weak coupling, move halfway in between the energies E_i when the coefficient of the contangent in (27) becomes large compared to f_{sp}.

The resonance scattering widths can be obtained from (18) and are found to be

$$\Gamma = \frac{2k}{K}\frac{D}{\pi}\left[\frac{\pi^2 H_c^2}{D\Delta} + \frac{D\Delta}{\pi^2 H_c^2}\cot^2 KR_0\right]^{-1}, \qquad \text{(Ap.V. 28)}$$

which is a generalization of (19), to which (28) reduces when the last term in the parenthesis dominates (weak coupling).

In the strong coupling region, the behaviour of the cross-section in between resonances is determined by the contribution of many far-off compound states, which dominates over the potential scattering. The variation of this background scattering depends on the coefficient of the cotangent in (27). Only when this coefficient is large compared to unity does the cross-section away from resonance approach a constant value, which then equals that of hard sphere scattering.

The foregoing analysis leads to the following picture of the scattering process in the various coupling regions (cf. Fig. 16).

For very small coupling

$$\frac{H_c^2}{D} \ll \Gamma_{\mathrm{sp}}, \qquad \text{(Ap.V. 29)}$$

the weak coupling situation applies for all incident energies and the principal part of the cross-section is determined by the potential scattering.

When (29) no longer holds, a strong coupling situation exists in the neighbourhood of the single-particle levels. Inside the region of strong coupling, the reduced scattering widths are of order (cf. (28))

$$\gamma = \left(\frac{D}{\pi H_c}\right)^2 \frac{\hbar^2}{MR_0^2} \qquad \text{(Ap.V. 30)}$$

while, at larger distances from the single-particle level, where the coupling is weak, the widths become very much smaller. A measure of the extent of the strong coupling region can be obtained as the energy interval W over which the reduced widths exceed half the maximum value (30). From (28) one finds

$$W = 2\pi\frac{H_c^2}{D}. \qquad \text{(Ap.V. 31)}$$

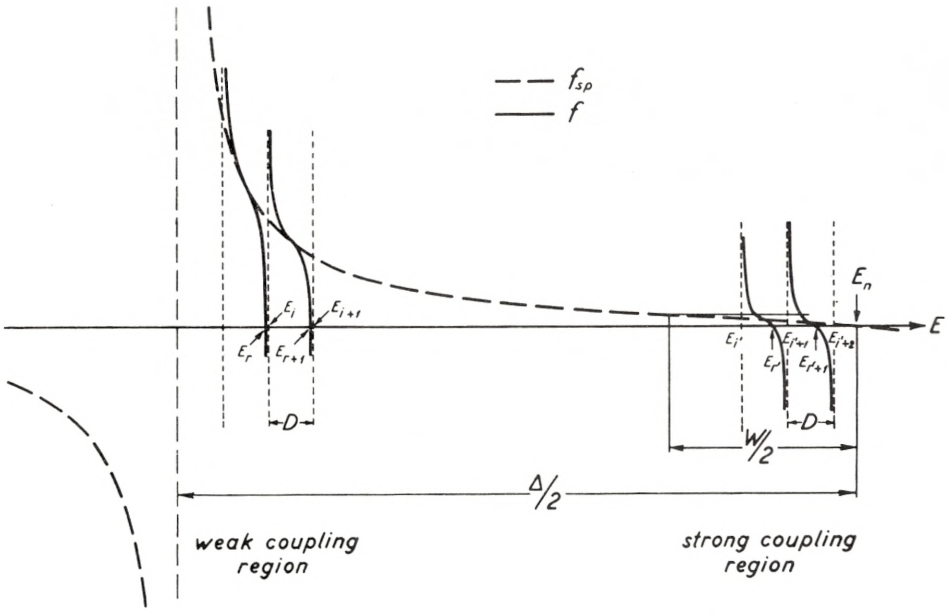

Fig. 16. *Scattering f-function in coupled model.* The scattering cross-sections can be simply expressed in terms of the logarithmic derivative f of the wave function at the nuclear surface (cf., e. g., (9)). The broken curve gives the f-function for pure single-particle scattering in the average nuclear potential. At the energies E_n, corresponding to the virtual single-particle states, with the spacing Δ, f_{sp} vanishes, while half way between these energies f_{sp} has poles. The coupling to the internal motion of the target nucleus, which is assumed to take place at the nuclear surface, adds a rapidly varying part to the total f-function (cf. (11)). The compound nucleus is described in terms of the states Ψ_i which would represent stationary states in the absence of the coupling to the entrance channel. At the energies E_i, which have on the average a spacing D, the f-function has a pole, while a resonance energy E_r of the compound nucleus (for which $f = 0$) occurs in each interval $E_i < E < E_{i+1}$.

The relative magnitude of the two contributions to f depends on the distance from the nearest single-particle level E_n. At large distances from E_n, the value of f_{sp} dominates and, to a first approximation, the cross-section is that of potential scattering. The coupling gives rise to resonances lying very close to the E_i and the scattering widths, which depend inversely on the energy derivative of f at resonance, are small (weak coupling region). Near to the E_n-values, the f-function is determined principally by the coupling term (strong coupling region). In this region, which extends over an energy interval W (cf. (31)), the resonance states result from the coupling of many Ψ_i-states, and the resonance energies lie essentially midway between the E_i. The scattering widths are relatively large in the strong coupling region, being of the order of Δ/W times the average resonance scattering width (cf. the sum rule (33 a)); the off-resonance scattering results mainly from the influence of many far-off resonances.

This energy is related to the probability per unit time for the formation of the compound nucleus, and can also be written in the form (VI.6), in terms of the mean free path of the particle for energy exchanges in the target nucleus.

For a coupling strength so great that W becomes comparable with or exceeds Δ, the region of strong coupling extends over the entire energy interval, and no structure associated with single-particle motion remains. In this situation, the entering particle shares its energy with many degrees of freedom of the compound nucleus before completing a single traversal of the nuclear field.

iii. *Sum rule for scattering widths.*

As long as the region of strong coupling W is small compared with the single-particle level spacing Δ, there exists a simple sum rule for the reduced scattering widths. This may be obtained, in its most general form, directly from (10). Since the scattering widths are appreciable only in regions around the single-particle levels E_n, one may use the form (24) for f_{sp}. The equation (10) is then equivalent to the secular equation for a bound state problem. The proper values and proper function for $f = 0$ give the resonance energies E_r of the compound nucleus and the state vectors of the scattering system at these resonances.

The reduced widths depend on $f'(E_r)$ and can be expressed in terms of the minors of (10) which, in turn, are simply related to the state vector at resonance. Thus, one obtains

$$\gamma_r = \left(\frac{\frac{1}{2} R_0 \varphi^2(R_0)}{\frac{1}{2} R_0 \varphi^2(R_0) + \sum_i c_i^2} \right)_r \frac{\hbar^2}{M R_0^2} \qquad \text{(Ap.V. 32)}$$

which expresses γ_r in terms of the reduced width of the single-particle level times the probability of finding the single-particle motion in the compound state (r). From the completeness of the states (r) one gets immediately

$$\sum_r \gamma_r = \frac{\hbar^2}{M R_0^2} \qquad \text{(Ap.V. 33)}$$

$$= \gamma_{\mathrm{sp}}, \qquad \text{(Ap.V. 33 a)}$$

where the sum is to be extended over the scattering resonances in the region $-\Delta/2 < E - E_n < \Delta/2$.*

As W approaches Δ, the single-particle level strength becomes approximately uniformly distributed over all the compound levels, corresponding to the relation (cf., e. g., WEISSKOPF, 1950)

$$\Gamma \approx \frac{D}{\Delta} \Gamma_{\mathrm{sp}} = \frac{2k}{K} \frac{D}{\pi}. \qquad \text{(Ap.V. 34)}$$

It may be noted that the sum rule (33a) is independent of the shape of the nuclear potential and of the particle angular momentum as well as of the types of couplings considered.

Similar sum rules hold for other properties of the compound levels, which depend on the content of a particular single-particle state. Thus, for a radiative transition to the ground state, the single-particle width may be considered as distributed over the compound levels, whose average radiative width, for the corresponding transition, may be represented by an expression equivalent to the first part of (34)**. However, for $W < \Delta$, the distribution will not be uniform, and the single-particle radiative width will be mainly concentrated on the compound levels in an energy region W around the unperturbed single-particle state.

c. Discussion.

In the application of the general formalism outlined in the preceding sections, the significant features of the nuclear structure are contained in the states Ψ_i in terms of which the properties of the compound nucleus are characterized.

The choice of a basis which diagonalizes all couplings except those to the entrance channel (cf. 7) is particularly appropriate

* Sum rules for reduced widths have been considered by TEICHMANN and WIGNER (1952) who have especially discussed the sums over channels leading from a particular compound state. Arguments for a relation similar to (33) are contained in the discussion following Eq. (31 b) of this reference. The factor 3/2 appearing in the estimate obtained by these authors arises from the assumption of a constant neutron wave function inside the nucleus.

** An expression for the partial radiative width of a compound state, similar to the first part of (34), has been given by BLATT and WEISSKOPF (1952; p. 646). However, as an estimate of the single-particle level spacing which enters in this expression, these authors have suggested a value of about 0.5 MeV for a medium heavy nucleus. The present estimate for Δ ($\sim$ 20 MeV) thus leads to a considerable decrease in the radiative widths.

if one can assume that, already after the first energy exchange between the incident particle and the target nucleus has taken place, the subsequent couplings proceed so rapidly that no structure associated with individual configurations remains.

In this situation, the states Ψ_i, though highly complex, have a certain uniformity of statistical nature. As a first approximation, one may assume the $|H_{0i}|$ to have a constant value H_c, and the level energies E_i to be approximately evenly spaced with a separation D. The gross features of the nuclear level structure may then be characterized by the coupling parameter W, representing the energy region around the single-particle resonances, where the compound nucleus is formed with appreciable probability (cf. Ap.V b.ii and also § VI d).

In general, one expects simple types of motion to manifest themselves also in intermediate stages of the reaction. The choice of the basis (7) is then less appropriate, since the assumption of a constant H_{0i} is no longer valid. The resulting features of the reaction process may be taken into account by including among the Ψ_i a number of states representing the structure of the intermediate stages.

Such effects may, for instance, be significant for very deformed target nuclei, where the entering particle has a large probability of setting the nucleus in rotation (cf. § VI c.ii). The rotational excitation energy is not easily transmitted to the other degrees of freedom of the nucleus, and may with appreciable probability be returned to the entrance channel, or may give rise to an inelastic process without the formation of a compound nucleus. To describe these features, one may consider as a first approximation only the potential scattering and the specific couplings to the rotational motion. It may be possible to include the additional couplings leading to the compound nucleus formation, by means of a uniform set of states, whose coupling to the simple motion may be characterized by parameters similar to W.

Recently, important evidence on the formation of the compound nucleus has been obtained from the analysis of total neutron cross-sections, averaged over many resonances (Barschall, 1952; Feshbach, Porter, and Weisskopf, 1953). The effect of the compound nucleus formation on such average cross-sections can be described as an absorption, since one may con-

sider the problem in terms of the scattering of neutron wave-packets with a time extension short compared with the periods of the compound states. A particle entering the complex motion is, therefore, effectively lost from the wave-packet. Such an absorption can be represented by an imaginary potential (cf., e. g., BETHE, 1940).

In the simplified situation discussed above, where specific structures of the intermediate stages of the coupling process can be neglected, the averaged total cross-sections can thus be obtained by considering single-particle scattering in a constant complex potential. The coupling energy W is related to the imaginary part of the potential V by

$$W = -2\,Im(V). \qquad \text{(Ap.V. 35)}$$

The analysis of the empirical data has shown that many features of the averaged total cross-sections can be accounted for in terms of such a complex potential with $Im(V) \approx -1$ MeV, corresponding to $W \approx 2$ MeV (FESHBACH, PORTER, and WEISSKOPF, 1953). Thus, the observed cross-sections resemble those of single-particle scattering, in which the individual resonances are broadened by about two MeV.*

The coupling which leads to the compound nucleus formation may result from the interaction of the incident particle with the surface oscillations or other collective modes of the target nucleus, or from direct collisions with individual nucleons. The contribution of the surface coupling to W may be estimated from the matrix elements in Chapter II. For the average coupling matrix element H_c, one has

$$H_c^2 \approx \frac{D}{\Delta} \sum_i |H_{0i}|^2, \qquad \text{(Ap.V. 36)}$$

where the sum is extended over all states within the single-particle level spacing Δ. This sum represents a closure over all variables

* In fitting the experimental cross-sections, FESHBACH, PORTER, and WEISSKOPF (1953) have used the parameters $V_0 = 19$ MeV, for the real part of the potential, and $R_0 = 1.45 \times A^{1/3} \times 10^{-13}$ cm for the nuclear radius. While the agreement between the calculated and measured cross-sections is striking, these parameters do not seem compatible with the positions of the single-particle levels, assumed by the shell model, which for the above radius requires a potential of about 30 MeV. Thus, for example, the observed large cross-sections below 1 MeV for elements with $A \approx 90$ result, for $V_0 = 19$ MeV, from a virtual $2p$ level, while already for lighter nuclei, $2p$ states, bound by about 8 MeV, have been identified (cf., e. g., Tables XII and XXV).

except the radial quantum number of the particle, and one obtains (cf. (II.9) and (A.38))

$$\sum_i |H_{0i}|^2 = <0|H_{\text{int}}^2|0> = \frac{5}{8\pi} k^2 \frac{\hbar\omega}{C} \qquad \text{(Ap.V. 37)}$$

for a particle incident on an undeformed nucleus. From (31), (36), and (37) one then finds

$$W = \frac{5}{4} \frac{k^2}{\Delta} \cdot \frac{\hbar\omega}{C}. \qquad \text{(Ap.V. 38)}$$

The hydrodynamical surface parameters (Figs. 1 and 2) and the expression (VI.7) for Δ lead to values for W of about 2 and 3 MeV for a heavy and medium heavy nucleus, respectively. It thus appears that the surface coupling is adequate to account for the observed probabilities for compound nucleus formation.

In the case of strongly deformed target nuclei, one obtains

$$<0|H_{\text{int}}^2|0> = \frac{1}{4\pi} k^2 \beta^2 \qquad \text{(Ap.V. 39)}$$

which represents an increase over (37) by a factor of the order of the number of phonons present in the deformed state. However, the major part of this very strong coupling leads to rotational excitations and thus gives rise to features in the reaction process that cannot be represented by the scattering in a fixed complex potential (see above). A detailed study of elastic as well as inelastic neutron cross-sections for very deformed nuclei (especially in the regions $155 < A < 185$ and $A > 225$) would thus be of interest. In addition to rotational interactions, the surface coupling gives rise to the excitation of vibrational modes, which may rather rapidly transmit their energy to additional degrees of freedom and result in the formation of a compound nucleus. An estimate of these couplings can be obtained from (39) by subtracting the rotational interactions, and one finds a value for the absorption parameter W of about 3/5 of the estimate (38).

With increasing energy of the impinging particle, couplings to collective modes of higher frequencies are expected to be of increasing importance, and also the direct particle forces can excite an increasing number of degrees of freedom of the target

nucleus. A compensating effect sets in when the particle energy becomes comparable with the kinetic energies of the target nucleons. The short time spent by the particle in the nucleus, together with the decreasing nucleon scattering cross-sections, then implies a decrease in the probability for formation of the compound nucleus. For bombarding energies in the region of 100 MeV, an appreciable transparency of the nucleus has been observed and has been interpreted in terms of the single-particle features embodied in the optical model of the nucleus (SERBER, 1947; FERNBACH, SERBER, and TAYLOR, 1949).

Appendix VI.

Nuclear Excitation by the Electric Field of Impinging Particles.

Important information may be obtained from the excitation of nuclei by bombardment with heavy charged particles whose energies are sufficiently below the Coulomb barrier to exclude the influence of nuclear forces. Since only electrostatic forces are then operative, the experiments can be analyzed in terms of relatively simple properties of the nuclear structure. Recently, TER-MARTIROSYAN (1952) has given a rather detailed treatment of such processes*. We here summarize some of the results of this analysis, attempting in particular to indicate the relations to the electromagnetic radiative transitions (cf. Chapter VII).

A great simplicity in the analysis arises from the fact that one can describe the projectile as following a classical trajectory. The condition for such a classical treatment is (cf. N. BOHR, 1948, § 1.3).

$$\varkappa = 2\frac{Z_1 Z_2 e^2}{\hbar v} \gg 1, \qquad \text{(Ap.VI. 1)}$$

where Z_1 and Z_2 are the charge numbers of the projectile and the target nucleus, respectively, and where v is the velocity of the incident particle.

This condition is always fulfilled when the bombarding energy is sufficiently low that penetration through the Coulomb barrier, and thus the influence of nuclear forces, is negligible.

One can then describe the influence of the particle on the nucleus in terms of a time-dependent potential

* Various aspects of these reactions have also been previously considered (WEISSKOPF, 1938; RAMSEY, 1951; MULLIN and GUTH, 1951; HUBY and NEWNS, 1951; BREIT, HULL, and GLUCKSTERN, 1952).

$$V(t) = \sum_{p=1}^{Z_2} \frac{Z_1 e^2}{|\vec{r}(t) - \vec{r}_p|}, \qquad \text{(Ap.VI. 2)}$$

where $\vec{r}_p$ are the coordinates of the target protons and where $\vec{r}(t)$ gives the trajectory of the incident particle, considered as a point charge. This potential gives rise to nuclear transitions of electric multipole character. Of special interest are the collective transitions, for which the excitation cross-sections are particularly large. The low energy collective transitions are induced by the quadrupole component of (2), given by

$$V_2(t) = \frac{4\pi}{5} Z_1 e^2 \sum_{\mu} \sum_{p} r_p^2 \, Y^*_{2\mu}(\vartheta_p, \varphi_p) \, Y_{2\mu}(\vartheta(t), \varphi(t)) \left[r(t)\right]^{-3}. \qquad \text{(Ap.VI. 3)}$$

The method of Coulomb excitation may also find application to other multipole transitions*, but these are in general expected to have appreciably smaller cross-sections. Magnetic transitions are weak due to the small velocity of the projectile.

Since the field of the particle produces only a small perturbation in the internal nuclear wave function, the probability for excitation of a given level may be written

$$P = \sum_{M_f} |b(M_f)|^2, \qquad \text{(Ap.VI. 4)}$$

where M_f is the magnetic quantum number of the final state and

$$b(M_f) = \frac{1}{i\hbar} \int_{-\infty}^{+\infty} \langle f | V(t) | i \rangle e^{i\omega t} dt \qquad \text{(Ap.VI. 5)}$$

with

$$\hbar\omega = E_f - E_i = \Delta E. \qquad \text{(Ap.VI. 6)}$$

For a quadrupole transition, one obtains

$$b(M_f) = \frac{4\pi}{5} \frac{Z_1 e}{i\hbar} \sum_{\mu} \langle i | \mathfrak{M}_e(2, \mu) | f \rangle \int_{-\infty}^{+\infty} \frac{1}{r^3} Y_{2\mu}(\vartheta, \varphi) \, e^{i\omega t} dt \qquad \text{(Ap.VI. 7)}$$

in terms of the nuclear matrix elements of the quadrupole operator $\mathfrak{M}_e(2, \mu)$ given by (VII.5).

* The electric dipole transitions have been considered in detail, for all values of $\varkappa$, by MULLIN and GUTH (1951), HUBY and NEWNS (1951), and TER-MARTIROSYAN (1952). MULLIN and GUTH (1951) have also considered the quantum mechanical treatment of $E2$ transitions, but their cross-sections seem to be too small, as a result of the assumption of a scalar property of the quantity $M_{2\,\mathrm{Born}}(\vec{k}, \vec{k}')$ implied in the equation following (29) of their paper.

The classical orbit of the projectile is a hyperbola and it is convenient to choose a coordinate system whose xy plane is that of the orbit and whose x-axis is the focal line. The orbit may be given in the following parametric representation

$$\left.\begin{aligned} x &= a\,(\cosh\omega + \varepsilon) \\ y &= a\sqrt{\varepsilon^2 - 1}\,\sinh w \\ r &= a\,(\varepsilon\cosh w + 1) \\ t &= \frac{a}{v}\,(\varepsilon\sinh w + w), \end{aligned}\right\} \qquad \text{(Ap.VI. 8)}$$

where

$$a = \frac{Z_1 Z_2 e^2}{m v^2} \qquad \text{(Ap.VI. 9)}$$

is half the distance of closest approach in a head-on collision. The reduced mass is denoted by m. The orbital eccentricity ε is

$$\varepsilon = \left[1 + \left(\frac{p}{a}\right)^2\right]^{1/2}, \qquad \text{(Ap.VI. 10)}$$

in terms of the impact parameter p. The angle of deflection ϑ in the center of mass system is given by

$$\tan\frac{\vartheta}{2} = \frac{a}{p}. \qquad \text{(Ap.VI. 11)}$$

The transition amplitude can now be written

$$) = i\sqrt{\frac{\pi}{5}}\,\frac{Z_1 e}{\hbar v}\,\frac{1}{a^2}\left\{B_e(2)\right\}^{1/2} < I_f\,2\,M_f M_i - M_f \,|\, I_f\,2\,I_i M_i > S^{(2)}_{M_f - M_i} \qquad \text{(Ap.VI. 12)}$$

where $B_e(2)$ is given by (VII.2). The non-vanishing components of $S^{(2)}_\mu$ are given by

$$S^{(2)}_0 = \int_{-\infty}^{+\infty} e^{i\xi(\varepsilon\sinh w + w)}\,\frac{1}{(\varepsilon\cosh w + 1)^2}\,dw \qquad \text{(Ap.VI. 13)}$$

$$= -\sqrt{\frac{3}{2}}\int_{-\infty}^{\infty} e^{i\xi(\varepsilon\sinh w + w)}\,\frac{(\cosh w + \varepsilon \mp i\sqrt{\varepsilon^2 - 1}\,\sinh w)^2}{(\varepsilon\cosh w + 1)^4}\,dw, \qquad \text{(Ap.VI. 14)}$$

where

$$\xi = \frac{\Delta E}{2E}\,\frac{Z_1 Z_2 e^2}{\hbar v}. \qquad \text{(Ap.VI. 15)}$$

The quantity $\varepsilon\xi$ represents the ratio of the collision time to the nuclear period $\tau = \omega^{-1}$. For values of $\varepsilon\xi$ of the order of or larger than unity, the collision becomes approximately adiabatic with a resulting small excitation probability, decreasing exponentially with $\varepsilon\xi$.

The differential cross-section for excitation associated with a scattering into the solid angle $d\Omega$ is

$$d\sigma_{\text{exc}}(\vartheta) = \frac{1}{4} a^2 \sin^{-4}\frac{\vartheta}{2} P d\Omega, \qquad \text{(Ap.VI. 16)}$$

while the total cross-section for excitation of the state in question becomes

$$\sigma_{\text{exc}} = \frac{2\pi^2}{25}\frac{1}{Z_2^2 e^2}\left(\frac{mv}{\hbar}\right)^2 B_e(2)\, g_2(\xi), \qquad \text{(Ap.VI. 17)}$$

with

$$g_2(\xi) = \sum_{\mu}\int_1^{\infty} \varepsilon\, d\varepsilon \left| S_{\mu}^{(2)}\right|^2. \qquad \text{(Ap.VI. 18)}$$

The function $g_2(\xi)$ is plotted in Fig. 17.

From the relative values of the transition amplitudes $b(M_f)$ the angular distribution of the γ-radiation following the excitation can be determined*.

While the angular distribution may give information about the spins of the states involved and about the multipole order of the emitted γ-rays, the measurement of σ_{exc} for the excitation from level c to level d leads to a determination of the quantity $\{B_e(2)\}_{c\to d}$. This information is thus similar to that obtained from a lifetime measurement for the inverse transition, for which the $E2$ radiative probability is given by (cf. (VII.1))

$$T = \frac{4\pi}{75}\frac{1}{\hbar}\left(\frac{\omega}{c}\right)^5 \{B_e(2)\}_{d\to c}. \qquad \text{(Ap.VI. 19)}$$

The nuclear matrix elements for the excitation and decay are related by

$$B_{c\to d} = B_{d\to c}\cdot\frac{2I_d+1}{2I_c+1}. \qquad \text{(Ap.VI. 20)}$$

* Recently, explicit expressions for the angular distribution of the γ-radiation following Coulomb excitation have been given by ALDER and WINTHER (1953).

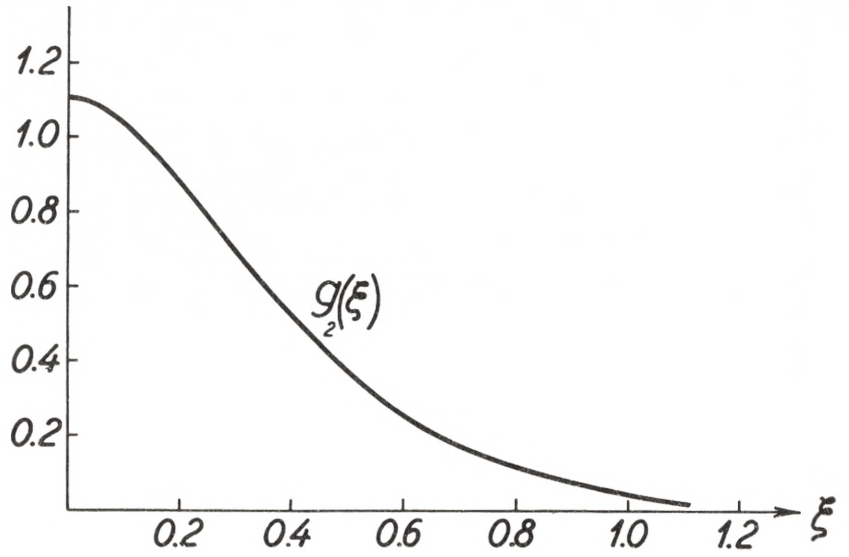

Fig. 17. *Function $g_2(\xi)$ appearing in cross-sections for Coulomb excitation.* The cross-section for Coulomb excitation produced by the electric quadrupole field of the impinging particles is given by (17), which contains the function $g_2(\xi)$, where ξ, given by (15), is a measure of the ratio between the collision time and the nuclear period. The function $g_2(\xi)$ is expressed by means of (13), (14), and (18) in terms of integrals over the trajectories of the particles. The integrals have been numerically evaluated by ALDER and WINTHER (1953), whose results we reproduce in this figure.

The evaluation of the reduced transition probabilities B for various types of transitions in the coupled system has been given in Chapter VII.

The large values of $B_e(2)$ for nuclear collective transitions make the method of Coulomb excitation especially suited for the study of rotational and vibrational states (§ VI c).

Note added in proof: Recently, the feasibility of Coulomb excitation has been exhibited by the observation of the γ-radiation following the nuclear excitation (MCCLELLAND and GOODMAN, 1953; HUUS and ZUPANČIČ, 1953). By this method important evidence has been obtained on the rotational spectrum of the odd-A nucleus, $_{73}Ta^{181}$ (cf. HUUS and ZUPANČIČ (1953), whose results we here summarize).

The first strongly excited level has been found at 137 keV. Since the ground state of Ta^{181} has $I_0 = 7/2$, the first rotational state is expected to have $I = 9/2$ and an energy of $9\hbar^2/2\Im$ (cf. VI. 4). Thus, assuming a similar moment of inertia as in the neighbouring even-even nucleus $_{72}Hf^{180}$, whose first excited (2+) state has an energy of 93 keV (cf. SCHARFF-GOLDHABER, 1953), the first rotational state in Ta^{181} should have an energy of about 140 keV, in good agreement with the observed value.

The second rotational state in Ta^{181}, with $I = 11/2$, should have an energy

of 20/9 times that of the first (9/2) state, and should also be strongly excited. This was confirmed by the observation of a γ-ray of 300 keV resulting from the Coulomb excitation.

The energy dependence of the excitation cross-sections for the two states was found to be in good agreement with (Ap. VI. 17), using the numerical results for $g_2(\xi)$ of ALDER and WINTHER (1953), thus supporting the $E2$ interpretation of the excitation process.

From the magnitude of the observed cross-section for the excitation of the 137 keV line, the reduced transition probability $B_e(2)$ can be obtained from (Ap. VI. 17). By means of (VII. 18) and (Ap. VI. 20), one derives an intrinsic quadrupole moment of $|Q_0| \sim 7 \times 10^{-24}$ cm^2, which is in good agreement with the trend of the deformations deduced from lifetime measurements of first excited states in even-even nuclei (cf. Table XXVII). The value of Q_0 may also be compared with the spectroscopic quadrupole moment (cf. Table XVIII) which yields, by means of the projection factor (V. 9), a deformation of $Q_0 \sim 14 \times 10^{-24}$ cm^2, which is again of the same order of magnitude; the difference may not be significant in view of the experimental uncertainties.

The cross-section for the production of the 300 keV γ-ray depends also on the branching ratio between the direct ground state transition ($11/2 \rightarrow 7/2$) and the cascading ($11/2 \rightarrow 9/2 \rightarrow 7/2$) via the first excited state. From a comparison of the cross-sections for the 300 keV and 137 keV γ-rays, a branching ratio of about 1:4 has been deduced. While the cross-over transition is of pure $E2$ type, the cascade may proceed by $M1$ as well as by $E2$ transitions. The $E2$ transition probabilities can be determined from the value of Q_0 (VII. 18 and 19), and the $M1$ transition probability can be related to the magnetic moment of the ground state (VII. 20 and IV. 9). From the observed magnetic moment (Table XVIII) and the value $Q_0 = 7 \times 10^{-24}$ cm^2, and using the internal conversion coefficients of ROSE et al. (1951) and of GOLDHABER and SUNYAR (1951), one calculates a branching ratio of about 1:1. While the observed branching ratio confirms the relatively strong competition of $E2$ with $M1$ radiation in rotational transitions, it is still somewhat smaller than the calculated ratio; however, the theoretical estimate is very sensitive to the value of the ground state magnetic moment, and a precision determination of μ (Ta^{181}) would thus be of interest.

References.

H. Aeppli, H. Albers-Schönberg, H. Frauenfelder, and P. Scherrer (1952), Helv. Phys. Acta **25,** 339 (Ad. v).

F. Ajzenberg and T. Lauritsen (1952), Rev. Mod. Phys. **24,** 321. (Ad. v; VIb; VIc.i; VIIIc.ii).

F. Alder and K. Halbach (1953), Helv. Phys. Acta **26,** 426. (Ad.iii).

K. Alder and A. Winther (1953), submitted to the Physical Review. (Ap. VI).

W. Arber and P. Stähelin (1953), Helv. Phys. Acta **26,** 433. (III. iv).

J. R. Arnold and T. Sugihara (1953), Phys. Rev. **90,** 332. (VI c.ii).

F. Asaro and I. Perlman (1952), Phys. Rev. **87,** 393. (VIc.ii).

F. Asaro and I. Perlman (1953), submitted to the Physical Review. (VI c.ii).

J. M. Baker, B. Bleaney, K. D. Bowers, P. F. D. Shaw, and R. S. Trenam (1953), Proc. Phys. Soc. A **66,** 305. (Ad. vii).

H. H. Barschall (1952), Phys. Rev. **86,** 431 (VId; Ap.Vc).

E. H. Bellamy and K. F. Smith (1953), Phil. Mag. **44,** 33. (Ad. v and xi).

A. Berthelot (1944), Ann. Phys. (11) **19,** 117. (VIIb.ii).

H. A. Bethe (1937), Rev. Mod. Phys. **9,** 69. (VIId.iii).

H. A. Bethe (1940), Phys. Rev. **57,** 1125. (Ap.Vc).

F. Bitter (1949), Phys. Rev. **76,** 150. (Ad. vi).

D. H. Black (1924), Proc. Roy. Soc. A **106,** 632. (VIc.ii).

J. M. Blatt (1953), Phys. Rev. **89,** 83. (VIIIc).

J. M. Blatt and V. F. Weisskopf (1952), Theoretical Nuclear Physics. J. Wiley and Sons, New York. (VII a; VII b.i; VII b.ii; VIII a; Ap. V a; Ap. V b.i and iii).

F. Bloch (1951); Phys. Rev. **83,** 839. (IV c).

G. S. Bogle, H. J. Duffus, and H. E. D. Scovil (1952), Proc. Phys. Soc. A **65,** 760. (Ad. vii).

A. Bohr (1951), Phys. Rev. **81,** 134. (I; II b.ii; IV; IVb; Vb).

A. Bohr (1951 a), Phys. Rev. **81,** 331. (Ad. iv and vi).

A. Bohr (1952), Dan. Mat. Fys. Medd. **26,** no. 14. (Quoted in the text as A).

A. Bohr, J. Koch, and E. Rasmussen (1952), Arkiv f. Fysik **4,** 455. (Ad. iv).

A. Bohr and B. R. Mottelson (1952), Physica **18,** 1066. (VIb; VIc.ii; VII d.i).

A. Bohr and B. R. Mottelson (1953), Phys. Rev. **89,** 316. (I; VI c.ii).

A. Bohr and B. R. Mottelson (1953 a), Phys. Rev. **90**, 717. (VI c.ii).
A. Bohr and V. F. Weisskopf (1950), Phys. Rev. **77**, 94. (Ad. iv and vi).
N. Bohr (1936), Nature **137**, 344. (I; VI d).
N. Bohr and F. Kalckar (1937), Dan. Mat. Fys. Medd. **14**, no. 10. (I).
N. Bohr and J. A. Wheeler (1939), Phys. Rev. **56**, 426. (I).
N. Bohr (1948), Dan. Mat. Fys. Medd. **18**, no. 8. (Ap. VI).
M. Born and W. Heisenberg (1924), Zs. f. Physik **23**, 388. (II a.iii).
R. Bouchez and R. Nataf (1952), C. R. **234**, 86; Phys. Rev. **87**, 155. (VIII c).
G. Bouissières, P. Falk-Vairant, M. Riou, J. Teillac, and C. Victor (1953), C. R. **236**, 1874. (VI c.ii).
G. Breit, M. H. Hull Jr., and R. L. Gluckstern (1952), Phys. Rev. **87**, 74. (Ap. VI).
P. Brix (1953), Phys. Rev. **89**, 1245. (Ad. v).
P. Brix and H. Kopfermann (1949), Zs. f. Physik **126**, 344. (V d; Ad. v).
P. Brix and H. Kopfermann (1952), Phys. Rev. **85**, 1050. (V d; Ad. v).
B. M. Brown and D. H. Tomboulian (1952), Phys. Rev. **88**, 1158. (Ad. viii).
H. B. G. Casimir (1936), On the Interaction between Atomic Nuclei and Electrons. Teyler's Tweede Genootschap, Haarlem. (I; V).
E. U. Condon and G. H. Shortley (1935), The Theory of Atomic Spectra. The University Press, Cambridge. (Ap. II).
S. M. Dancoff (1950), Phys. Rev. **78**, 382. (II b.iii).
J. M. Daniels, M. A. Grace, H. Halban, N. Kurti, and F. N. H. Robinson (1952), Phil. Mag. **43**, 1297. (Ad. xi).
J. P. Davidson Jr. (1951), Phys. Rev. **82**, 48. (VIII a; VIII c.iv).
J. P. Davidson and E. Feenberg (1953), Phys. Rev. **89**, 856. (II a.iii; II b.ii; II b.iii; IV; Ad. i; VIII b.ii).
H. G. Dehmelt (1952), Zs. f. Physik **133**, 528. (Ad. iii and xi).
H. G. Dehmelt and H. Krüger (1951), Zs. f. Physik **129**, 401. (Ad. iii).
H. G. Dehmelt and H. Krüger (1951 a), Zs. f. Physik **130**, 385. (Ad. v).
D. M. Dennison (1940), Phys. Rev. **57**, 454. (VI c.i).
A. de-Shalit (1951), Helv. Phys. Acta **24**, 296. (IV c).
S. S. Dharmatti and H. E. Weaver Jr. (1952), Phys. Rev. **85**, 927. (Ad. vi).
S. S. Dharmatti and H. E. Weaver Jr. (1952 a), Phys. Rev. **86**, 259. (Ad. ii).
W. C. Dickinson (1950), Phys. Rev. **80**, 563. (Ad.).
P. A. M. Dirac (1947), The Principles of Quantum Mechanics. (3rd Ed.). Oxford University Press. (II b.i).
A. S. Douglas (1953), Nature **171**, 868 (II a.iii).
A. R. Edmonds and B. T. Flowers (1952), Proc. Roy. Soc. A **214**, 515. (II c.iii).
A. R. Edmonds and B. T. Flowers (1952 a), Proc. Ryo. Soc. A **215**, 120. (II c.iii; III.ii, iii, and iv).
J. T. Eisinger, B. Bederson, and B. T. Feld (1952), Phys. Rev. **86**, 73. (Ad. iv; Ad. vi; Ad. xi).

R. J. Elliot and K. W. H. Stevens (1952), Proc. Phys. Soc. A **65**, 370. (Ad. vii).
C. D. Ellis and G. H. Aston (1930), Proc. Roy. Soc. A **129**, 180. (VII d.iii).
E. Feenberg (1947), Rev. Mod. Phys. **19**, 239. (II a.i).
E. Feenberg and K. C. Hammack (1949), Phys. Rev. **75**, 1877. (IV).
E. Feenberg and K. C. Hammack (1951), Phys. Rev. **81**, 285. (II a.iii; V b).
L. Feldman and C. S. Wu (1952), Phys. Rev. **87**, 1091. (VIII c.iv).
S. Fernbach, R. Serber, and T. B. Taylor (1949), Phys. Rev. **75**, 1352. (Ap. V c).
H. Feshbach and V. F. Weisskopf (1949), Phys. Rev. **76**, 1550. (VI d).
H. Feshbach, C. E. Porter, and V. F. Weisskopf (1953), Phys. Rev. **90**, 166. (VI d; Ap. V c).
M. Fierz (1937), Zs. f. Physik **104**, 553. (VIII a).
M. Fierz (1943), Helv. Phys. Acta **16**, 365. (VII b.ii).
B. H. Flowers (1952), Proc. Roy. Soc. A **212**, 248. (II c.iii).
B. H. Flowers (1952 a), Proc. Roy. Soc. A **215**, 398. (II c.iii; III.iii).
B. H. Flowers (1952 b), Phys. Rev. **86**, 254. (II c.iii; III.ii; VI c.ii).
B. H. Flowers (1952 c), Phil. Mag. (7), **43**, 1330. (IV a; Ad. iv).
S. Flügge (1941), Ann. d. Phys. (5), **39**, 373. (VII b.ii).
S. Flügge and K. Woeste (1952), Zs. f. Physik **132**, 384. (II a.i).
L. L. Foldy and F. J. Milford (1950), Phys. Rev. **80**, 751. (II b.i; IV).
K. W. Ford (1953), Phys. Rev. **90**, 29. (II b.ii; II b.iii; II c.ii; V d; VI c.ii).
S. Gallone and C. Salvetti (1951), Phys. Rev. **84**, 1064. (V b).
S. Gallone and C. Salvetti (1951 a), Il Nuovo Cimento (9) **8**, 970. (V b).
S. Gallone and C. Salvetti (1953), Il Nuovo Cimento (9) **10**, 145. (II a.ii; Ap. I).
S. Geschwind, G. R. Gunther-Mohr, and G. Silvey (1952), Phys. Rev. **85**, 474. (Ad. v).
M. Goldhaber and R. D. Hill (1952), Rev. Mod. Phys. **24**, 179. (III.iii; VI b; VI c.ii; VII d; VII d.i).
M. Goldhaber and A. W. Sunyar (1951), Phys. Rev. **83**, 906. (I; VI b; VI c.ii; VII d; VII d.i; VII d.ii; Ap.VI).
M. Goldhaber and E. Teller (1948), Phys. Rev. **74**, 1046. (II a.i).
W. Gordy (1949), Phys. Rev. **76**, 139. (V; V a).
C. J. Gorter, H. A. Tolhoek, O. J. Poppema, M. J. Steenland, and J. A. Beun (1952), Physica **18**, 135. (Ad. xi).
R. L. Graham and R. E. Bell (1953), Canadian J. of Physics **31**, 377. (VII d.i).
E. Greuling (1942), Phys. Rev. **61**, 568. (VIII a).
W. A. Hardy, G. Silvey, and C. H. Townes (1952), Phys. Rev. **85**, 494. (Ad. viii).
J. A. Harvey (1951), Phys. Rev. **81**, 353. (VI b).
J. A. Harvey (1953), Canadian J. of Physics **31**, 278. (VI b).
O. Haxel, J. H. D. Jensen, and H. E. Suess (1950), Zs. f. Physik **128**, 295. (I; III.i; III.ii; IV).

O. Haxel, J. H. D. Jensen, and H. E. Suess (1952), Ergebn. d. Exakten Wiss. **26**, 244. (I).
G. Herzberg (1950), Molecular Spectra and Molecular Structure I. D. van Nostrand, New York. (II b.ii; VI c.ii; VII c.i).
D. L. Hill and J. A. Wheeler (1953), Phys. Rev. **89**, 1102. (I; II a.ii; VI d; VII c.i; Ap. I).
R. D. Hill (1949), Phys. Rev. **76**, 998. (V).
R. D. Hill (1950), Phys. Rev. **79**, 1021. (VI b).
A. J. M. Hitchcock (1952), Phys. Rev. **87**, 664. (II c.iii; III.iv; IV a; Ad. xi).
A. J. M. Hitchcock (1952 a), Dissertation, Cambridge. (II c.iii; III.iv).
J. M. Hollander, I. Perlman, and G. T. Seaborg (1953), Rev. Mod. Phys. **25**, 469. (VI c.ii; VII d.iii).
N. J. Hopkins (1952), Phys. Rev. **88**, 680. (VII d.i).
H. Horie, M. Umezawa, Y. Yamaguchi, and S. Yoshida (1951), Progress Theor. Phys. **6**, 254. (VI c.ii).
H. Horie and S. Yoshida (1951), Progress Theor. Phys. **6**, 829. (IV a).
R. Huby and H. C. Newns (1951), Proc. Phys. Soc. A **64**, 619. (Ap. VI).
T. Huus and Č. Zupančič (1953), Dan. Mat. Fys. Medd. **28**, no. 1. (VI c.iii; VII d.iii; Ap. VI).
D. R. Inglis (1952), Phys. Rev. **87**, 915. (III.iv; Ad. iii; VI b).
V. Jaccarino, B. Bederson, and H. H. Stroke (1952), Phys. Rev. **87**, 676. (Ad. xi).
C. D. Jeffries (1953), Phys. Rev. **90**, 1130. (III.iii; Ad. vii).
C. D. Jeffries, H. Loeliger, and H. H. Staub (1952), Phys. Rev. **85**, 478. (Ad. vii).
W. Jekeli (1952), Zs. f. Physik **131**, 481. (II b.i; VII b.ii).
J. H. D. Jensen and M. G. Mayer (1952), Phys. Rev. **85**, 1040. (IV c).
F. M. Kelly (1952), Proc. Phys. Soc. A **65**, 250. (Ad. iv).
K. G. Kessler (1950), Phys. Rev. **79**, 167 (Ad. iii).
C. Kikutchi, M. H. Sirvetz, and V. W. Cohen (1952), Phys. Rev. **88**, 142. (Ad. xi).
J. G. King and V. Jaccarino (1953), Bul. Am. Phys. Soc. **28**, nr. 2, p. 11. (Ad. iii).
P. F. A. Klinkenberg (1952), Rev. Mod. Phys. **24**, 63. (Ad.).
L. J. Koester, H. L. Jackson, and R. K. Adair (1951), Phys. Rev. **83**, 1250. (Ad.i; VI b).
O. Kofoed-Hansen and A. Winther (1952), Phys. Rev. **86**, 428. (IV a; VIII c).
E. J. Konopinski (1943), Rev. Mod. Phys. **15**, 209. (VIII a).
E. J. Konopinski and G. E. Uhlenbeck (1941), Phys. Rev. **60**, 308. (VIII a).
H. Kopfermann (1951), Naturwiss. **38**, 29. (V d; Ad. iii).
H. Krüger and U. Meyer-Berkhout (1952), Zs. f. Phys. **132**, 171. (Ad. iii).
H. Kuhn and G. K. Woodgate (1951), Proc. Phys. Soc. A **64**, 1090. (Ad. ii).

D. KURATH (1950), Phys. Rev. **80,** 98. (II c.iii; III.iii).
D. KURATH (1952), Phys. Rev. **87,** 218 (A). (II c.iii; III.iv).
D. KURATH (1952 a), Phys. Rev. **88,** 804. (Ad. iii).
D. KURATH (1953), submitted to the Physical Review. (II c.iii; III.iv).
H. LEW (1953), Phys. Rev. **89,** 530. (Ad. v).
L. LIDOFSKY, P. MACKLIN, and C. S. WU (1952) Phys. Rev. **87,** 391. (VIII c.iv).
I. S. LOWEN (1941) Phys. Rev. **59,** 835. (VII b.ii).
J. E. MACK (1950), Rev. Mod. Phys. **22,** 64. (III.iii; Ad.).
H. M. MAHMOUD and E. J. KONOPINSKI (1952), Phys. Rev. **88,** 1266. (VIII a).
K. G. MALMFORS (1953), Arkiv f. Fysik **6,** 49. (VII d.iii).
M. G. MAYER (1950), Phys. Rev. **78,** 16. (I; III i; III ii; IV).
M. G. MAYER (1950 a), Phys. Rev. **78,** 22. (II c.iii; III.ii; III.iii).
M. G. MAYER, S. A. MOSZKOWSKI, and L. W. NORDHEIM (1951), Rev. Mod. Phys. **23,** 315. (IV a; VI b; VIII c.ii and iii).
C. L. MCCLELLAND and C. GOODMAN (1953), submitted to the Physical Review. (Ap. VI).
L. MEITNER and O. R. FRISCH (1939), Nature **143,** 239. (I).
D. W. MILLER, R. K. ADAIR, C. K. BOCKELMAN, and S. E. DARDEN (1952), Phys. Rev. **88,** 83. (VI d).
A. C. G. MITCHELL (1951), Phys. Rev. **83,** 183. (VI b).
H. MIYAZAWA (1951), Progress Theor. Phys. **6,** 263. (IV c).
H. MIYAZAWA (1951 a), Progress Theor. Phys. **6,** 801. (IV, IV c; V d; Ad. iii).
M. MIZUSHIMA and M. UMEZAWA (1952), Phys. Rev. **85,** 37; **86,** 1055. (IV a).
S. A. MOSZKOWSKI (1951), Phys. Rev. **83,** 1071. (VI b; VII a; VII d.i; VII d.ii).
S. A. MOSZKOWSKI (1953), Phys. Rev. **89,** 474. (VII a; VII b.i; VII d.i).
C. J. MULLIN and E. GUTH (1951), Phys. Rev. **82,** 141. (Ap. VI).
K. MURAKAWA and S. SUWA (1952), Reports of the Institute of Science and Technology, University of Tokyo **6,** no. 4. (Ad. iii).
K. MURAKAWA and S. SUWA (1952 a), Phys. Rev. **87,** 1048. (Ad. iii; Ad. iv).
N. NERESON and S. DARDEN (1953), Phys. Rev. **89,** 775. (VI d).
H. H. NIELSEN (1951), Rev. Mod. Phys. **23,** 90. (VI c.ii).
M. NOGAMI (1948), Progress Theor. Phys. **3,** 362. (II b.i).
L. W. NORDHEIM (1949), Phys. Rev. **75,** 1894. (IV).
L. W. NORDHEIM (1951), Rev. Mod. Phys. **23,** 322. (VI b; VIII b.i; VIII c.ii).
S. A. OCHS and P. KUSCH (1952), Phys. Rev. **85,** 145. (Ad. vi).
S. A. OCHS, R. A. LOGAN, and P. KUSCH (1950), Phys. Rev. **78,** 184. (Ad. iv).
R. K. OSBORN and L. L. FOLDY (1950), Phys. Rev. **79,** 795. (IV c).
D. PFIRSCH (1952), Zs. f. Physik **132,** 409. (II a.iii; V c).
P. PREISWERK and P. STÄHELIN (1952), Physica **18,** 1118. (VI c.ii).

M. H. L. Pryce (1952), Proc. Phys. Soc. A **65**, 773. (VI b; VI c.i).
G. Racah and I. Talmi (1952), Physica **18**, 1097. Cf. also recent work by G. Racah quoted in this reference. (II c.iii; III. ii and iii).
J. Rainwater (1950), Phys. Rev. **79**, 432. (I; II a.iii; V; V c).
N. F. Ramsey (1951), Phys. Rev. **83**, 659. (Ap. VI).
M. E. Rose, G. H. Goertzel, B. I. Spinrad, J. Harr, and P. Strong (1951), Phys. Rev. **83**, 79. (Ap.VI).
S. Rosenblum and M. Valadares (1952), C. R. **235**, 711. (VI c.ii).
L. Rosenfeld (1948). Nuclear Forces. North-Holland Publishing Company, Amsterdam. (II a.ii).
L. Rosenfeld (1951), Physica **17**, 461. (V).
M. Ross (1952), Phys. Rev. **88**, 935. (IV c).
A. Russek and L. Spruch (1952), Phys. Rev. **87**, 1111. (IV c).
A. Rytz (1951), C. R. **233**, 790. (VII d.iii).
R. G. Sachs (1948), Phys. Rev. **74**, 433; Phys. Rev. **75**, 1605. (IV; IV c).
G. Scharff-Goldhaber (1952), Physica **18**, 1105. (VI c.ii).
G. Scharff-Goldhaber (1953), Phys. Rev. **90**, 587. (VI c.ii; Ap.VI).
L. I. Schiff (1951), Phys. Rev. **84**, 1. (IV c).
T. Schmidt (1937), Zs. f. Physik **106**, 358. (IV; IV a).
R. Serber (1947), Phys. Rev. **72**, 1114. (Ap. V c).
W. von Siemens (1951), Naturwiss. **38**, 455. (Ad. iv).
A. B. Smith, R. S. Caird, and A. C. G. Mitchell (1952), Phys. Rev. **88**, 150. (III.iii).
L. Spruch (1950), Phys. Rev. **80**, 372. (IV c).
P. Stähelin and P. Preiswerk (1951), Helv. Phys. Acta **24**, 623 (VI c.ii).
B. Stech (1952), Zs. f. Naturforsch **7 a**, 401. (VII a; VII b.i).
H. Steinwedel and J. H. D. Jensen (1950), Zs. f. Naturforsch. **5 a**, 413. (II a.i).
R. Sternheimer (1951), Phys. Rev. **84**, 244. (Ad.).
R. Sternheimer (1952), Phys. Rev. **86**, 316. (Ad.).
A. Steudel (1952), Zs. f. Phys. **132**, 429. (Ad. v).
A. Storruste (1951), Investigation of Gamma-Rays by the Scintillation Method. Dissertation, Oslo. (VII d.iii).
H. E. Suess and J. H. D. Jensen (1952), Arkiv f. Fysik **3**, 577. (VI b).
S. Suwa (1952), Phys. Rev. **86**, 247. (Ad. v).
W. J. Swiatecki (1951). Proc. Phys. Soc. A**64**, 226. (II a.i).
I. Talmi (1951), Phys. Rev. **83**, 1248. (Ad. xi).
I. Talmi (1952), Helv. Phys. Acta **25**, 185. (II c.iii; III.iii).
I. Tamm (1945), J. Phys. (USSR) **9**, 449. (II b.iii).
T. Teichmann and E. P. Wigner (1952), Phys. Rev. **87**, 123. (Ap. V b.iii).
E. Teller and J. A. Wheeler (1938), Phys. Rev. **53**, 778. (II a.i).
K. A. Ter-Martirosyan (1952), Zh. Eksper. Teor. Fiz. **22**, 284. (VII a; Ap. VI).
S. Tomonaga (1946), Progress Theor. Phys. **1**, 83, 109. (II b.ii).

C. H. Townes, H. M. Foley, and W. Low (1949), Phys. Rev. **76,** 1415. (I; V; V a).
G. L. Trigg (1952), Phys. Rev. **86,** 506. (VIII c; VIII c.i).
F. Villars (1947), Helv. Phys. Acta **20,** 476. (IV; IV c).
R. van Wageningen and J. de Boer (1952), Physica **18,** 369. (V c).
H. Walchli, R. Livingston, and W. J. Martin (1952), Phys. Rev. **85,** 479. (Ad. ix).
H. E. Walchli, W. E. Leyshon, and F. M. Scheitlin (1952 a), Phys. Rev. **85,** 922. (Ad. xi).
M. Walt, R. L. Becker, A. Okazaki, and R. E. Fields (1953), Phys. Rev. **89,** 1271. (VI d).
A. H. Wapstra (1952), Physica **18,** 799. (VI c.ii).
A. H. Wapstra (1953), The Decay Scheme of Pb^{209}, Bi^{207} and Bi^{214} and the Binding Energies of the Heavy Nuclei. Dissertation, Amsterdam. (VI c.ii; VII d.iii).
K. Way, L. Fano, M. R. Scott, and K. Thew (1950). Nuclear Data. National Bureau of Standards, Circular 499. (VII d.iii).
V. F. Weisskopf (1938), Phys. Rev. **53,** 1018. (Ap. VI).
V. F. Weisskopf (1950), Helv. Phys. Acta **23,** 187. (Ap. V b.iii).
V. F. Weisskopf (1951), Phys. Rev. **83,** 1073. (VII a).
V. F. Weisskopf (1952), Physica **18,** 1083. (II c.iii; VI d).
E. P. Wigner (1931), Gruppentheorie und ihre Anwendung auf die Quantenmechanik der Atomspektren. F. Vieweg, Berlin. (II b.ii).
E. P. Wigner and E. Feenberg (1941), Reports on Progress in Physics, **8,** 274. (VIII b.i).
A. Winther (1952), Physica **18,** 1079. (VIII c.i).
A. Winther and O. Kofoed-Hansen (1953), Dan. Mat. Fys. Medd. **27,** no. 14. (VIII a; VIII c; VIII c.i).
K. Woeste (1952), Zs. f. Physik **133,** 370. (II a.i).
C. S. Wu (1950), Rev. Mod. Phys. **22,** 386. (VIII c.iv).

Det Kongelige Danske Videnskabernes Selskab
Matematisk-fysiske Meddelelser, bind **27**, no. 16.

Mat. Fys. Medd. Dan. Vid. Selsk. **27**, no. 16 (1953)(ed. 2, 1957)

COLLECTIVE AND INDIVIDUAL-PARTICLE ASPECTS OF NUCLEAR STRUCTURE

BY

AAGE BOHR AND BEN R. MOTTELSON

SECOND EDITION

København 1957
i kommission hos Ejnar Munksgaard

Fotografisk optryk

STATENS TRYKNINGSKONTOR

Un 27-2

Preface to the Second Edition

The general approach to the analysis of nuclear structure which was followed in this paper has been considerably developed during the past four years and has been applied in the interpretation of a large body of experimental data. The 1953 paper is being reproduced without changes, but we take the present opportunity to indicate some of the main lines along which the development has proceeded and to give a number of references to later work.

The description of nuclear dynamics in terms of individual particle motion and collective oscillations is based on a set of equations representing the coupled motion of the particle and collective degrees of freedom. The form of these equations follows largely from considerations of the symmetry properties of the system, and is thus expected to have a rather general validity. Some of the parameters involved, however, such as the stability of the nuclear shape against distortion or the mass associated with the collective flow, depend on more specific features of the nuclear collective motion.

As a first orientation, one attempted to employ values for these parameters obtained from a liquid drop model, but already the early analysis of various nuclear properties showed the limitations of this comparison. The inadequacy of the liquid drop estimates was especially clearly brought out by the comparison of the nuclear moments of inertia with the deformations deduced from the rate of the electric quadrupole rotational transitions (§ VIc. ii; Ford, 1954; Sunyar, 1955).

An improved understanding of the collective nuclear properties has come from the efforts to derive these directly from the motion of the nucleons; this analysis has revealed the important influence of the nuclear shell structure on the collective motion. The effect on the moment of inertia is at present the best understood (Inglis, 1954; Bohr and Mottelson, 1955; Moszkowski,

1956), but also tentative beginnings have been made with respect to the analysis of other collective parameters (cf. Ap. I; INGLIS, 1955; MOSZKOWSKI, 1956; ARAÚJO, 1956; ALDER et al., 1956). The inadequacy of the liquid drop model with irrotational flow implies that the collective coordinates considered as functions of the nucleonic variables are of more general form than (II.2), and depend on the nucleonic velocities as well as positions (BOHR and MOTTELSON, 1955). The problem of deriving the collective nuclear properties from the equations for a system of interacting particles has been considered by a number of different methods; in addition to the references quoted in ALDER et al. (1956, p. 528), the following papers on the subject have recently appeared: COESTER (1956), DAVIDOV and FILLIPOV (1956), LIPKIN, DESHALIT, and TALMI (1956), LÜDERS (1956), NATAF (1957), SKYRME (1957), TOMONAGA (1956), PEIERLS and YOCCOZ (1957), YOCCOZ (1957); cf. also the review article by TAMURA (1957).

In 1953, it was not always clear which coupling scheme would be most appropriate to a particular nucleus. As a result of the extensive experimental study of nuclear rotational and vibrational spectra, it seems now established that the strong coupling scheme, characterized by a relatively large equilibrium deformation and a rotational band structure of the energy levels, provides a good starting point for nuclei in the regions $A \sim 25$, $150 < A < 190$, and $A > 222$ (cf. the data summarized in ALDER et al., 1956). Outside these regions, and excluding the nuclei immediately adjacent to closed shells, it has been possible to interpret many features of the observed lowest states of even-even nuclei in terms of quadrupole vibrations about a spherical equilibrium (SCHARFF-GOLDHABER and WENESER, 1955; JEAN and WILETS, 1955; ALDER et al., 1956). In these latter regions, the odd-A nuclei present a more complicated picture, which is not yet well understood, but which may possibly be related to intermediate coupling schemes (§ IIb. iii; FORD, 1953; CHOUDHURY, 1954; J. RAZ, 1955).

In the region where the strong coupling scheme applies, the great simplicity of the nuclear structure has made possible a rather detailed description of the low energy excitation spectrum as well as of the different types of transitions between the nuclear states. The simple relationships between the states within a rotational band have been further exploited (ALAGA, ALDER, BOHR, and

MOTTELSON, 1955; BOHR, FRÖMAN, and MOTTELSON, 1955; SATCHLER, 1955; KERMAN, 1955) and, in addition, the analysis of independent particle motion in non-spherical fields has made possible the interpretation of intrinsic excitations and the calculation of equilibrium shapes (NILSSON, 1955; MOSZKOWSKI, 1955; MOTTELSON and NILSSON, 1955, 1957; GOTTFRIED, 1956). In the α-decay of the heavy elements, the influence of the nuclear shape on the intensities of the fine structure components has been analyzed (RASMUSSEN and SEGALL, 1956; STRUTINSKY, 1956; FRÖMAN, 1957). In the β- or γ-transitions between different intrinsic states, there are important selection rules associated with quantum numbers appropriate to the motion in a deformed field (ALAGA et al., 1955; ALAGA, 1955; MOTTELSON and NILSSON, 1957). More detailed estimates have shown that the readjustment of the collective field (cf. p. 107) has in most cases only a small effect on the transition rate (SUEKANE, 1953; REDLICH and WIGNER, 1954).

While a great amount of evidence has been accumulated on the rotational and single particle excitation spectra of the deformed nuclei, relatively little information has been obtained regarding collective vibrations in these nuclei. Quite recently, however, there has appeared some evidence for the occurrence of levels with the expected properties of β- and γ-vibrations; also odd parity states resembling octupole vibrations have been observed in certain regions of elements (cf. the data summarized by ALDER et al., 1956, and by PERLMAN and RASMUSSEN, 1957).

The important influence of the residual two body interactions on various features of the low energy nuclear properties has been emphasized by recent work. One may especially mention the analysis of nuclear spectra for configurations with a few particles outside of closed shells (cf., e. g., the review by ELLIOTT and LANE, 1957) and the interpretation of magnetic moments which provides an especially sensitive test of configuration mixing (BLIN-STOYLE and PERKS, 1954; ARIMA and HORIE, 1954; and the review by BLIN-STOYLE, 1956). Moreover, the role of the pairing energy is reflected in the intrinsic excitation spectra of even-even nuclei as well as by the analysis of the kinetic and potential energy of the collective motion(cf., e. g., ALDER et al., 1956). It is not yet clear to what extent these forces simply represent the direct interactions between the particles outside of closed shells, and to

what extent they are to be ascribed to the effective forces resulting from the polarization of the nucleus (cf. § IIc. i).

A description of nuclear reaction processes, similar to that developed in § VId and Ap. V, has been considered by a number of authors (SCOTT, 1954; LANE, THOMAS, and WIGNER, 1955; FRIEDMAN and WEISSKOPF, 1956). An instructive example which exhibits some of the conditions for the applicability of the optical model is provided by the direct coupling between the incident particle and the nuclear rotational motion (cf. the discussion in Ap. Vc). A number of consequences of an extended optical model which includes the effect of such direct couplings have been derived (cf., e. g., BRINK, 1955; HAYAKAWA and YOSHIDA, 1955; DROZDOV, 1956; MOSHINSKY, 1956; MARGOLIS and TROUBETZKOY, 1957; GRIBOV, 1957). In the nuclear fission reaction, the strong coupling scheme should provide a good description of the spectrum of fission channels at the saddle point, and some of the consequences of such a model have been discussed (BOHR, 1955).

In this brief summary, it has not been possible to mention explicitly the many experimental studies which have guided the theoretical developments. For the understanding of the low energy nuclear structure, the decay scheme studies and the Coulomb excitation experiments have in recent years played an especially important part. The first definite results of Coulomb excitation experiments were reported in 1953, shortly after this article was sent to the printer. For a review of the developments in this field, cf. HEYDENBURG and TEMMER (1956) and ALDER, BOHR, HUUS, MOTTELSON, and WINTHER (1956).

Aage Bohr and Ben R. Mottelson.

March 1, 1957.
Institute for Theoretical Physics
University of Copenhagen,
and
CERN, Theoretical Study Division,
Copenhagen, Denmark.

References.

G. Alaga (1955), Phys. Rev. **100,** 432.

G. Alaga, K. Alder, A. Bohr, and B. R. Mottelson (1955), Mat. Fys. Medd. Dan. Vid. Selsk. **29,** no. 9.

K. Alder, A. Bohr, T. Huus, B. R. Mottelson, and A. Winther (1956), Revs. Mod. Phys. **28,** 432.

J. M. Araújo (1956), Nuclear Physics **1,** 259.

A. Arima and H. Horie (1954), Prog. Theor. Phys. **11,** 509.

R. J. Blin-Stoyle (1956), Revs. Mod. Phys. **28,** 75.

R. J. Blin-Stoyle and M. A. Perks (1954), Proc. Phys. Soc. (London) A **67,** 885.

A. Bohr, (1955), Proc. Intern. Conf. Geneva, **2,** 151. U. N., New York 1956.

A. Bohr, P. O. Fröman, and B. R. Mottelson (1955), Mat. Fys. Medd. Dan. Vid. Selsk. **29,** no. 10.

A. Bohr and B. R. Mottelson (1955), Mat. Fys. Medd. Dan. Vid. Selsk. **30,** no. 1.

D. M. Brink (1955), Proc. Phys. Soc. (London), A **68,** 994.

D. C. Choudhury (1954), Mat. Fys. Medd. Dan. Vid. Selsk. **28,** no. 4.

F. Coester (1956), Nuovo Cimento **4,** Ser. 10, 1307.

A. S. Davydov and G. F. Filipov (1956), Physica **XXII,** 1167.

S. I. Drozdov (1955, 1956), Journ. Exp. Theor. Physics USSR **28,** 734, 736; **30,** 786.

J. P. Elliott and A. M. Lane (1957), to appear in Handbuch der Physik (Springer Verlag, Berlin).

K. W. Ford (1953), Phys. Rev. **90,** 29.

K. W. Ford (1954), Phys. Rev. **95,** 1250.

F. L. Friedman and V. F. Weisskopf (1955), Niels Bohr and the Development of Physics, Pergamon Press, London, W. Pauli ed.

P. O. Fröman (1957), Mat. Fys. Skr. Dan. Vid. Selsk. **1,** no. 3.

K. Gottfried (1956), Phys. Rev. **103,** 1017.

S. Hayakawa and S. Yoshida (1955), Prog. Theor. Phys. **14, 1.**

N. P. Heydenburg and G. M. Temmer (1956), Ann. Rev. of Nuclear Science, vol. 6, J. G. Becheley ed.

D. R. Inglis (1954), Phys. Rev. **96,** 1059.

D. R. Inglis (1955), Phys. Rev. **97,** 701.

M. Jean and L. Wilets (1955), C. R. **241,** 1108; Phys. Rev. **102,** 788 (1956).

A. K. Kerman (1956), Mat. Fys. Medd. Dan. Vid. Selsk. **30,** no. 15.

A. M. Lane, R. G. Thomas, and E. P. Wigner (1955), Phys. Rev. **98,** 693.
H. J. Lipkin, A. de-Shalit, and I. Talmi (1956), Phys. Rev. **103,** 1773.
G. Lüders (1956), Z. f. Naturforsch. **11a,** 617 and in press.
B. Margolis and E. Troubetzkoy (1957), Phys. Rev. **106,** 105.
M. Moshinsky (1956), Revista Mexicana de Fisica **5,** 1.
S. A. Moszkowski (1955), Phys. Rev. **99,** 803.
S. A. Moszkowski (1956), Phys. Rev. **103,** 1328.
B. R. Mottelson and S. G. Nilsson (1955), Phys. Rev. **99,** 1615.
B. R. Mottelson and S. G. Nilsson (1957), to appear in Mat. Fys. Medd. Dan. Vid. Selsk.
R. S. Nataf (1957), Nuclear Physics **2,** 497.
R. E. Peierls and J. Yoccoz (1957), Proc. Phys. Soc. (London) **A 70,** 381.
S. G. Nilsson (1955), Mat. Fys. Medd. Dan. Vid. Selsk. **29,** no. 16.
I. Perlman and J. O. Rasmussen (1957), to appear in Handbuch der Physik (Springer Verlag, Berlin).
J. O. Rasmussen and B. Segall (1956), Phys. Rev. **103,** 1298.
B. J. Raz (1955), Dissertation, Rochester University.
M. G. Redlich and E. P. Wigner (1954), Phys. Rev. **95,** 122.
G. R. Satchler (1955), Phys. Rev. **97,** 1416.
G. Scharff-Goldhaber and J. Weneser (1955), Phys. Rev. **98,** 212.
J. M. C. Scott (1954), Phil. Mag. **45,** 441.
T. H. R. Skyrme (1957), Proc. Roy. Soc. A (London), to be published.
S. Suekane (1953), Prog. Theor. Phys. **10,** 480.
A. W. Sunyar (1955), Phys. Rev. **98,** 653.
V. M. Strutinsky (1956), J.E.T.P., USSR, **30,** 411.
T. Tamura (1957), to appear in Fortschritte der Physik.
S. Tomonaga (1956), Report at the Intern. Congress of Theor. Phys., Seattle.
F. Villars (1957), Nuclear Physics **3,** 240.
J. Yoccoz (1957), Proc. Phys. Soc. (London) **A 70,** 388.